FISH OIL DISRUPTS B CELL PLASMA MEMBRANE LATERAL ORGANIZATION AND IMMUNOLOGICAL SYNAPSE FORMATION

by

Benjamin Drew Rockett

November, 2012

Director of Dissertation: Saame Raza Shaikh

Biochemistry and Molecular Biology

East Carolina University

Fish oil has immunosuppressive properties that could provide treatment for numerous inflammatory and autoimmune disorders. The primary bioactive components of fish oil, which are the n-3 polyunsaturated fatty acids (PUFAs) eicosapentaenoic acid (EPA) and docosahexaenoic acid (DHA), can exert differential effects on many cell types in the body. A major limitation in the development of fish oil as a therapeutic is the lack of mechanistic understanding of how fish oil exerts its functional effects. One emerging mechanism is that EPA and DHA have unique biophysical properties that could disrupt the lateral organization of plasma membrane lipids and proteins critical for signaling and cell-cell communication, such as lipid rafts and the immunological synapse. In this study, we investigate a potential mechanism for this disruption in B cells, a cell type poorly represented in the field of n-3 PUFA research. The central hypothesis for this study was that fish oil disrupts lateral organization of lipid rafts and suppresses downstream B cell function. Using high and low fat fish oil diets in mice, we demonstrated that fish oil dispersed clustering of B cell lipid rafts on a micron scale, and enhanced membrane molecular order upon cross-linking raft domains. We found that

the effects on lipid rafts are primarily driven by DHA and not EPA, and that n-3 PUFAs have a limited influence on non-raft lateral organization. Finally, we show that fish oil suppresses B cell antigen presentation and subsequent $CD4^+$ T cell IL-2 secretion, by disrupting the B cell side of the immunological synapse. Taken together, this work highlights the utility of fish oil, more specifically DHA, as a tool for disrupting plasma membrane lateral organization. We add to the biochemical understanding of how these fatty acids may disrupt various downstream signaling events and cell-cell interactions. It also emphasizes the importance of the plasma membrane as a target for suppressing other cellular functions mediated through lipid raft domains. Finally, these studies add B cells as key targets for suppression of antigen presentation in diseases such as autoimmune disorders.

FISH OIL DISRUPTS B CELL PLASMA MEMBRANE LATERAL ORGANIZATION AND IMMUNOLOGICAL SYNAPSE FORMATION

A Dissertation

Presented To the Faculty of the Department of Biochemistry and Molecular Biochemistry

East Carolina University

In Partial Fulfillment of the Requirements for the Degree

Doctor of Philosophy

by

Benjamin Drew Rockett

November, 2012

FISH OIL DISRUPTS B CELL PLASMA MEMBRANE LATERAL ORGANIZATION AND IMMUNOLOGICAL SYNAPSE FORMATION

by

Benjamin Drew Rockett

APPROVED BY:

DIRECTOR OF DISSERTATION:

_____

Saame Raza Shaikh, Ph.D.

COMMITTEE MEMBER:

_____

Joseph M. Chalovich, Ph.D.

COMMITTEE MEMBER:

_____

Lance C. Bridges, Ph.D.

COMMITTEE MEMBER:

_____

Barbara J. Muller-Borer, Ph.D.

CHAIR OF THE DEPARTMENT OF BIOCHEMISTRY AND MOLECULAR BIOLOGY:

_____

Phillip H. Pekala, Ph.D.

DEAN OF THE GRADUATE SCHOOL:

_____

Paul J. Gemperline, Ph.D.

ACKNOWLEDGEMENTS

I would first like to thank my parents, Ron Rockett and Annette Adams, for providing me every opportunity I ever wanted to pursue my dreams. I cannot be more grateful for all you have done to guide me through each stage of me life. I next want to thank my wife, Alexis Rockett. Without you, I would not be where I am today. You give me strength and purpose. To my mentor, Dr. Raz Shaikh, before starting this stage of my career, I never would have imagined where I would end up. I owe much of my success to you. To the my lab-mates Kristen, Mo, Kaitlin, Heather, Mitch, and Mark, all science is a team effort. I could not accomplish this without your hard work and dedication. To my committee, the faculty and staff at ECU, and our collaborators, thank you for the opportunity to work with you, and all the guidance and assistance you have given me.

TABLE OF CONTENTS

PAGE

PAGE

PAGE

LIST OF TABLES

LIST OF FIGURES

PAGE

PAGE

LIST OF ABBREVIATIONS

AA	Arachidonic acid
ALA	α-Linolenic acid
APC	Antigen presenting cell
BSA	Bovine serum albumin
c-SMAC	Central supramolecular activation cluster
C16-Bodipy	4,4-Difluoro-5,7-dimethyl-4-bora-3a,4a-diaza-s-indacene-3-hexadecanoic acid
CD	Control diet
CTx-B	cholera toxin subunit B
DC	Dendritic cell
DHA	Docosahexaenoic acid
$DiIC_{18}$	1,1'-dioctadecyl-3,3,3′,3′-tetramthylindocarbocyanine perchlorate
DRM	Detergent-resistant membrane
DSM	Detergent-soluble membrane
E	Energy transfer
ELA	Elaidic acid
EPA	Eicosapentaenoic acid
FAST-DiI	1,1′-Dilinoleyl-3,3,3′,3′-tetramethylindocarbocyanine perchlorate
FFA	Free fatty acid
FO	Fish oil
fPALM	Fluorescence Photoactivation Localization Microscopy
FRET	Förster resonance energy transfer
GC	Gas chromatography

GP	Generalized polarization
GPI	Glycosylphosphatidylinositol
GPR	G-protein coupled receptor
HF	High-fat
I	Intensity
IFN	Interferon
IL	Interleukin
LF	Low-fat
LPS	Lipopolysaccharide
MHC	Major histocompatibility complex
MβCD	Methyl-beta-cyclodextrin
OA	Oleic acid
$OVA_{323–339}$	Chicken ovalbumin 323–339
p-SMAC	Peripheral supramolecular activation cluster
PC	Phosphatidylcholine
PE	Phosphatidylethanolamine
PPAR	Proliferator-activated receptor
PUFA	Polyunsaturated fatty acid
RER	Respiratory exchange ratio
SFA	Saturated fatty acid
SM	Sphingomyelin
SMAC	Supramolecular activation cluster
STED	Stimulated emission depletion
STORM	Stochastic optical reconstruction microscopy
TCR	T cell receptor
TG	Triglycerides
Th1	T helper 1

Th2	T helper 2
TIRF	Total internal reflection fluorescence
TLR	Toll-like receptor
TNF	Tumor necrosis factor
VCO_2	Maximal CO_2 consumption
VO_2	Maximal O_2 consumption

CHAPTER 1: INTRODUCTION

Overview

n-3 polyunsaturated fatty acids (PUFAs), also known as omega 3 fatty acids, are important bioactive molecules with many potential health benefits (1). In particular, consumption of eicosapentaenoic acid (EPA) and docosahexaenoic acid (DHA), the major n-3 PUFA bioactive components of fish oil, have been established as regulators of immune function (2). However, a major roadblock to widespread clinical utility of fish oil is the lack of clear understanding of the mechanisms for its beneficial effects. This dissertation addresses that limitation by investigating how incorporation of EPA and DHA into the plasma membrane modifies B cell function.

Historical perspective

Research on n-3 PUFAs originated in the 1970s, when scientists began studying Greenland's Inuit populations due to their incredibly low incidence of ischemic heart disease compared to the rest of the world (3). What they discovered was the Inuit population consumed a unique diet that led to decreased plasma lipid concentrations (4). Unlike most industrialized civilizations, this diet consisted of very high levels of n-3 PUFAs from fish and other seafoods. The dietary n-3 PUFA levels amounted to around 7% of total daily energy (5, 6). Some modern Japanese populations also have elevated n-3 PUFA intakes, especially when compared to the western diet, though not to the degree of the Greenland Inuits. The Japanese consume roughly 1-2% of daily energy from n-3 PUFA, which also correlates to moderate decrease in total mortality (7, 8).

Not until the 1990s and the early 2000s did increased awareness of the additional possible health benefits of consuming n-3 PUFAs become widespread. n-3

PUFAs have been shown to be beneficial in a number of conditions such as cardiovascular disease (9-13), cancer (14-16), various inflammatory disorders (17-20), and cognitive health (21-23). A link between many of these conditions is the immunosuppressive properties of n-3 PUFAs (24). Therefore, this dissertation is focused on unveiling a mechanism for how fish oil suppresses immune cell function.

Biochemistry of n-3 PUFAs

The unique structure of n-3 PUFAs is distinguished by multiple double bonds starting 3 carbons from the methyl end of the acyl chain. Similarly, n-6 PUFAs, a structurally related group of fatty acids, are distinguished by multiple double bonds starting 6 carbons from the methyl end. Animal tissues, unlike plants, are unable to synthesize either group of these fatty acids due to an inability to insert double bonds further than 9 carbons from the carboxyl end of the acyl chain (25). Once consumed through the diet, α-linolenic acid (ALA), 18:3 (n-3), or linoleic acid, 18:2 (n-6), can be converted into the longer chain PUFAs through a series of elongation and desaturation reactions (Figure 1.1). Retroconversion or β-oxidation of DHA can also generate EPA and docosapentaenoic acid (26). However, since ALA is at the top of this pathway, this makes ALA and linoleic acid essential dietary fatty acids. There are two major metabolic fates for ALA when consumed in the diet: 1) β-oxidation for use as a fuel source, 2) conversion into longer chain n-3 PUFAs for a variety of uses. Some studies suggest that most is used for β-oxidation (27, 28). In addition, the conversion of ALA to longer-chain n-3 PUFA is very inefficient, although the rate is slightly higher in pre-menopausal women (29). For instance, studies of plasma lipid levels in healthy individuals found that only 0.2% of radio-labeled ALA was able to be converted into EPA, whereas 63% of

Figure 1.1: PUFA synthesis

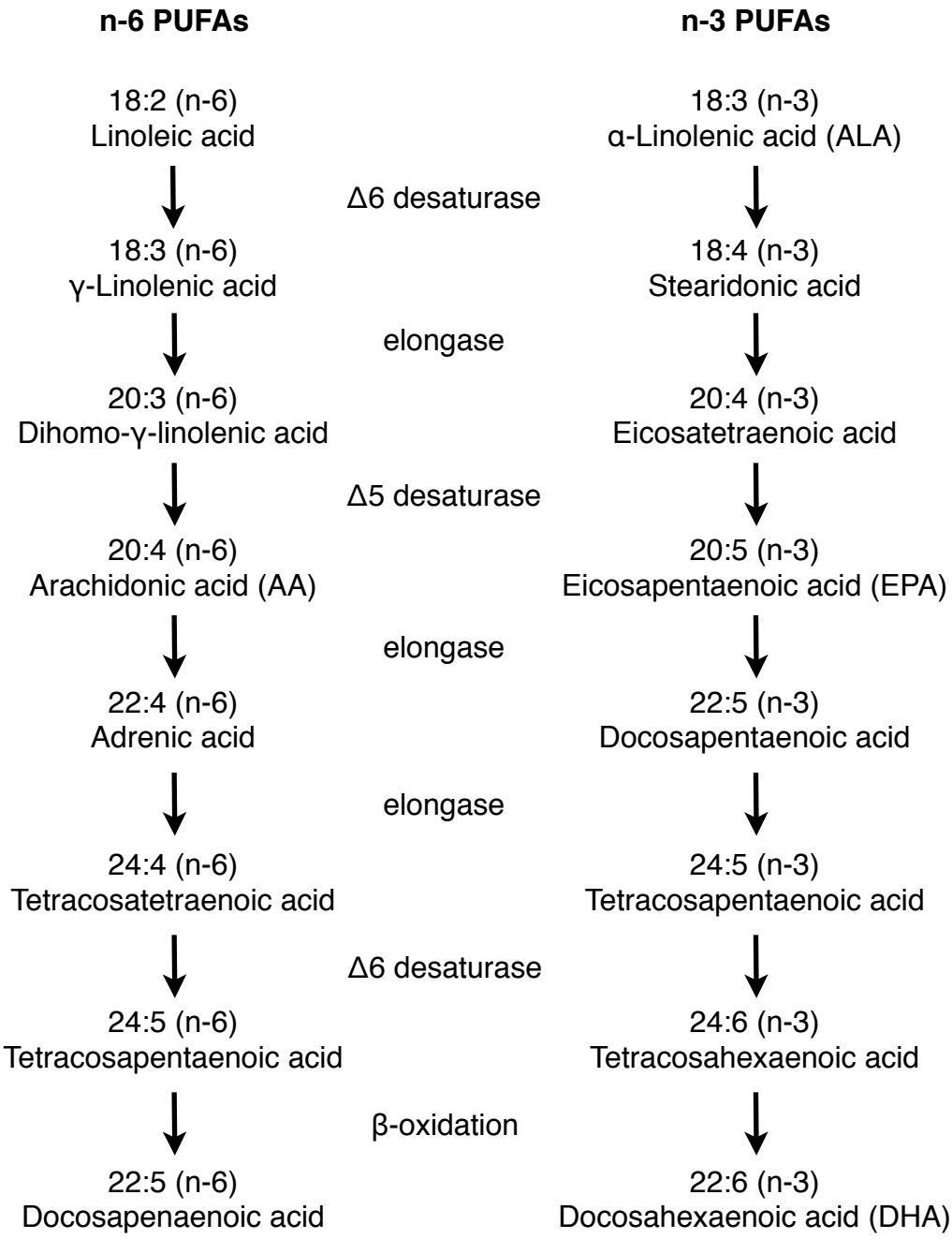

Figure 1.1: Polyunsaturated fatty acid (PUFA) synthesis. n-6 PUFA (left) and n-3 PUFA (right) elongation pathways. Each step in either pathway uses the same enzymes.

EPA was able to be converted into DHA (30). This finding suggested that direct dietary consumption of EPA/DHA may be more beneficial for studying the effects of EPA/DHA than consumption of ALA alone. On the other hand, additional evidence suggests this limitation could be tissue dependent (31).

An additional limitation of longer chain n-3 PUFA synthesis from ALA is the competition between the synthesis pathways of n-3 versus n-6 PUFAs. This competition is due to the fact that they share the elongase and desaturase enzymes for this process (32-34). Furthermore, animals are not able to convert an n-3 PUFA into an n-6 PUFA or vice versa. However, the *C. elegans* gene, fat-1, was identified for this process (35). Consequently, this discovery led to development of a transgenic mouse line where the fat-1 gene was expressed, resulting in abundant n-3 PUFA and reduced n-6 PUFA levels, without a dietary n-3 PUFA supply (36).

Recommended intake of n-3 PUFAs

According to the American Heart Association, World Health Organization, and European Food Safety Agency, n-3 PUFAs should be added to the daily diet for good overall health and to prevent many diseases (37). The daily dietary recommended level of n-3 PUFAs has continually evolved, increasing as more information about their beneficial effects is gathered. Currently these organizations recommend healthy individuals consume on average 1 - 2.5 grams per day of total n-3 PUFA, including 200 to 600 mg per day of EPA/DHA (37-40). Due to the limited conversion rate described above, and the evidence of the necessity of DHA for overall health, there has been a push to recognize DHA in addition to ALA as an essential dietary fatty acid (41, 42). These recommended levels can be achieved through a minimum of 2 servings of fish

per week, with one being oily fish (tuna, mackerel, salmon, or sardine). Consumption of fish does not come without some risks. Some contaminants in fish are methylmercury, dioxins, polychlorinated biphenyls, and organic pollutants from industrial processes. Advancement in dietary enrichment of milk, eggs, meat and other products with n-3 PUFAs provides many new alternatives to fish consumption alone (43). In fact, market research by Packaged Facts predicts the n-3 PUFA food and beverage market, excluding fish, will become a $7 billion commercial industry by 2015 (44).

As supplements or food additives, n-3 PUFAs exist as two major forms, triglycerides or ethyl esters. The n-3 PUFAs present in fish or other oils are mostly in the triglyceride form. The triglyceride form seems to show increased efficiency in being absorbed through dietary intake compared to the ethyl ester form (45, 46). In both forms, the fatty acids are absorbed in the small intestine, cleaved by lipases, and reassembled into triglycerides. However, in the ethyl ester form, absorption and re-synthesis is delayed, perhaps making this form less effective as a clinical treatment (47, 48). Ethyl ester n-3 PUFAs can be re-esterified into a glycerol backbone during manufacturing, but this is usually not done because of the added costs. However, all forms seem to have similar abilities in treating hypertriglyceridemia (49, 50).

Purified fish oil as ethyl esters has been clinically developed to lower elevated triglyceride levels with a drug called Lovaza. This is the only use for n-3 PUFAs that is clinically approved in the United States by the FDA, although the mechanism of action is still unclear. Four grams per day of EPA and DHA is prescribed for severe hypertriglyceridemia (≥500 mg/dL). This treatment represents approximately 465 mg of EPA and 375 mg of DHA per 1 g capsule of ethyl ester fatty acids. Lovaza is thought to

work by reducing triglyceride production and liver secretion, in addition to removing excess triglycerides from the blood (51). Both the types of n-3 PUFA and the dose used in many other therapeutic applications have varied widely, making it very difficult to make specific clinical recommendations for further applications (52). Fully elucidating the mechanisms remains a major theme of n-3 PUFA research. Specifically, this dissertation addresses that limitation by investigating how a specially formulated fish oil diet disrupts plasma membrane lateral organization and immunological function of B cells.

n-3 PUFAs and the immune system

n-3 PUFAs have been extensively studied with regards to targeting immune cell function (53). Although there are many differential findings, common themes are that n-3 PUFAs, specifically EPA/DHA, are immune system regulators. They assist in resolution of inflammation and act as immunosuppressants by regulating immune cell function (2, 54, 55). The immune system, however, is layered in complexity, and n-3 PUFAs are thought to play a role in modifying many of its components. Immune cells are produced in bone marrow from multipotent progenitor cells, or hematopoietic stem cells, and migrate to the thymus, spleen, and lymph nodes, as well as many other organs. Multipotent hematopoietic stem cells further differentiate into either lymphoid progenitor or myeloid progenitor cells (56). Lymphoid progenitor cells will become B and T lymphocytes or natural killer cells (56). Myeloid progenitor cells develop to become monocytes, macrophages, basophils, neutrophils, erythrocytes, mast cells, and dendritic cells (56). These cell types make up the major cells of the immune system. The immune system can be broken down into two primary types of immune responses, which are the

innate response and the adaptive response.

Innate function is evolutionarily conserved and is the first line of defense against invading pathogens and other infectious agents. Inflammation plays a critical role in this process as a protective response to an injury or infection. The vascular and immune systems work together to respond to invasion of pathogens, irritants, or damaged cells by increasing blood flow and cell permeability to the affected area (57). Inflammation can be characterized as either acute or chronic. Resolving acute inflammation promptly is critical for overall health, as chronic inflammation is associated with a variety of diseases such as atherosclerosis, rheumatoid arthritis, metabolic syndrome, and some types of cancer (58). Cytokine release by damaged cells recruits immune cells. Phagocytic immune cells, such as macrophages, dendritic cells, and neutrophils, are recruited to the area to engulf and eliminate pathogens that could cause further infection. Some pathogens are recognized by pattern recognition receptors such as the Toll-like receptors (TLRs) (59). Phagocytized foreign pathogens are degraded, processed and various proteins are presented to cells of the adaptive immune system. This is a critical link between the two types of immune responses (60).

The adaptive immune response can also be broken down into two parts: humoral and cellular. Humoral immunity is mediated primarily by B cell antibody secretion. Cell-mediated immunity involves T cells activated by antigen presenting cells (APCs). The primary APCs are dendritic cells, but B cells and macrophages can also serve this function. Cell-mediated immunity involves direct contact through immunological synapses, described in detail below. Unlike the innate immune system, the adaptive immune system is designed to protect against many foreign contagions, and not just

specific evolutionarily conserved patterns. However, the two types of immune responses often work together to clear pathogens and maintain health.

A number of studies have shown that n-3 PUFAs can be immunosuppressive by inhibiting proliferation of lymphocytes in both rodents and humans (24, 61-64). However, in some studies with human patients, conjugated linoleic acid was found to have limited results (65, 66). There is also evidence that cytokine secretion can be inhibited by n-3 PUFA dietary supplementation. For example, secretion of pro-inflammatory cytokines IL (interleukin)-6 and TNF (Tumor necrosis factor)-α by macrophages was inhibited in rats (67). In dendritic cells, TNF-α and IL-12 cytokine secretion was diminished by n-3 PUFAs (68). n-3 PUFAs have also been shown to suppress APCs ability to present antigen (69, 70). In addition, they have been shown to inhibit $CD4^+$ T cell signaling and function (71, 72). Other studies suggest that the response between cell types may not be universally suppressive (73). However, B cells are a cell type poorly represented in the field of n-3 PUFA research. Therefore, a major focus of this work is on how n-3 PUFAs modify B cell function.

B cells

B cells are continually generated throughout the lifespan of most mammals. In the fetus, B cells differentiate in the liver. After birth, B cell generation moves to the bone marrow where they must undergo a differentiation and maturation process before becoming functioning members of the immune system (74). B cells leave the bone marrow and migrate through the periphery and into the lymphoid tissues of the lymph nodes and spleen. Currently there are ten known B cell–specific cell surface markers that have been identified: CD19, CD20, CD21, CD22, CD23, CD24, CD40, CD72, and

CD79a,b (75). The two major mature B cell subtypes are B-1 and B-2. B-1 cells are self-renewing and long-lived. They are crucial for innate immune function in defense against encapsulated bacterial infections (76, 77). B-1 cells produce natural antibodies, which are secreted before an infection occurs. B-2 cells are the major adaptive immune response B cell type. There are two major splenic subpopulations, marginal zone and follicular cells. Marginal zone B cells mature from transitional type 1 and transitional type 2 precursors (78, 79) Marginal zone B cells are non-circulating and are also critical for defense against blood-borne encapsulated bacterial pathogens (79). Upon encountering an antigen, naïve mature follicular B cells process and present that antigen to cognate helper T cells in the periphery of a lymphoid follicle. The activated B cells become short-lived antibody secreting plasma cells, or migrate to a germinal center to rapidly proliferate and differentiate. In the germinal center, antibody affinity is refined through a process known as affinity maturation (80). The differentiated B cells then become long-lasting memory B cells that can rapidly proliferate and differentiate into plasma cells upon a second encounter with the same antigen (81).

While the primary role of B cells is antibody production, they are also recognized as important APCs for the initiation of immune responses (82-85). B cell MHC class II antigen presentation is critical for many autoimmune diseases like rheumatoid arthritis, lupus, allograft rejection, and chronic allergic lung disease (86-89). Suppression of B cell antigen presentation is a potential target for treatment of these disorders. For example, rituximab, a chimeric monoclonal antibody against CD20, suppresses B cell antigen presentation, which has some clinical benefits, especially in rheumatoid arthritis (90-93). B cells can also play a role in cytokine production, tumor immunity, cell

regulation, antiviral immunity, and wound healing (75, 94).

Potential mechanisms for n-3 PUFAs

Consumption of n-3 PUFAs can affect nearly every cell in the body. In doing so, there are a variety of mechanisms that n-3 PUFAs can target. They can directly bind to receptors and modify gene regulation. For instance, n-3 PUFAs have been shown to bind peroxisome proliferator-activated receptors (PPARs) and liver x receptors (95, 96). In addition, there has been a recent discovery of a specific n-3 PUFA receptor, the G-protein coupled receptor (GPR) 120 (97, 98). These studies with knockout mice demonstrated that GPR120 signaling plays a major role in obesity, inflammation, insulin resistance, and other symptoms of metabolic syndrome.

n-3 and n-6 PUFAs also serve as precursors for pro- and anti-inflammatory metabolites. The discovery of these metabolites has established that the resolution of inflammation is not a passive process, but requires a variety of metabolites to activate inflammatory pathways, followed by further synthesis of pro-resolving mediators to resolve the inflammation once the process is complete (99-101). These pro-inflammatory molecules are primarily the n-6 PUFA arachidonic acid (AA) derived eicosanoids, made up of leukotrienes, prostaglandins, thromboxanes, and prostacyclins. However, EPA competes for enzyme activity with AA, limiting the AA production pathway and promoting alternative EPA derived eicosanoid production (102). The eicosanoids derived from EPA have weaker pro-inflammatory bioactivity than AA derived products (103). EPA and DHA also serve as precursors for the potent inflammation-resolving molecules known as E or D series resolvins, protectins/ neuroprotectins and, more recently, maresins. (104). After an inflammatory response,

these resolvins/protectins promote resolution of inflammation through removal of leukocytes (104).

n-3 PUFAs also have unique structural properties. They can be esterified at the sn-2 position of phospholipids. As a phospholipid constituent, it has been shown that DHA can cause significant alteration to fluidity and permeability, as well as surrounding membrane protein function (105). Molecular dynamic simulations have shown that DHA acyl chains have an unusually high degree of conformational flexibility in membranes compared to other acyl chains (106). It is therefore proposed that DHA modifies plasma membrane order by disrupting hydrogen bonding between surrounding acyl chains and cholesterol (105). This results in an incompatibility between the rigid structure of cholesterol and DHA. In addition, DHA is thought to form DHA rich domains that are segregated from cholesterol rich membrane domains (107). These cholesterol rich membrane domains, known as lipid rafts, have critical functions for many cellular processes. Defining how dietary n-3 PUFAs disrupt lateral organization of lipid rafts in B cells is one of the primary aims for this dissertation.

Lipid rafts

Our understanding of the complexities of the plasma membrane has advanced greatly since the establishment of the fluid mosaic model in the 1970‘s by Singer and Nicolson (108). We now have evidence for non-random associations of proteins and lipids in functional membrane domains of various sizes and functions (109). Lipid rafts are membrane domains of recent importance (110). Highly ordered in nature, they are defined as sphingolipid and cholesterol-rich domains. They are heterogeneous in composition but small in size, roughly 10 - 200 nm in diameter (111). Functionally, lipid

rafts are thought to compartmentalize important cell signaling events by serving as platforms for protein clustering (110, 112, 113).

Despite extensive characterization of lipid raft components and properties, there remains controversy associated with the existence of *in vivo* lipid raft domains (114, 115). Much of this controversy lies in the methods used to isolate or image these membrane domains (116-118). Many of the early studies relied on insolubility in mild detergent followed by density centrifugation, but this method is now highly debated because of the potential for artifacts (119). Furthermore, detergent methods homogenize lipid raft components and give no information about how they were distributed in an intact plasma membrane.

Progress in fluorescence microscopy has allowed for limited visualization of these elusive domains by fluorescently tagging raft-associated proteins identified by the detergent extraction studies (120, 121). One such raft constituent, the ganglioside GM-1, binds the non-lethal subunit of cholera toxin (CTx-B) and is commonly used for imaging lipid rafts (122). This protein is readily available as a kit, with a variety of fluorescent proteins. The CTx-B proteins are then cross-linked by antibodies to aggregate larger lipid raft clusters that are now visible on the micron scale. However, a limitation to this application is that the CTx-B/antibody kit induces raft formation, and the natural *in vivo* state may not be represented by this method. Other studies use quantitative microscopy techniques such as Förster resonance energy transfer (FRET) to obtain nanoscale spatial information about components of rafts, and attempt to visualize these domains with minimal disruption. FRET can detect changes in protein distribution less than 10 nm apart, the size scale in which lipid raft protein clustering

occurs. FRET measures non-radiative energy transfer from a donor fluorophore on one protein to that of an acceptor on another closeby protein (117). One such study found evidence for highly dynamic nanoclusters of GPI-linked proteins using FRET (123). Further advances in super resolution microscopy like stimulated emission depletion (STED), stochastic optical reconstruction microscopy (STORM), and fluorescence photoactivation localization microscopy (fPALM) have revealed dynamic nanoscale lipodomains in living cells (124). Recently, advanced single-molecule fluorescent tracking methods were used to study the lateral organization of glycosylphosphatidylinositol-anchored (GPI) proteins in rafts (125). Suzuki et al. found homodimer formation of GPI proteins may be a critical mechanism for raft assembly (125). Further advances in studying lipid rafts will enhance understanding of numerous cellular processes because of the diversity of signaling pathways that utilize lipid rafts.

As mentioned above, DHA has a low affinity for cholesterol due to steric incompatibility (126). This property makes DHA, and likewise other n-3 PUFAs, a potential disrupter of lipid rafts. Subsequently it has been shown that n-3 PUFAs do affect cell signaling by altering lipid raft domains (127-129). However, most n-3 PUFAs actually end up in non-raft domains. Therefore, there are also implications to protein organization in non-raft domains (130). This dissertation further investigates the mechanism of how dietary n-3 PUFAs disrupt plasma membrane lateral organization in B cells.

The immunological synapse

In APCs such as B cells, direct cell-cell communication and subsequent activation can occur through contact between complementary regions of the plasma

membrane on B and T cells. This contact region is defined as the immunological synapse, and its formation is thought to be dependent on lipid rafts (131). APCs use major histocompatibility complex (MHC) proteins on the plasma membrane surface to present antigens to T cells. The antigen-loaded complex is recognized and bound by the T cell receptor (TCR). This contact, along with a host of other proteins, constitutes the immunological synapse. The immunological synapse can be further defined as a supramolecular activation cluster (SMAC), which consists of central, peripheral, and distal regions. The complex is actively assembled and matures over time (132). Initially, MHC class II, found on B cells, is bound to TCR and gradually clustered to the central SMAC (c-SMAC), along with other proteins such as protein kinase Cθ (PKCθ), CD2, CD4, CD8, CD28, Lck, and Fyn (132). Cytoskeletal elements such as talin and actin surround this central region in the peripheral SMAC (p-SMAC), driving other proteins toward the c-SMAC (133). The functional anatomy of some of the elements involved in this contact region is depicted in Figure 1.2.

At high antigen levels synapse formation initiates very quickly and maturation occurs over as much as 6 hours (134). First the APC and T cell scan the surface to find complementary TCR and MHC class II molecules, respectively. In order to check antigen specificity, T cells also undergo a form of kinetic proofreading, similar to mechanisms in DNA synthesis (135). During this process, phosphorylation events pause signal transduction after antigen recognition to discriminate self and foreign antigens (135). This greatly enhances the receptor's ability to discriminate between a foreign antigen and self-antigens and ensures incorrect signals are not processed. When antigen levels are low or TCR affinity to antigen is low, many TCRs are triggered

Figure 1.2

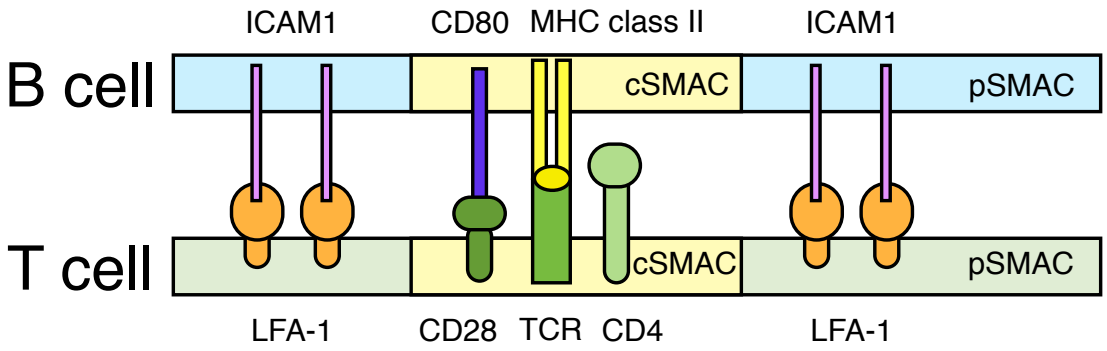

Figure 1.2: The B-T cell immunological synapse. Shown in blue (top) is the B side of the immunological synapse. In green (bottom) is the T cell side. B proteins MHC class II and CD80, as well as T cell proteins TCR, CD28, and CD4 cluster in the cSMAC shown in yellow. Adhesion molecules, ICAM1 and LFA-1, cluster in the pSMAC, which surrounds the cSMAC.

sequentially through a process called serial triggering to resolve the lower affinity (136). Once the antigen is recognized and verified, calcium signaling and synapse assembly begins immediately. After initial APC contact with a T cell, signaling can begin at as early as 45 seconds. However, full maturation and T cell activation requires SMAC formation (137). As the synapse matures over the course of 5-60 minutes, SMAC formation and segregation occurs. Some evidence shows that although dendritic cells are professional APCs, full synapse maturation does not occur in these cells (138). Finally, after a few hours when signaling is complete, the TCR internalizes and the synapse is dissolved.

The immunological synapse is a potential target for n-3 PUFAs as a mechanism for their immunosuppressive properties (71, 139). Dietary n-3 PUFAs are known to suppress recruitment of PKCθ, as well as other structural proteins, to the site of the immunological synapse in $CD4^+$ T cells by increasing lipid raft formation (140). Dietary n-3 PUFAs also limit mitochondrial translocation to the immunological synapse in T cells, an early step in T cell activation (141). Additionally, studies in other immune cell types yield similar lipid raft disruption and impaired function (142, 143). Much less is known, however, about B cells. B cells have a critical function in antibody production, but, like dendritic cells, they also are involved in activating T cells through the immunological synapse. Therefore, the goal of this dissertation is to describe how EPA and/or DHA can target lipid rafts in B cells, thereby disrupting antigen presentation.

Specific aims

n-3 PUFAs are the primary bioactive components of fish oil. Consumption of fish oil can elicit immunosuppressive effects, as well as many other potential health benefits. However, a limitation in the clinical utility of n-3 PUFAs is the lack of understanding of

how they exert their effects. To address this limitation, we investigated a potential mechanism for how n-3 PUFAs suppress B cell immune function. The central hypothesis was that n-3 PUFAs disrupt lipid rafts, as well as the direct contact of plasma membrane regions between B cells and T cells in the immunological synapse, thereby suppressing B cell function. This study serves to aid in potential treatment for chronic inflammatory and autoimmune disorders where immunosuppression of B cell antigen presentation by n-3 PUFAs would be beneficial (86-89). To address the central hypothesis, the specific aims are:

Aim 1: Test the hypothesis that dietary n-3 PUFAs disrupt B cell lipid raft organization and function.

Proteins important for B cell function localize to lipid rafts where they can cluster for signal transduction. Disruption of protein and lipid lateral organization in lipid rafts could lead to modification of B cell function. To investigate the hypothesis that dietary n-3 PUFAs disrupt lipid raft organization, we first identified how n-3 PUFAs incorporate into the plasma membrane. We then determined the types of phospholipids into which dietary n-3 PUFAs incorporate. Using various fluorescent probes, we determined how high and low fat n-3 PUFA diets modified raft and non-raft biophysical properties. Finally, we measured the effect of fish oil on micron and nanoscale clustering of lipid raft localized functional proteins vital to immunological synapse formation.

Aim 2: Test the hypothesis that n-3 PUFA diet modified B cells diminish stable immunological synapse formation.

The immunological synapse is structurally organized into cSMAC- and pSMAC-containing antigen receptors and adhesion molecules. Disruption of this structure in T

cells by n-3 PUFAs has been shown. Here we tested the functional consequences of dietary modifications on B cell plasma membranes by n-3 PUFAs. In doing so, we tested the hypothesis that B cells from n-3 PUFA fed mice would inhibit the formation of the immunological synapse, and therefore suppress T cell activation. We first measured the effect n-3 PUFAs have on the kinetics of initial immunological synapse or conjugate formation. We then directly imaged the immunological synapse using confocal microscopy to determine how n-3 PUFA dietary modification of B cells modified lateral organization of key T cell proteins. Finally, we determined the functional outcomes of dietary B cell modification on $CD4^+$ T cell activation efficiency.

Taken together, this study defines a mechanism through which n-3 PUFAs modify B cell function and regulate immunological synapse formation. In addition, we characterized various n-3 PUFA rich diets and some of the metabolic implications of consuming very high doses of these unique fatty acids. We also further established that relevant dietary doses of fish oil can modify lipid raft organization in B cells as well as immunological synapse formation. This study will aid in the clinical application of n-3 PUFAs as immunosuppressants.

CHAPTER 2: MEMBRANE RAFT ORGANIZATION IS MORE SENSITIVE TO DISRUPTION BY N-3 PUFA THAN NONRAFT ORGANIZATION IN EL4 AND B CELLS[1]

Introduction

EPA and DHA, the bioactive n-3 PUFA of fish oil, are increasingly available and consumed by the general public as over-the-counter supplements (43, 144). Clinically, EPA and DHA have applications for the prevention and/or treatment of some metabolic diseases (50, 145-147); in addition, they have potential utility for treating the symptoms associated with inflammatory and autoimmune disorders (2, 54, 148). However, one major limitation of further developing these fatty acids for clinical use is an incomplete understanding of their targets and molecular mechanisms.

An emerging mechanism of the action of n-3 PUFA, due to their unique molecular structure, is modification of plasma membrane lipid rafts (149), which are sphingolipid-cholesterol enriched domains that compartmentalize signaling proteins (124). We recently discovered an n-3 PUFA disrupted lipid raft clustering of EL4 cells (150). The data raised a new question, i.e. could n-3 PUFA also disrupt the organization of nonraft domains. These membrane domains are broadly defined as those regions that are not enriched in sphingolipids and cholesterol that also compartmentalize specific proteins (e.g. MHC class I, TLR4, etc.) (151). There were 2 reasons to hypothesize n-3 PUFA would disrupt nonraft organization. First, experiments using model membranes demonstrated DHA acyl chains, due to their structural incompatibility with cholesterol, primarily incorporated into nonrafts to enhance nonraft formation (130, 152, 153).

[1]This research was originally published in The Journal of Nutrition. Rockett, B. D., Franklin, A., Harris, M., Teague, H., Rockett, A., & Shaikh, S. R. Membrane raft organization is more sensitive to disruption by (n-3) PUFA than nonraft organization in EL4 and B Cells. *J Nutr*. 2011; 141:1041–1048. © the American Society for Nutrition.

Second, biochemical detergent extraction studies showed a large fraction (up to 70%) of EPA and DHA localized into nonrafts (150, 154-156). Thus, these studies suggest that a major role of n-3 PUFA acyl chains is to modify nonraft domain organization.

The first objective of this study was to extend our previous work by determining if EPA and DHA treatment disrupted nonraft organization of EL4 cells. The second objective was to translate the findings on EL4 cells by testing the impact of dietary n-3 PUFA on both nonraft and lipid raft organization in an animal model. To address our objectives, we relied on quantitative imaging methods of confocal and FRET microscopy. Application of these methods to the study of n-3 PUFA and membrane domains advances the field by overcoming the use of cold detergent extraction as a primary method of studying how n-3 PUFA modify membrane domains. Although detergent resistance has great predictive value, the detergent can induce artifacts (157-159). Furthermore, the biochemical detergent method does not report on the effects of n-3 PUFA on the appropriate length scales on which membrane domains form (124). Therefore, we used more appropriate imaging methods to address the effects of n-3 PUFA on membrane domain organization.

Materials and Methods

Cells

EL4 cells were maintained in RPMI 1640–1× (Mediatech) with 10% heat-inactivated defined FBS (Hyclone), 2 mmol/L L-glutamine (Mediatech), and 1% penicillin/streptomycin (Mediatech) at 37°C in a 5% CO_2 incubator. The lipid composition of the FBS was as previously reported (150).

Fatty acid treatment

A total of 9–10 × 10^5 EL4 cells was treated for 15.5 h with 25 μmol/L FFA (free fatty acid, Nu-Check Prep) complexed to fatty acid-free BSA (Bovine serum albumin, Roche Biochemicals) in serum-free medium as previously described (150). For select experiments, EL4 cells were treated in the presence of 10% FBS. The rationale for selecting the fatty acid concentration and time of treatment was to be consistent with our previous study on EL4 cells and membrane domains (150). Oleic (OA) and AA were tested to rule out general effects of fatty acid treatment and to ensure specificity of EPA and DHA.

Mice, diets, and B cell isolation

Male C57BL/6 mice (Charles River), aged 4–6 wk (~18 g), were fed the following diets (Harlan-Teklad) for 3 wk: a purified control diet (CD) (5% fat wt:wt), a n-6 PUFA diet (20% fat wt:wt), a low-fat (LF) n-3 PUFA diet (5% fat wt:wt), or a high fat (HF) n-3 PUFA diet (20% fat wt:wt) (Table 2.1) (160, 161). For the CD and LF n-3 PUFA diets, ~13% of the total energy was from fat. For the HF n-6 and n-3 PUFA diets, ~41% of the total energy was from fat. For the LF n-3 PUFA diet, 3.3% of the total energy was from α-linolenic acid, 1% from EPA, and 0.6% from DHA (160). For the HF n-3 PUFA diet, 10.5% of the total energy was from α-linolenic acid, 3% from EPA, and 2% from DHA (160). The diets were analyzed for their fatty acid composition (Supplemental Table 2.1). For B cell isolation, mice were killed using CO_2 inhalation after 3 wk of feeding. Naïve $B220^+$ B cells (>90% purity) from splenocytes were purified with negative selection (Miltenyi Biotec) as previously described (160). All experiments with mice fulfilled guidelines established by the East Carolina University for euthanasia and humane treatment.

Table 2.1: Composition of experimental diets

Ingredients (g/kg)	CD	HF (n-6) PUFA	LF (n-3) PUFA	HF (n-3) PUFA
Casein	185.0	220.0	185.0	220.0
L-Cystine	2.5	3.0	2.5	3.0
Corn starch	370.0	173.9	370.0	173.9
Maltodextrin	140.0	140.0	140.0	140.0
Sucrose	150.0	150.0	150.0	150.0
Cellulose (fiber)	50.0	50.0	50.0	50.0
Flaxseed oil	0.0	0.0	23.1	92.5
Fish oil (Menhaden)	0.0	0.0	23.1	92.5
Soybean oil	50.0	30.0	3.75	15.0
Safflower oil	0.0	125.0	0.0	0.0
Hydrogenated coconut oil	0.0	45.0	0.0	0.0
Mineral mix, AIN-93M[2]	35.0	42.0	35.0	42.0
Vitamin mix, AIN-93[2]	15.0	18.0	15.0	18.0
Choline bitartate	2.5	3.0	2.5	3.0
TBHQ	0.02	0.06	0.02	0.06

C57BL/6 mice were fed for 3 weeks CD, HF (n-6) PUFA, LF and HF (n-3) PUFA diets.

Composition of mineral and vitamin formulas are as reported in (161).

Fatty acid analysis

For analysis of diets, ~0.01–0.05 g of the diet pellets was homogenized using a Dounce homogenizer prior to extraction. Total lipids were extracted and analyzed relative to standards (Restek) from the differing cell types or diets with gas chromatography (GC) using our previously published protocol (150, 160). Areas of identified peaks were summed and each peak area is expressed as the percentage of total peak area for a given treatment (150, 160).

Column chromatography

To assess incorporation of EPA and DHA into neutral lipid, FFA, and polar lipid fractions, 2×10^6 EL4 cells were treated with fatty acids spiked with 185 kBq [^{14}C]EPA or [^{14}C]DHA (American Radiolabeled Chemicals). Extracted lipids were separated into different lipid classes using aminopropyl beads (Sigma) loaded in a Pasteur pipette with a fiberglass plug and elution with HPLC-grade organic solvents (Fisher Scientific) as previously described (160, 162).

Staining and imaging with 1,19-dilinoleyl-3,3,39,39-tetramethylin-docarbocyanine perchlorate and 4,4-difluoro-5,7-dimethyl-4-bora-3a,4a-diaza-s-indacene-3-hexadecanoic acid

A total of 2×10^6 cells was washed twice with cold PBS, stained with 0.66 mg/L of the nonraft probe 1,1′-dilinoleyl-3,3,3′,3′-tetramethylindocarbocyanine perchlorate (FAST-DiI; Invitrogen) or 4,4-difluoro-5,7-dimethyl-4-bora-3a,4a-diaza-s-indacene-3-hexadecanoic acid (C16-Bodipy; Invitrogen) for 5 min on ice followed by 2 washes with cold PBS (163, 164). Cells were fixed in 4% paraformaldehyde (Fisher Scientific) for 1 h, washed twice, placed in Vitrotubes (Fiber Optic Center), and mounted onto slides

with nail polish. All imaging studies, described below, relied on a Zeiss LSM510 confocal microscope using a 100× oil objective. Pinhole, detector gain, and laser settings were kept constant between samples for a given experiment. For some experiments, images were acquired as z-stacks.

Sample preparation for FRET microscopy

MHC class I molecules were used as the probe to measure nanometer scale molecular proximity, because these molecules are localized to nonrafts and are established to serve as excellent reporters for measuring changes in membrane organization (165-167). Cells were stained with varying concentrations of Cy3 (donor) and Cy5 (acceptor) separately labeled M1/42.3.9.8 anti-MHC class I antibodies (BioXCell). Fluorophores were conjugated to the antibody using a standard fluorophore conjugation kit (GE Healthcare). Specificity of the antibody was confirmed by using isotype controls (BioXCell) (150). Total antibody levels were held constant at 0.02 mg/ sample using unlabeled antibody as donor:acceptor ratios were varied from 1:1, 1:2, and 1:3 in 1×10^{-4} L PBS (168, 169). Cells were stained for 15 min on ice, washed twice with PBS, fixed, washed, and mounted to slides as described above. A positive control M1/42.3.9.8 antibody was generated by simultaneously conjugating Cy3 and Cy5 fluorophores, yielding a dual labeled antibody to ensure high FRET. Negative control samples were labeled with donor fluorophore only to check for donor channel bleaching during acceptor fluorophore bleaching and acceptor fluorophore only to optimize bleaching time.

FRET microscopy

FRET was measured in terms of the efficiency of energy transfer (E) from donor

(Cy3) to acceptor (Cy5) fluorophores separated by distance r, given by the following equation: $E = 1/\{1 + (r/Ro)^6\}$, where Ro is the Förster radius of the donor and acceptor fluorophore pairs and is 54 Å for Cy3/Cy5 (170, 171). The filter sets were 560- to 615-nm band pass for Cy3, and 650-nm long pass for Cy5 in 2 separate tracks. Excitation relied on 543- and 633-nm lasers, respectively, for Cy3 and Cy5. Eight-bit 512 × 512 pixel images were acquired. Acceptor photobleaching was carried out by iterative scanning of the 633-nm laser for ~2 min. Gain settings were optimized to ensure images were not saturated after photobleaching.

Lipid raft staining

B cells were labeled with cholera toxin subunit B-FITC (Invitrogen) for cross-linking lipid rafts and imaged as previously described (150).

Image analysis

All images were analyzed with NIH ImageJ. Approximately 20–33 cells per treatment per experiment were analyzed as previously described (150). For FAST-DiI and C16-Bodipy studies, differential interference contrast images were routinely used to confirm plasma membrane compared with intracellular staining. For image intensity analysis, images were background subtracted and manually thresholded for regions of interest either inside the cell or on the plasma membrane. The approach was confirmed by selecting several regions of interest manually drawn on the cell surface and inside the cell. Cells were also scored as high intensity if they were in the top one-third of the distribution of fluorescence intensities.

FRET images were analyzed with FRETcalc v3.0 plug-in for NIH ImageJ (172). Some cells could not be properly registered and were not included in the analysis.

Images were registered by manual translation or rotation. All images were background subtracted and smoothed using a 3 × 3 filter. The threshold values for the donor and acceptor images were determined manually. This was required to calculate FRET efficiency of the entire cell by the FRETcalc plug-in (172).

Images of lipid rafts were background subtracted and raft size was determined in terms of Feret diameter using NIH ImageJ as previously described (150).

Cell growth and apoptosis measurements

Cell growth was determined by counting cells in duplicate or triplicate using a hemacytometer. Dead cells were excluded with Trypan blue (HyClone, Fisher Scientific) staining. Measurements were routinely confirmed by a second person using blinded samples. We verified that this approach gave the same results as a cell proliferation testing kit (GenScript). The advantage of counting cells over the kit was the absolute number of cells could be determined rather than relative changes. Cell survival was measured in terms of Annexin V-Cy5/Sytox Blue (BD Pharmingen) staining with a BD LSR II flow cytometer as previously described (160).

Statistical analysis

Reported values are means ± SEM from several independent experiments. For animal studies, independent experiments were conducted using 1 mouse from each diet group. All statistical analyses were conducted using Excel and GraphPad Prism (GraphPad Software). Parametric statistics were used, because the data were normally distributed. Unequal variances were tested for prior to ANOVA using a Levene's test. For FRET studies, efficiency values varied between experiments due to variation in the fluorophore to antibody ratios; thus, significance was established against the control

using repeated-measures 1-way ANOVA followed by a Dunnett's t test. For cell growth and apoptosis measurements as a function of time, 2-way ANOVA analysis was used followed by a Bonferroni t test. The 2-way ANOVA used treatment and time as factors and there was no interaction effect. For all other studies, significance was established against the control using a 1-way ANOVA followed by a Dunnett's t test. P-values < 0.05 were considered significant.

Results

EPA and DHA treatment disrupted nonraft organization of EL4 cells

EPA and DHA treatment of EL4 cells increased accumulation of the nonraft probe FAST-DiI in the plasma membrane by ~50–70% relative to the BSA control (Figure 2.1A,B). The OA and AA treatments did not significantly increase FAST-DiI uptake compared with BSA (Figure 2.1B). The intensity of FAST-DiI inside of the cell was not changed by treatment with any of the fatty acids (Figure 2.1B). The increase in FAST-DiI plasma membrane binding with EPA and DHA was also confirmed by scoring the cells for intensity. EPA and DHA treatment resulted in the largest percentage of cells with a high intensity of plasma membrane staining compared with BSA (Figure 2.1C).

A major concern was that the EPA and DHA treatment exerted a general effect on fluorescent probe uptake. Therefore, we tested the effects of fatty acid treatment on the uptake of a nonspecific probe, C16-Bodipy (173). C16-Bodipy did not merely report on the same subcellular organization as FAST-DiI. Colocalization analysis of z-stacks of EL4 cells costained with FAST-DiI and C16-Bodipy showed the percent colocalization between the 2 probes was ~32%, as measured by Mander's coefficients (Supplemental Figure 2.1A) (150). Relative to BSA, EPA and DHA treatment did not promote uptake of

Figure 2.1

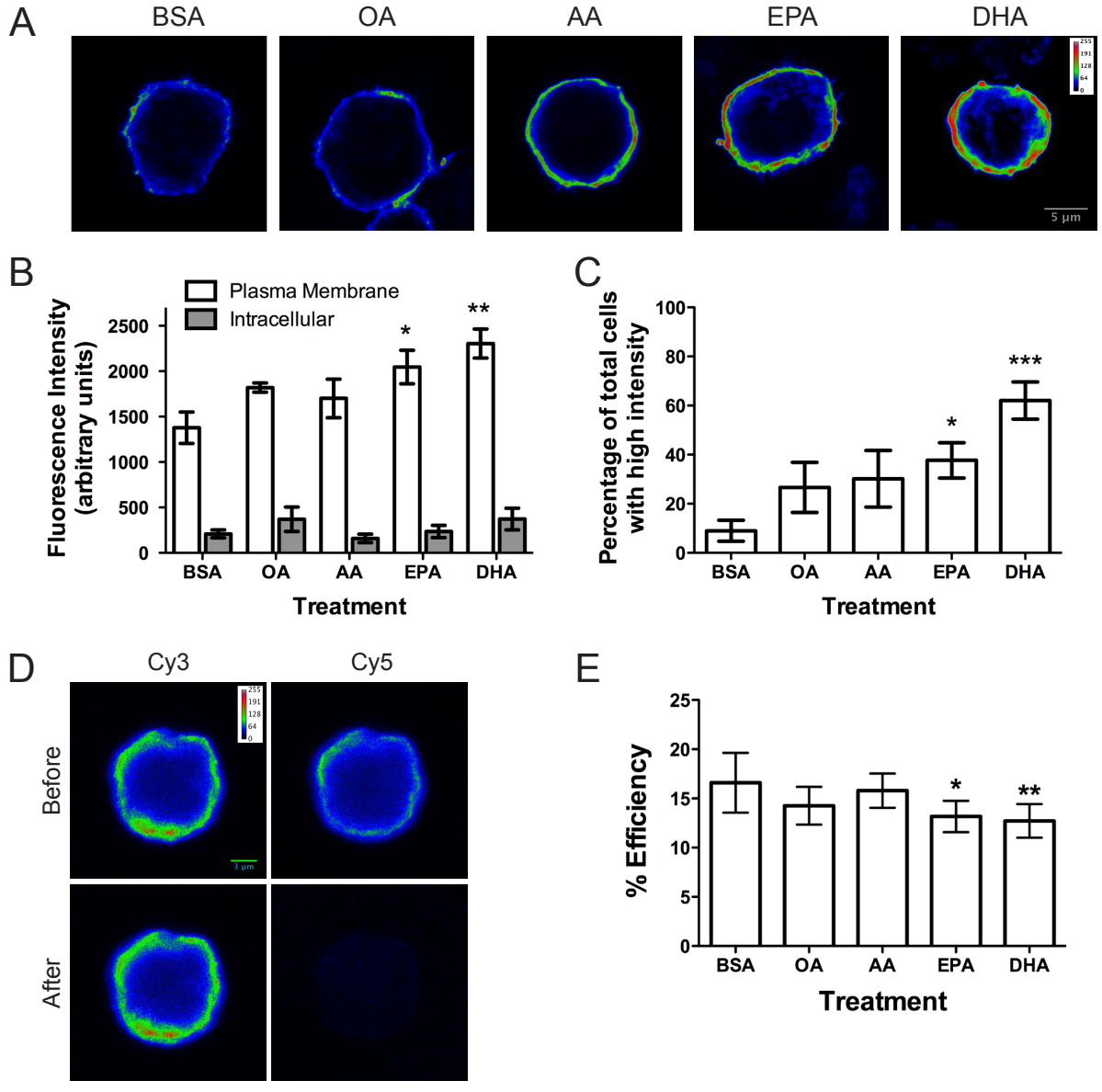
A
BSA
OA
AA
EPA
DHA
5 µm
B
Plasma Membrane
Intracellular
Fluorescence Intensity (arbitrary units)
2500
2000
1500
1000
500
0
*
**
BSA
OA
AA
EPA
DHA
Treatment
C
Percentage of total cells with high intensity
100
80
60
40
20
0
*
***
BSA
OA
AA
EPA
DHA
Treatment
D
Cy3
Cy5
Before
After
3 µm
E
% Efficiency
25
20
15
10
5
0
*
**
BSA
OA
AA
EPA
DHA
Treatment

Figure 2.1: EPA and DHA treatment disrupted nonraft organization of EL4 cells. (A) Fluorescence images of EL4 cells treated with BSA, OA, AA, EPA, or DHA and stained with FAST-DiI. (B) FAST-DiI intracellular and plasma membrane image intensity. (C) Percentage of cells with high FAST-DiI intensity as a function of treatment. (D) Sample images of BSA-treated cells from acceptor photobleaching FRET. (E) FRET efficiency values for treated EL4 cells. Images are on a rainbow palette to discriminate differences in relative fluorescence intensity. Red and blue values indicate high and low intensity, respectively. Data are means ± SEM, n = 3–4. Data in E are from 60-90 total cells analyzed. Asterisks indicate different from BSA: *$P < 0.05$, **$P < 0.01$, ***$P < 0.001$. Data in A-B were collected by Franklin, A.

C16-Bodipy into the plasma membrane or inside the cell (Supplemental Figure 2.1B). OA and AA treatments also had no effect.

We also determined if EPA and DHA treatment modified nonraft organization on a nanometer scale using FRET microscopy. Positive control experiments showed the acceptor photobleaching approach with Cy3 and Cy5 antibodies increased FRET (Supplemental Figure 2.2A). The distribution of MHC class I molecules on the surface of EL4 cells was then determined as random, clustered, or a mixture of random and clustered by increasing the donor:acceptor fluorophore ratios. FRET efficiency did not increase with increasing donor:acceptor ratios (Supplemental Figure 2.2B), which is the signature pattern of a random distribution of molecules (168, 169). This allowed us to combine FRET acceptor:donor ratios in the subsequent analyses.

Analysis of FRET efficiency values from FRET images (Figure 2.1D) in every single experiment showed EPA and DHA treatment consistently decreased FRET by 25–30% relative to the BSA control (Figure 2.1E). OA and AA treatments did not lower FRET relative to BSA. The most plausible explanation for an increase in the distance between neighboring MHC I molecules with n-3 PUFA was an increase in cell size, which was investigated next.

EPA and DHA treatment increased cell size and growth

Cell size was measured in terms of forward scatter with flow cytometry (Figure 2.2A). EPA and DHA treatment increased cell size by ~26% relative to BSA after 15.5 h of treatment. OA and AA treatment had no effect. A similar trend was confirmed with microscopy measurements (data not shown). EPA and DHA, in addition to AA, treatment also increased side scatter relative to BSA (data not shown).

Figure 2.2

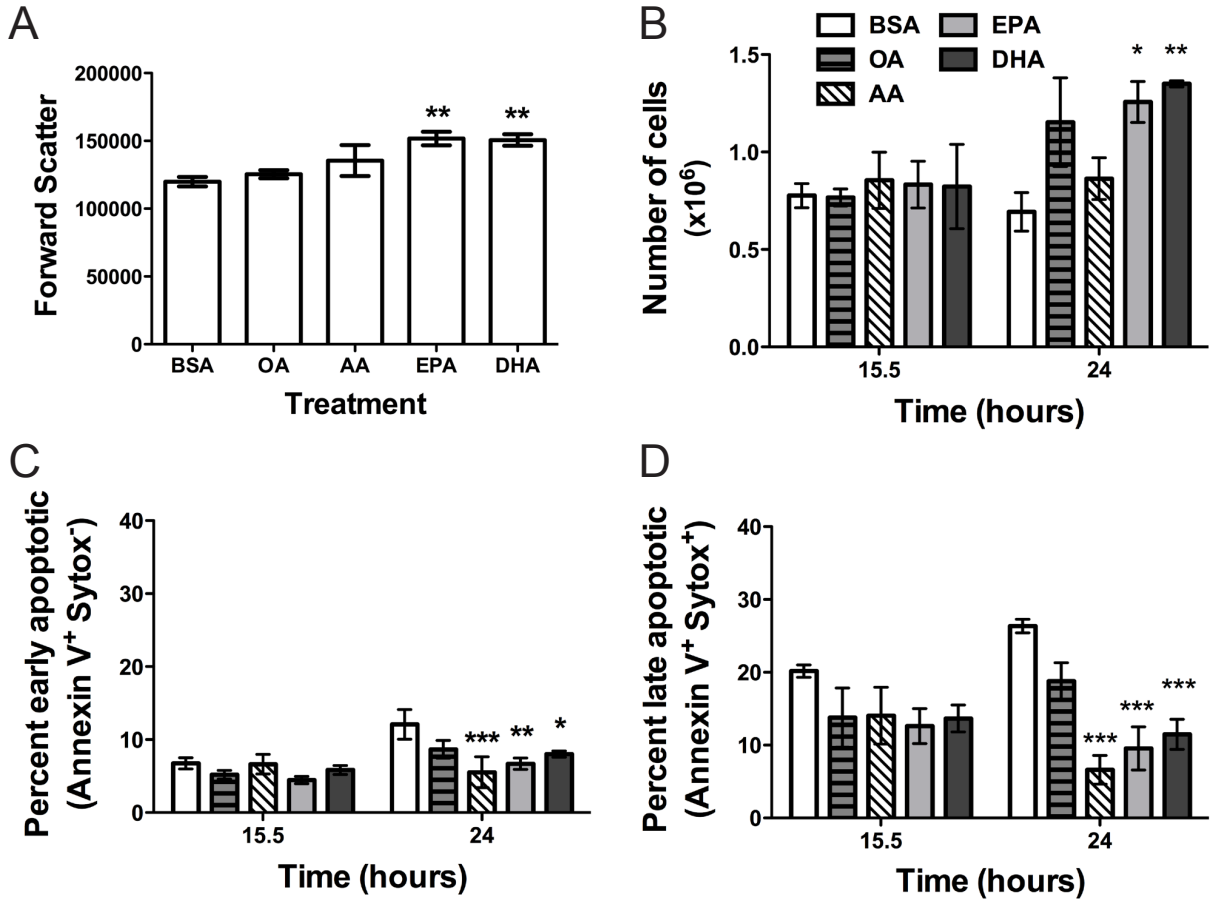

Figure 2.2: EPA and DHA treatment increased EL4 cell size and growth and prevented cell death. (A) Median forward scatter values for EL4 cells treated with BSA, OA, AA, EPA, or DHA. (B) Cell growth, (C) early apoptosis, and (D) late apoptosis as a function of time for the different treatment groups. Data are means 6 SEM, n = 4. Asterisks indicate different from BSA: *P < 0.05, **P < 0.01, ***P < 0.001.

The subsequent experiment tested if the increase in cell size related to a change in cell growth (Figure 2.2B). At 15.5 h of treatment, cell number between the BSA control and the differing fatty acids did not differ. After 24 h, EPA and DHA treatment increased the number of viable cells. In contrast, OA and AA treatment did not increase cell growth compared with BSA. We then tested if the increased ability to grow was driven by an ability to prevent cell death. At 15.5 h of treatment, the cells were equally viable when measured for early and late apoptosis (Figure 2.2C,D) (150). After 24 h of treatment, all 3 PUFA (AA, EPA, and DHA) prevented early and late apoptosis relative to the BSA control (Figure 2.2C,D). OA treatment had no effect relative to BSA. EPA and DHA treatment did not modify nonraft organization when cell size was unchanged.

We determined if preventing the expansion of cell size prevented changes in nonraft organization. Treatment conditions were first optimized to prevent an increase in cell size but still allowed for efficient uptake of the fatty acids. Cells were treated in the presence of 10% FBS, which significantly elevated EPA and DHA levels (Figure 2.3A). Uptake of EPA and DHA into polar lipids did not change relative to treatment in serum free conditions, as measured with radiolabeled fatty acids (Figure 2.3B). Forward scatter values did not differ between EPA and DHA treatment compared with the BSA control (data not shown). Image analysis of cells stained with FAST-DiI (Figure 2.3C) showed no change in fluorescence intensity with EPA- or DHA-treated cells relative to BSA. Similarly, subsequent FRET imaging showed treatment of EL4 cells with n-3 PUFA did not lower FRET relative to BSA. FRET efficiency values were ~10% for BSA-, EPA-, and DHA-treated cells.

Figure 2.3

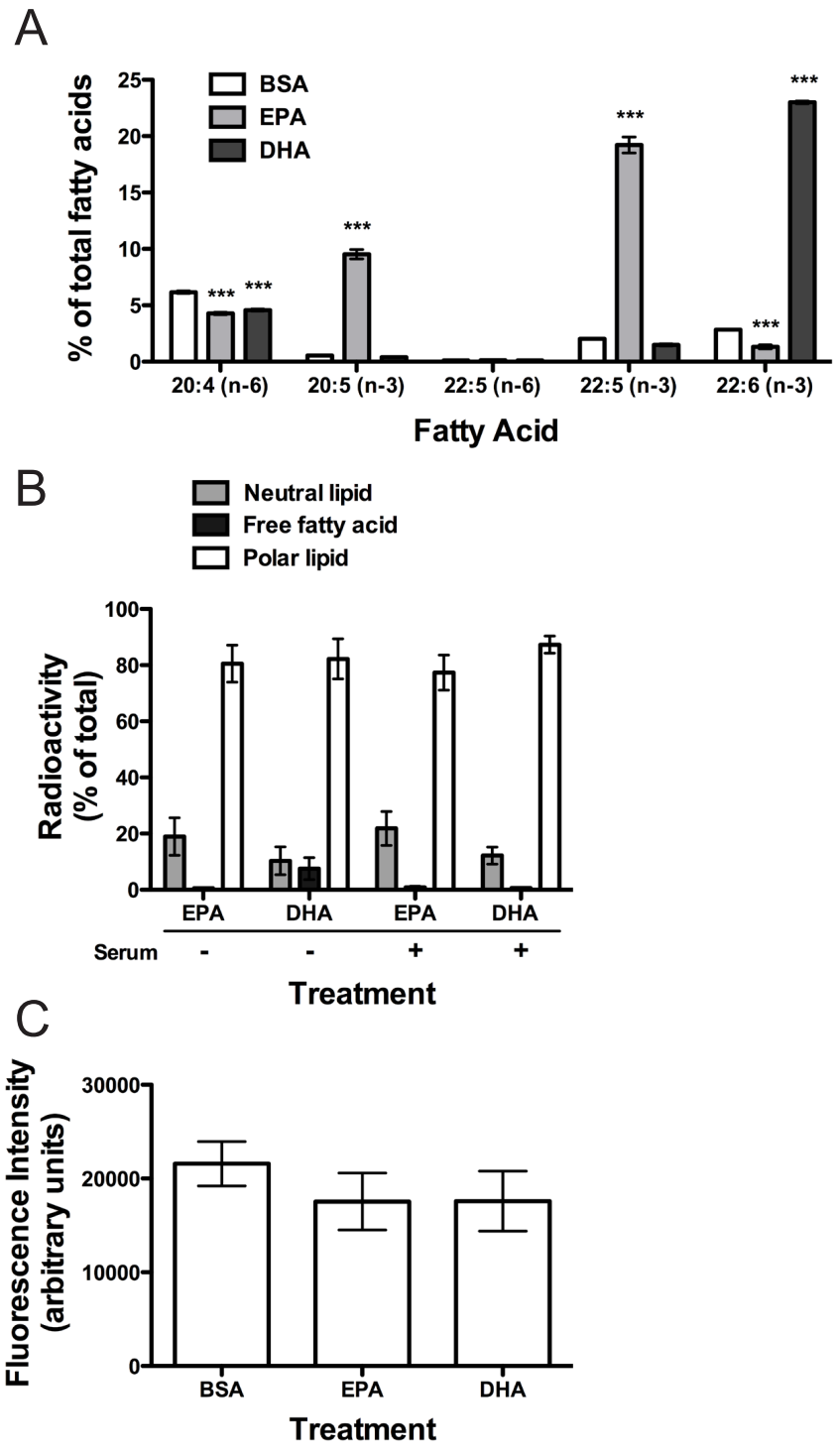
A
% of total fatty acids
25
20
15
10
5
0
BSA
EPA
DHA
***
***
***
***
***
20:4 (n-6)
20:5 (n-3)
22:5 (n-6)
22:5 (n-3)
22:6 (n-3)
Fatty Acid
B
Neutral lipid
Free fatty acid
Polar lipid
Radioactivity (% of total)
100
80
60
40
20
0
EPA
DHA
EPA
DHA
Serum
-
-
+
+
Treatment
C
Fluorescence Intensity (arbitrary units)
30000
20000
10000
0
BSA
EPA
DHA
Treatment

Figure 2.3: EPA and DHA treatment had no effect on nonraft organization when cell size was unchanged. (A) Total levels of 20:4, 20:5, 22:5, and 22:6 upon treatment of EL4 cells with BSA, EPA, or DHA in serum-containing medium. (B) Incorporation of radiolabeled EPA and DHA into neutral lipids, FFA, and polar lipid fractions in serum-free and serum-containing medium. (C) FAST-DiI intensity of EL4 cells treated with BSA, EPA, or DHA in serum-containing medium. Data are means ± SEM, n = 3. Asterisks indicate different from BSA: ***$P < 0.001$. Data in B were collected by Shaikh, S. R. and Harris, M.

In vivo administration of n-3 PUFA did not modify nonraft organization but disrupted lipid raft clustering

Body weights of C57BL/6 mice fed the HF (n-6), LF n-3, and HF n-3 PUFA diets did not differ from the CD group after 3 wk (~22 ± 0.3 g). Energy intakes also did not differ between these groups and the CD group (11.4 ± 0.1 kcal/d). GC measurements confirmed uptake of fatty acids from the diet into B cells (Table 2.2). Cell size did not differ between the B cells from the CD group and those from the other groups (data not shown).

Relative to CD, the HF (n-6), LF n-3, and HF n-3 PUFA diets did not increase FAST-DiI uptake into B cells (Figure 2.4A). Unexpectedly, the HF n-3 PUFA diet decreased plasma membrane and intracellular uptake of C16-Bodipy by ~33% (Figure 2.4B). The LF n-3 and HF n-6 PUFA diets did not affect C16-Bodipy binding. Sample images of FAST-DiI and C16-Bodipy staining are presented in Supplemental Figure 2.3. To verify the conclusion that n-3 PUFA did not disrupt nonrafts, MHC I FRET experiments were conducted with the HF n-3 PUFA diet, because it lowered C16-Bodipy uptake. FRET imaging showed nearly identical FRET efficiency values (~12%) for B cells isolated from the CD and HF n-3 PUFA diet-fed mice.

Finally, we investigated if the HF n-3 PUFA diet disrupted B cell lipid raft organization. Microscopy images showed the HF n-3 PUFA diet decreased the clustering of lipid rafts (Supplemental Figure 2.4) and increased the Feret diameter of the domains by ~40% (Figure 2.4C) compared with CD. In contrast, the HF n-6 and LF n-3 PUFA diets, relative to CD, did not affect lipid raft organization.

In this study, we addressed if n-3 PUFA disrupted nonraft organization of EL4

Table 2.2: Fatty acid analysis of B cells isolated from mice fed differing diets

Fatty Acid	CD	HF (n-6) PUFA	LF (n-3) PUFA	HF (n-3) PUFA
14:0	0.9 ± 0.2	0.7 ± 0.1	0.6 ± 0.2	0.8 ± 0.1
16:0	24.9 ± 1.7	23.1 ± 2.0	25.8 ± 0.8	24.6 ± 0.5
16:1	0.8 ± 0.2	0.5 ± 0.1	1.0 ± 0.2	1.1 ± 0.1
18:0	16.5 ± 1.2	18.5 ± 2.3	18.5 ± 4.0	19.4 ± 2.8
18:1 *trans*	0.7 ± 0.2	0.9 ± 0.6	0.9 ± 0.4	0.5 ± 0.2
18:1 *cis*	14.2 ± 2.4	9.7 ± 0.6	13.2 ± 0.6	12.4 ± 0.6
18:1 (n-7)	1.9 ± 0.5	0.8 ± 0.2	1.7 ± 0.1	1.7 ± 0.1
18:2 (n-6)	17.6 ± 1.6	16.5 ± 1.3	17.1 ± 2.0	18.5 ± 1.0
18:3 (n-6)	0.5 ± 0.3	1.7 ± 0.7	3.6 ± 0.8**	1.6 ± 0.6
18:3 (n-3)	1.6 ± 0.2	1.1 ± 0.1	1.7 ± 0.2	2.3 ± 0.3
20:1	1.1 ± 0.4	1.4 ± 0.4	0.4 ± 0.1	0.7 ± 0.2
20:2 (n-6)	1.4 ± 0.7	1.6 ± 0.7	0.5 ± 0.3	0.7 ± 0.5
20:3 (n-6)	3.5 ± 1.6	0.5 ± 0.2	0.9 ± 0.3	1.0 ± 0.3
20:3 (n-3)	1.1 ± 0.5	1.4 ± 0.2	0.7 ± 0.2	0.8 ± 0.3
20:4 (n-6)	5.1 ± 1.6	3.5 ± 2.0	3.2 ± 0.4	2.4 ± 0.7
20:5 (n-3)	0.2 ± 0.0	0.4 ± 0.1	2.0 ± 0.2*	3.8 ± 0.6***
22:2 (n-6)	1.2 ± 0.4	0.4 ± 0.2	0.1 ± 0.0*	0.4 ± 0.1
22:4 (n-6)	1.2 ± 0.2	1.1 ± 0.4	0.5 ± 0.0*	0.5 ± 0.1*
22:5 (n-6)	0.3 ± 0.1	2.3 ± 1.7	0.3 ± 0.1	0.4 ± 0.1
22:5 (n-3)	1.0 ± 0.4	1.2 ± 0.1	2.7 ± 0.7	2.4 ± 0.4
22:6 (n-3)	1.7 ± 0.4	1.5 ± 0.3	3.0 ± 0.4	3.5 ± 0.6*
24:1	0.9 ± 0.2	0.2 ± 0.1*	0.4 ± 0.0	0.4 ± 0.1
∑SFA	44.6 ± 2.3	46.2 ± 5.2	45.6± 4.5	45.8 ± 2.4
∑MUFA	19.8 ± 3.2	13.6 ± 1.3	17.8 ± 0.6	16.9 ± 0.5
∑PUFA (n-6)	30.6 ± 2.5	26.3 ± 3.9	26.5 ± 3.1	25.6 ± 2.0
∑PUFA (n-3)	5.0 ± 0.7	4.3 ± 0.7	10.1 ± 0.9**	11.7 ± 0.8***
∑PUFA	35.6 ± 3.0	30.7 ± 4.6	36.6 ± 4.0	37.3 ± 2.0
n-6/n-3	6.6 ± 1.0	6.1 ± 0.2	2.6 ± 0.1**	2.2 ± 0.2***

Values (% of total) are mean ± SEM, n=4-5. Values below 0.5 are not shown for clarity.

Asterisks indicate different from CD, *P<0.05, **P<0.01, ***P<0.001.

Figure 2.4

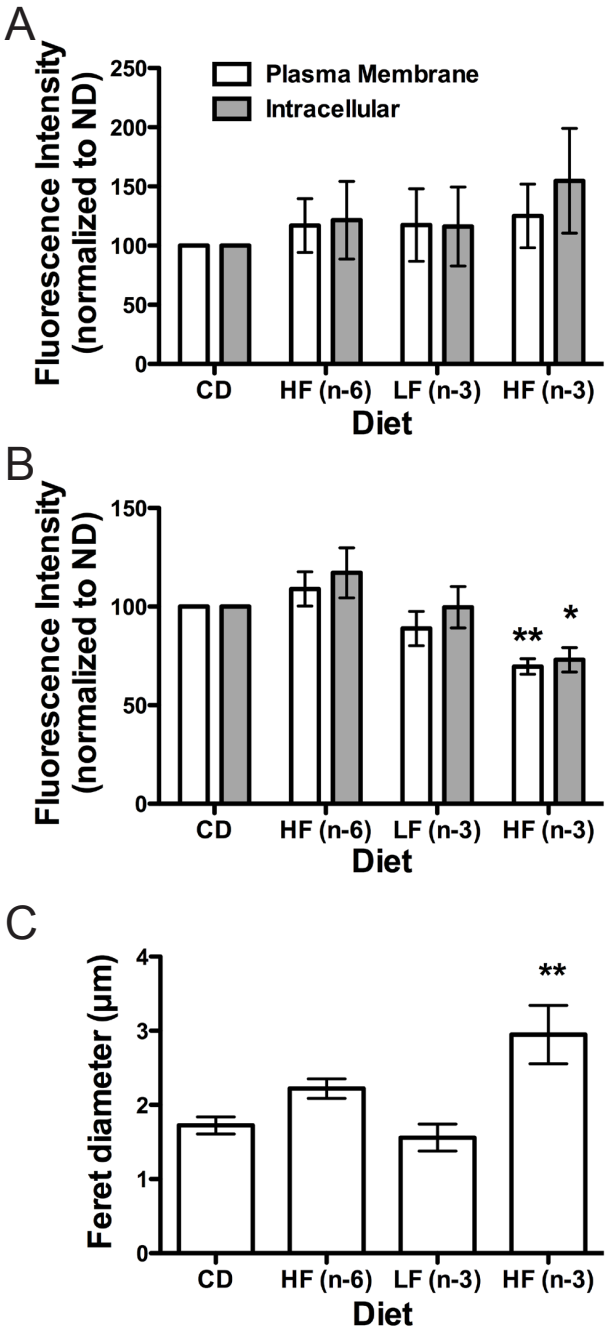
A
Fluorescence Intensity (normalized to ND)
Plasma Membrane
Intracellular
250
200
150
100
50
0
CD
HF (n-6)
LF (n-3)
HF (n-3)
Diet
B
Fluorescence Intensity (normalized to ND)
150
100
50
0
**
*
CD
HF (n-6)
LF (n-3)
HF (n-3)
Diet
C
Feret diameter (µm)
4
3
2
1
0
**
CD
HF (n-6)
LF (n-3)
HF (n-3)
Diet

Figure 2.4: (n-3) PUFA diets did not modify nonraft organization, but the HF (n-3) PUFA diet disrupted lipid raft clustering. (A) FAST-DiI intracellular and plasma membrane image intensity of B cells isolated from mice fed CD, HF (n-6), LF (n-3), and HF (n-3) PUFA diets. (B) C16-Bodipy intracellular and plasma membrane image intensity. Fluorescent values in A and B are normalized to CD, because gain settings were not the same between differing sets of experiments. (C) Feret diameter of lipid rafts. Data are means ± SEM, n = 3–5. Data in C are from 48-143 total cells analyzed per diet. Asterisks indicate different from CD: *$P < 0.05$, **$P < 0.01$. Data in A-B were collected by Franklin, A.

cells followed by translational studies that determined the impact of n-3 PUFA on nonraft and lipid raft organization ex vivo. The approach relied on quantitative imaging methods to overcome limitations of using detergent extraction (157, 158). As discussed below, the data point to an emerging model in which lipid rafts appears more sensitive to disruption than nonrafts in response to n-3 PUFA intervention in EL4 and primary B cells.

Disruption of nonraft organization in vitro

In serum free conditions, EPA and DHA treatment modified nonraft organization of EL4 cells. There were several possibilities by which EPA or DHA treatment increased FAST-DiI in the plasma membrane. One possibility was uptake of FAST-DiI with n-3 PUFA represented EPA- and/or DHA-rich domains (130, 151). Alternatively, increased FAST-DiI accumulation with EPA or DHA represented a dissolving of rafts. Thus, the area of nonrafts could have increased upon treatment, but these nonrafts were not organizationally distinct domains. To address these 2 possibilities, specific fluorescent probes will have to be designed, synthesized, and extensively tested in the future.

Some other interpretations of the results with FAST-DiI staining were ruled out. One possibility was BSA, OA, and AA treatment made FAST-DiI staining of the membrane less efficient than EPA or DHA. This was highly unlikely, because we observed similar uptake of C16-Bodipy for most of the treatments. A second possibility was EPA and DHA decreased the microviscosity of the membrane, which allowed for more uptake of the probe (105). Although this was possible, one would then have expected increased internalization of the probe with EPA or DHA treatment compared with BSA; furthermore, increased uptake of C16-Bodipy would have occurred.

The FRET data with EL4 cells revealed EPA and DHA could modify membrane organization on a nanometer scale. To the best of our knowledge, this was the first study to use FRET imaging to study nanometer scale organization of n-3 PUFA in a cellular system. The data highlight the use of this methodology to determine effects of n-3 PUFA on the appropriate size scale. The FRET studies showed EPA and DHA increased the distance between randomly distributed nonraft MHC class I molecules. The increase in cell size with EPA or DHA treatment did not maintain the relative density of MHC class I surface molecules compared with the BSA control. We previously reported MHC I surface levels on EL4 cells increased by ~30–35% with EPA or DHA treatment (150). Here, we found cell size increased by ~26–30% with EPA or DHA. Given that forward scatter roughly reports on the diameter of the cell and if we assume the cell is a sphere, a ~30% increase in diameter of the cell with EPA and DHA treatment should increase surface area by ~60%. Thus, MHC I surface expression should have increased >30–35% with EPA or DHA treatment to maintain the same density of molecules as the BSA-treated cells. Therefore, as cell size increased, MHC I molecules were pushed further apart.

Nonraft organization was not disrupted by n-3 PUFA in vitro or ex vivo when cell size was unaffected

Mechanistically, we speculate an increase in cell size with EPA and DHA treatment under serum free conditions caused a redistribution in the lateral organization of lipids and proteins. The increase in cell size appeared to be related to the ability of EPA and DHA to promote cell growth and prevent cell death. The growth data were consistent with previous studies that showed EPA and DHA enhanced cell growth in

some cell types (174, 175). Although the numbers of EL4 cells were equivalent across the treatment groups at 15.5 h (time point at which studies were conducted), by 24 h, there were differences in cell number. Therefore, the data suggest cells treated with EPA or DHA at 15.5 h grew in size at a faster rate than the BSA-treated cells and were likely poised to divide. It has been reported with primary cells that cell size, measured with forward scatter, increased as cells started to divide, because a homogenous population of cells can have varying thresholds for entry into the cell cycle (176).

The ex vivo data also showed n-3 PUFA administered to mice at 2 different doses had no effect on nonraft organization. The ex vivo data were consistent with the in vitro studies in which EPA and DHA did not affect cell size but inconsistent with the in vitro studies in which cell size increased. Several possibilities, which may not be mutually exclusive, could explain the discrepancy. First, there was the obvious difference in cell size, as discussed above. Second, n-3 PUFA in vitro were administered as single fatty acids, whereas the diet provided a complex mixture of differing fatty acids. Third, B cells from the mice incorporated much lower levels of n-3 PUFA compared with EL4 cells. However, in vivo levels were more physiologically relevant than those administered in vitro. Indeed, 2 independent imaging experiments showed treatment of EL4 cells in serum free conditions with a lower dose (10 μmol/L EPA or DHA) did not affect FAST-DiI uptake relative to BSA (data not shown). Overall, the in vitro studies using serum free conditions suggest the changes in nonraft organization had limited physiological relevance. Of course, our studies do not rule out the possibility that nonraft organization could be disrupted with n-3 PUFA in other cell types.

Lipid raft clustering was sensitive to n-3 PUFA

Unexpectedly, the HF n-3 PUFA diet lowered uptake of C16-Bodipy in B cells. It was unlikely the lowered uptake was due to a modification in nonraft organization, because we measured no change in FAST-DiI intensity or FRET. One possibility could be that as n-3 PUFA increased raft size, it made the membrane more ordered, which prevented uptake of C16-Bodipy. Overall, it was unclear why this probe was not efficiently recruited into the cell, which we aim to investigate in the future. Nevertheless, the HF n-3 PUFA diet disrupted lipid raft organization, which was highly consistent with our previous data with EL4 cells in which DHA diminished raft clustering (150). The data were also consistent with several studies using in vitro or fat-1 transgenic mouse model systems that showed n-3 PUFA disrupted lipid raft molecular organization (128, 140, 155, 177-179). Specifically, the ex vivo data from this study agreed with an electron microscopy study that demonstrated treatment of HeLa cells with DHA had a more robust effect on cholesterol-dependent raft domains compared with cholesterol-independent nonraft domains of the inner plasma membrane leaflet (180).

The discovery that the HF n-3 PUFA diet made rafts appear larger was the first visual evidence of n-3 PUFA dietary intervention having an effect on lipid rafts in an animal model. Note that although we interpret the rafts to be larger in size, it is possible that they could represent rafts that are much smaller in size but only seem larger due to increased levels of GM1. Future studies will have to address whether the disruption in raft organization represents the formation of highly ordered raft domains or many small raft domains. We also propose lipid raft clustering was diminished, because it was reported that cholera toxin binds more efficiently to GM1 raft molecules when they are

declustered (181). Surprisingly, the LF n-3 PUFA diet did not exert an effect on raft organization. Thus, the levels of n-3 PUFA in this diet may not have been high enough to modify lipid rafts. Future studies will have to determine at what dose n-3 PUFA serve to disrupt rafts.

Implications

Although numerous studies have established that n-3 PUFA modify the global membrane parameter of microviscosity (105), the specific effects of n-3 PUFA on membrane domain organization have generally remained elusive. We show n-3 PUFA specifically target the organization of lipid rafts more than nonrafts, which has relevance toward understanding how these fatty acids disrupt downstream intracellular signaling events or cell-cell communication. The data from this study have implications for several model systems. We present 2 examples for simplicity. A recent study demonstrated DHA treatment prevented dimerization and recruitment of the Toll-like Receptor 4 into lipid rafts (182). Our data suggest DHA could prevent recruitment of the protein into lipid rafts from nonrafts as a consequence of the disruption in the spatial distribution of rafts (which may be occurring on several length scales). As another example, it was proposed that suppression of MDA-MB-231 breast cancer migration with n-3 PUFA was due to an inability of the chemokine receptor CXCR4 to cluster, but the mechanism was not investigated (183). We propose a disruption in lipid rafts could prevent CXCR4 clustering and one approach would be to measure CXCR4 clustering with FRET imaging on a nanometer scale.

In summary, data from EL4 and primary B cells suggest lipid rafts are far more sensitive to disruption in response to intervention with n-3 PUFA than nonraft domains.

Future studies will have to address how n-3 PUFA acyl chains initiate a change in the spatial distribution of lipid rafts in the plasma membrane and how this affects protein clustering and ultimately cellular function.

CHAPTER 3: HIGH DOSE OF AN N-3 POLYUNSATURATED FATTY ACID DIET LOWERS ACTIVITY OF C57BL/6 MICE[2]

Introduction

n-3 PUFAs, the bioactive components of fish and flaxseed oil, are routinely consumed by the public as food additives or supplements. They are also recognized to have utility for treating metabolic and inflammatory diseases (2, 50, 51, 144, 146). Generally, dietary studies evaluating n-3 PUFA efficacy in differing model systems have relied on low doses of n-3 PUFAs. With animal studies, investigators have commonly used ~5% (weight/weight) fish or flaxseed oil as intervention, corresponding to approximately 2–6% of total energy as n-3 PUFAs (52). This dose, especially of fish oil, is often selected to model n-3 PUFA intake of Greenland Eskimos that consume n-3 PUFAs in the range of 1–6% of total energy (4, 5). A few studies have tested the effects of fish or flaxseed oils at higher doses with mixed results on functional endpoints (184-186). Overall, very little is known about the effects of high doses of n-3 PUFAs, which could have a unique therapeutic niche or could exert negative side effects, raising potential safety issues for the general public.

We previously reported long-term administration of high levels of a mixed fish/ flaxseed oil diet to C57BL/6 mice promoted significant body weight gain (160). These findings suggested high doses of n-3 PUFAs increased body weight by lowering activity since we ruled out changes in food consumption (160). Therefore, the objective of this study was to determine if short-term dietary consumption of a high dose of n-3 PUFAs

[2]This research was originally published in Prostaglandins, Leukotrienes, and Essential Fatty Acids. Rockett, B. D., M. Harris, & S. R. Shaikh. 2012. High dose of an n-3 polyunsaturated fatty acid diet lowers activity of C57BL/6 mice. Prostaglandins Leukot. Essent. Fatty Acids. 86: 137–140. © Elsevier Ltd.

could lower energy expenditure prior to any large differences in body weight. Studies were conducted in comparison to a LF purified mouse CD and a LF n-3 PUFA diet.

Experimental methods

Mice and diets

All experiments with mice fulfilled guidelines established by the East Carolina University Brody School of Medicine for euthanasia and humane treatment. Male C57BL/6 mice (~4–6 weeks old) were placed for 3 weeks on two experimental diets, developed in collaboration with Harlan-Laboratories (Madison, WI). Mice were administered either a purified CD, 5% fat by weight, a LF n-3 PUFA diet, or a HF n-3 PUFA diet, 20% fat by weight, as previously described (187). The composition of the diets is listed in Table 3.1.

Metabolic cage studies

Mice were placed in fully automated metabolic cages (TSE Systems) for 4 days to monitor activity during week 2. Mice were placed one per cage and were acclimated for 48 h followed by data collection for 48 h. Airflow through the cages was held constant at 0.5 L/min. 12 h light and dark cycles were maintained with ad libitum access to food and water. Locomotor activity in the metabolic cages was measured by the breaking of 32 infrared laser beams that span each cage in the xy and yz planes. TSE LabMaster software recorded in 20 min intervals each time a series of laser beams were broken by ambulatory, rearing, and running wheel activity. Metabolic activity was measured via indirect calorimetry recording maximal O_2 consumption (VO_2) and CO_2 production (VCO_2). VO_2 and VCO_2 values were normalized by the software to body weight in kilograms and are reported as ml/h/kg (188). Respiratory exchange ratio

Table 3.1: Composition of control, low fat, and high fat n-3 PUFA diets

Formula (g/Kg)	CD	LF n-3 PUFA	HF n-3 PUFA
Casein	185	185	220
L-Cystine	2.5	2.5	3.0
Corn Starch	370	370	174
Mineral Mix, AIN-93M-MX (94049)	35	35	42
Vitamin Mix, AIN-93-VX (94047)	15	15	18
Choline Bitartrate	2.5	2.5	3.0
TBHQ, antioxidant	0.02	0.02	0.06
Maltodextrin	140	140	140
Sucrose	150	150	150
Cellulose	50	50	50
Soybean Oil	50	3.8	15
Flaxseed Oil	-	23.1	92.5
Fish Oil	-	23.1	92.5

(RER) was calculated as VCO_2/VO_2. The data were analyzed for average light and dark activity (188). Significance was established using a two-way ANOVA followed by a Bonferroni Multiple Comparison t test using GraphPad Prism (188). P values less than 0.05 were considered significant.

Results

Body weight and food consumption

Mice weighing 16–19 g were placed on diets. Final body weight gain, confirmed with measurements of adipose mass with Echo-MRI, was identical between the CD and the experimental diets (data not shown). Mice on the HF n-3 PUFA diet consumed less food relative to CD; however, there was no difference in the total kcal consumed between the differing diets relative to CD (data not shown).

Metabolic cage studies

The time course of ambulatory, rearing, and running wheel activities are shown in Figure 3.1A–C. These data were used to calculate the average activity for the entire light and dark cycles (Figure 3.1D–F). There was a significant increase in activity during the dark cycle with all of the diets relative to the light cycle for all measurements (Figure 3.1D–F).

There were no statistical differences between the diets during the light cycle. The HF n-3 PUFA diet lowered average dark cycle ambulatory activity by 62% relative to CD (Figure 3.1D). The LF n-3 PUFA diet had no significant effect compared to CD. Rearing activity was significantly lowered with the HF n-3 PUFA diet by 63% compared to CD (Figure 3.1E). The LF n-3 PUFA diets had no effect on rearing activity relative to CD. For the ambulatory and rearing measurements of activity, there were no significant

Figure 3.1

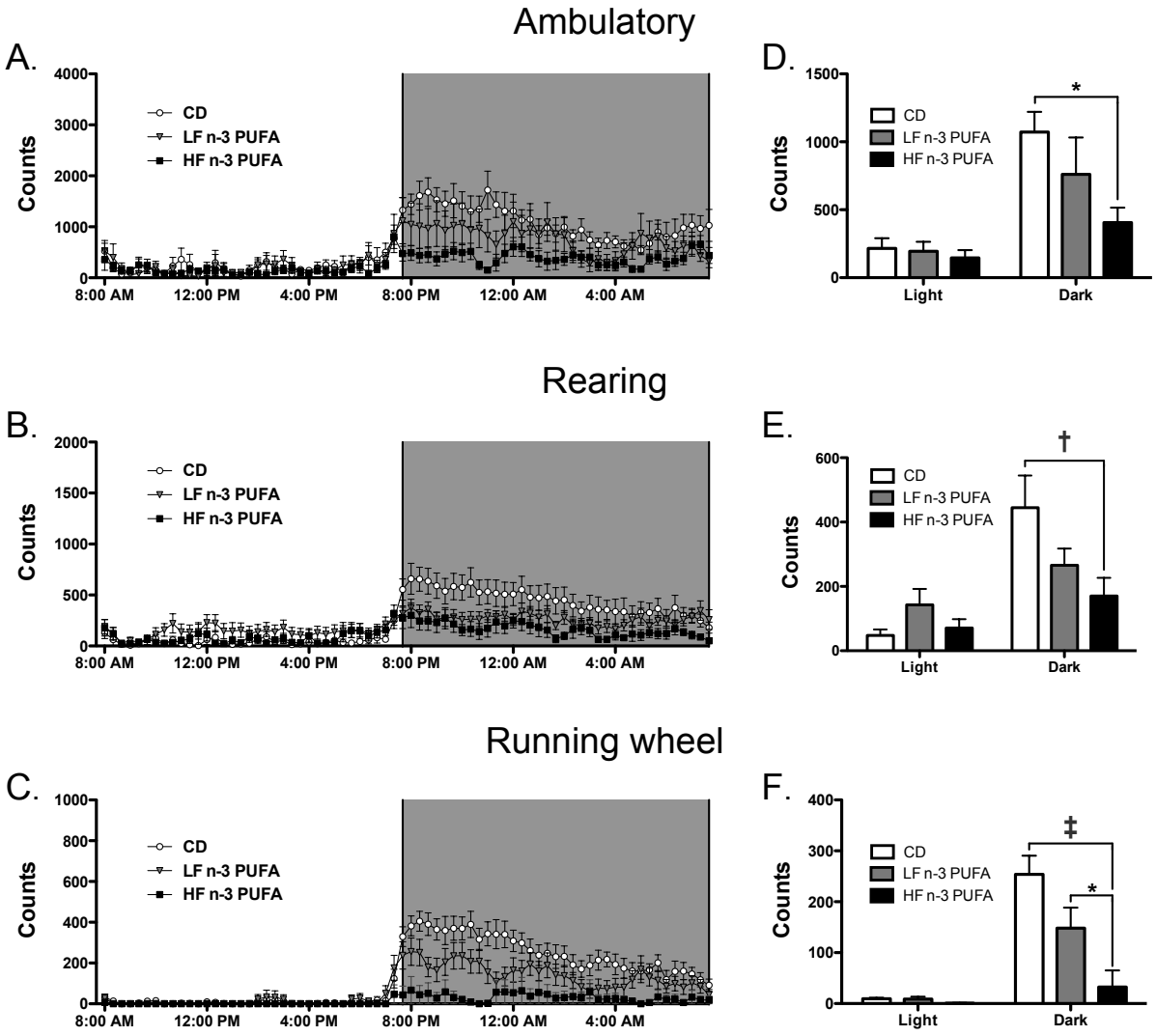

Figure 3.1: HF n-3 PUFA diet lowered activity. (A) Ambulatory, (B) rearing, and (C) running wheel activities as a function of time for mice fed differing diets. Corresponding average light and dark cycle (D) ambulatory, (E) rearing and (F) running wheel activities. Counts represent the number of laser beams broken due to movement in the cage. Data are mean ± SEM, n = 7 mice per diet. Significance during the dark cycle compared to CD is indicated by *$P < 0.05$, †$P < 0.01$, ‡$P < 0.001$.

differences in activity between the LF n-3 PUFA and HF n-3 PUFA diets. Running wheel activity was lowered with the HF n-3 PUFA diet relative to CD by 87%, and 78% relative to the LF n-3 PUFA (Figure 3.1F). The LF n-3 PUFA diet had no effect on running wheel activity relative to CD.

The time course of VO_2, VCO_2, and RER values is shown in Figure 3.2A–C. These data were then used to calculate the average VO_2, VCO_2, and RER for the entire light and dark cycles (Figure 3.2D–F). The average dark cycle VO_2 (Figure 3.2D) and VCO_2 (Figure 3.2E) were significantly higher for all of the diets relative to the light cycle. There were no differences between the diets on VO_2. The HF n-3 PUFA diet lowered dark cycle VCO_2 by 20% relative to CD and LF n-3 PUFA. RER values were significantly different for all of the diets between the light and dark cycles (Figure 3.2F). During the dark cycle, the HF n-3 PUFA had lower RER values relative to CD and LF n-3 PUFA.

Discussion

We present evidence for the first time that a high dose of n-3 PUFAs lowered mouse activity. The reduction in activity with the HF n-3 PUFA diet was consistent with our previous study demonstrating this diet promoted significant body weight gain in mice (160). The LF n-3 PUFA diet also had a tendency to reduce energy expenditure in some of the measurements. This raises the question of whether mixing fish and flaxseed oils has some potential effect that does not promote body weight loss and perhaps even increase body weight gain after long-term feeding due to a reduction in activity. More studies are needed to address this in addition to determining the effects of other fat sources (i.e. hydrogenated oils, coconut oil) on activity. Overall, the reduction in all three measures of activity (ambulatory, rearing, and running wheel) appeared dose

Figure 3.2

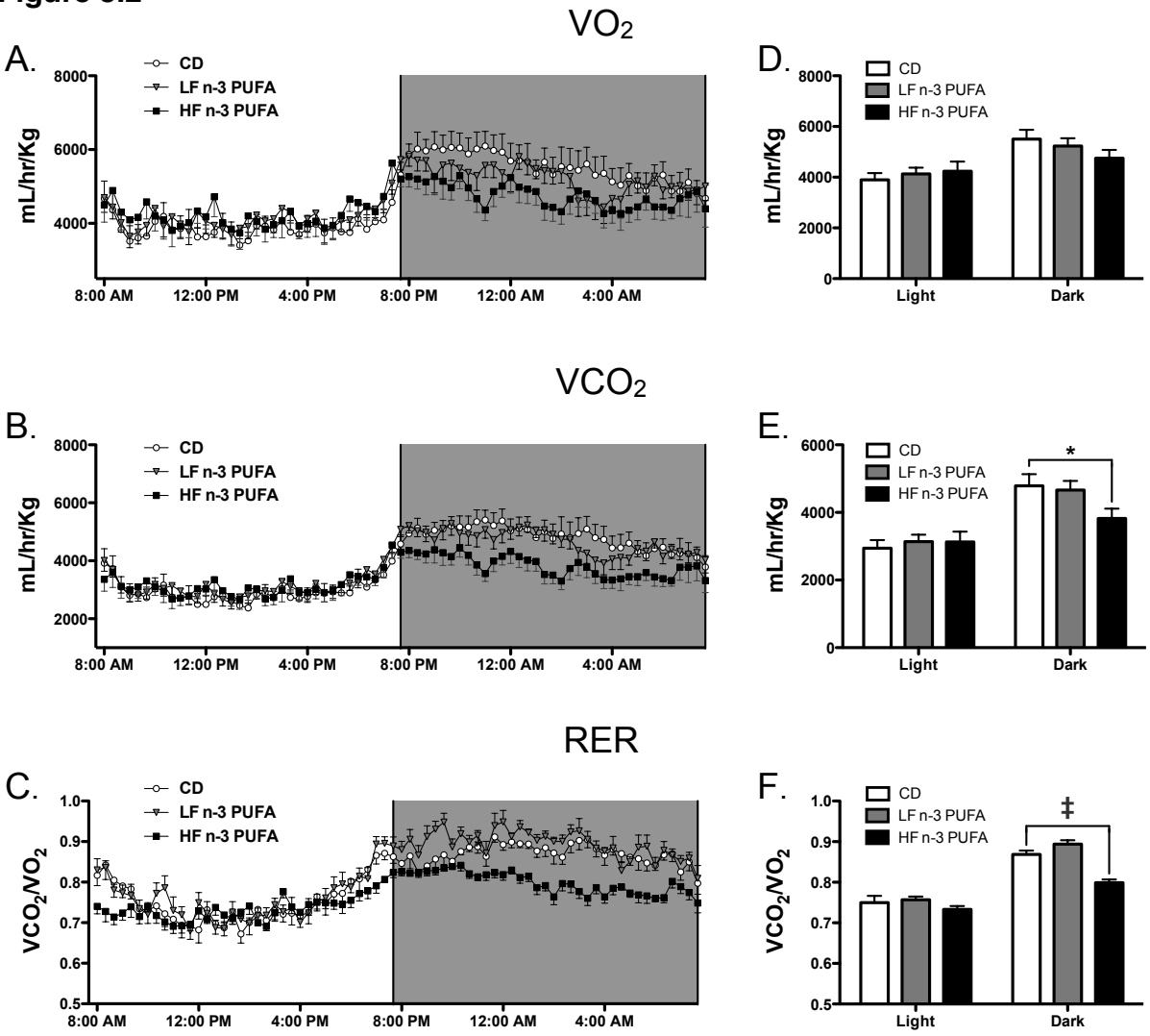

Figure 3.2: HF n-3 PUFA diet lowered VCO_2 and RER. (A) VO_2, (B) VCO_2, and (C) RER as a function of time for mice fed differing diets for 3 weeks. Corresponding average light and dark cycle (D) VO_2, (E) VCO_2, and (F) RER. VO_2 and VCO_2 are mL of gas consumed or expelled per hour normalized to body weight. Data are mean ± SEM, n = 7 mice per diet. Significance during the dark cycle compared to CD is indicated by *$P < 0.05$, ‡$P < 0.001$.

dependent with the n-3 PUFA diets.

It is difficult to directly compare our data to other studies since there are very few studies in this area, which are not in complete agreement. For instance, an EPA enriched oral food supplement provided to advanced pancreatic cancer patients, who are prone to losing weight, enhanced energy expenditure, and provided some improvement in their metabolism (189). However, in another set of studies, supplementing the diet of healthy males with fish or flaxseed oil had no effect on energy expenditure (190, 191). Clearly, more studies are needed in this area with n-3 PUFAs in both animals and humans.

Overall, the potential therapeutic value of high n-3 PUFA doses appears very limited. It is interesting that despite lowering activity, the HF n-3 PUFA diet reduced serum triglycerides (data not shown). Therefore, the data suggest high doses of n-3 PUFAs are effective in their accepted role of lowering triglycerides (TG) even when they lower activity. There are a few cases where an increase in body fat mass due to lower activity could have some value. For instance, HIV positive patients can have elevated TGs and high energy expenditure, yet low body weight, which are in part driven by aggressive anti-viral therapy (192, 193). The elevated TGs are a risk factor for cardiovascular disease, which is prevalent in HIV positive patients (194). Perhaps short-term intervention with a high dose of fish/flaxseed oils would assist in lowering TGs and lowering energy expenditure. Of course, extensive functional and mechanistic studies in animals and eventually humans would be required to address at what specific dose, composition of n-3 PUFAs, and duration could these fatty acids be utilized for these cohorts.

CHAPTER 4: FISH OIL INCREASES RAFT SIZE AND MEMBRANE ORDER OF B CELLS ACCOMPANIED BY DIFFERENTIAL EFFECTS ON FUNCTION[3]

Introduction

Fish oil (FO) enriched in n-3 PUFAs is increasingly hypothesized to have beneficial health effects for treating symptoms for a wide range of diseases associated with chronic inflammation (17, 195, 196). However, several hurdles have prevented the therapeutic use of FO in the clinic, including a limited understanding of the molecular targets and mechanisms of n-3 PUFAs. The proposed mechanisms by which the n-3 PUFAs of FO, EPA and DHA, exert immunosuppressive effects are pleiotropic (197). These include incorporating into membrane phospholipids and modifying plasma membrane microdomain organization, serving as precursors for bioactive lipid molecules, disrupting intracellular signaling, and regulating gene expression (197). Recently, manipulation of lipid raft microdomains with n-3 PUFAs has gained attention because this mode of action is central to many of the downstream effects of n-3 PUFAs (149).

Several models, which are not in complete agreement, have emerged to explain how n-3 PUFAs disrupt raft molecular organization. One model, based on ex vivo studies of the $CD4^+$ T-cell immunological synapse, is that n-3 PUFAs, relative to controls, enhance the formation of more ordered and possibly larger lipid rafts upon stimulation of the cell (140). This model is the most relevant because it relied on the

[3]This research was originally published in The Journal of Lipid Research. Rockett, B. D., H. Teague, M. Harris, M. Melton, J. Williams, S. R. Wassall, & S. R. Shaikh. Fish oil increases raft size and membrane order of B cells accompanied by differential effects on function. *J Lipid Res*. 2012; 53; 674–685.

fat-1 transgenic mouse that has higher endogenous levels of n-3 PUFAs compared with control mice. A second model developed with studies in model membranes is that phosphatidylethanolamines containing DHA largely avoid raft molecules to form their own entities as nonraft domains (198, 199). Finally, a more integrated model, based mostly on in vitro studies, is that n-3 PUFAs incorporate directly into rafts and in some cell types force cholesterol molecules to undergo displacement between rafts and nonrafts (149, 200, 201). Overall, the majority of these models have not relied on physiologically relevant conditions that model human intake of FO.

Based on studies with $CD4^+$ T cells, macrophages, and splenocytes, disruption of rafts with n-3 PUFAs generally suppresses cellular function (140, 142, 143). Far less is known about the relationship between disruption of lipid rafts with n-3 PUFAs and downstream function in other cell types. In particular, B cells are increasingly recognized to have a role in inflammatory processes and autoimmune diseases (202, 203); however, there is limited understanding about how FO affects B cell membrane organization and function, especially at the animal level. We previously demonstrated that feeding C57BL/6 mice a very high dose of n-3 PUFAs for 3 weeks diminished B cell lipid raft clustering (187). We also showed that mice consuming this very high dose for 14 weeks displayed enhanced B cell activation, which we speculated was due to an increase in body weight (160). However, we did not completely test the effects of a physiologically relevant dose of FO on raft organization, the mode of raft disruption, or its relationship with innate and adaptive B cell function.

The specific objectives of this study were 1) to determine if administration of a dose of FO, modeling human intake, disrupted lipid raft organization of mouse B cells;

2) to address the conflicting models on how n-3 PUFAs disrupted raft molecular organization; and 3) to test the hypothesis that altering raft organization with FO would promote immunosuppressive effects on downstream innate and adaptive B cell function. The approach relied on biochemical and imaging measurements of B cells isolated from mice fed FO, supplemented with in vitro and model membrane studies. The data revealed for the first time that a relevant dose of FO increased B cell raft size and membrane molecular order upon cross-linking rafts, which was accompanied by novel downstream functional effects.

Materials and Methods

Mice and diets

Male C57BL/6 mice (Charles River), 4–6 weeks old, were fed for 3 weeks a purified CD or a FO diet (Harlan-Teklad). Both diets consisted of 5% total fat by weight or 13% by total energy. All ingredients were essentially identical except the fat source, which was soybean oil in the CD and menhaden fish oil in the FO diet (Table 4.1). The FO diet also contained food coloring, which we ensured had no effects on the measurements described below. The fatty acid distribution of the diet, measured with GC, was within experimental error to that reported by the vendor (Harlan-Teklad) (Supplementary Table 4.1). Approximately 2% of the total kcal came from EPA and 1.3% from DHA. This level of EPA/DHA corresponded to approximately 4 g of FO consumed by a human on a daily basis, which can be achieved through the diet and is currently in use pharmacologically for treating elevated triglycerides (52). Mice were euthanized using CO_2 inhalation and cervical dislocation followed by isolation of spleens. All of the experiments with mice fulfilled the guidelines established by the East Carolina

Table 4.1: Composition of control and fish oil diets.

Formula (g/Kg)	Control	Fish oil
Casein	185.0	185.0
L-Cystine	2.5	2.5
Corn Starch	369.98	369.88
Maltodextrin	140.0	140.0
Sucrose	150.0	150.0
Cellulose	50.0	50.0
Soybean Oil	50.0	-
Fish Oil	-	50.0
Mineral Mix, AIN-93M-MX (94049)	35.0	35.0
Vitamin Mix, AIN-93-VX (94047)	15.0	15.0
Choline Bitartrate	2.5	2.5
TBHQ, antioxidant	0.02	0.02
Yellow food coloring	-	0.1

University Brody School of Medicine for euthanasia and humane treatment.

Cell isolation and cell culture

$B220^+$ B cells (> 90% purity) were isolated from splenocytes by negative selection (Miltenyi Biotech) as previously described (160). For some experiments, $CD4^+$ T cells (> 85% purity) were purified from B6.Cg-Tg(TcraTcrb)425Cbn/J mice (OT-II) (Jackson Laboratory) that express α- and β-chain T-cell receptor and CD4 co-receptor specific for recognizing chicken ovalbumin 323–339 ($OVA_{323–339}$) presented by H-2 IAb molecules. For in vitro studies, mouse EL4 lymphomas were treated with 25 μM EPA or DHA complexed to BSA for 15.5 h as previously described (150). BSA without complexed fatty acid served as the control (150).

Isolation of detergent-resistant membranes and analysis

A total of 30×10^6 B cells or 20×10^6 EL4 cells were prepared for detergent extraction and layered on a sucrose gradient as previously described (150). Sucrose gradients were centrifuged at 40,000 rpm for 20 h at 4°C in a swinging bucket SW41Ti rotor (Beckman). Twelve 1 ml fractions were collected. Fractions 3–6 representing detergent-resistant membranes (DRMs) or fractions 9–12 representing detergent-soluble membranes (DSMs) were combined based on their cholesterol content, which was measured with an Amplex Red cholesterol assay kit (Invitrogen) relative to protein levels. Lipids were extracted as described previously (150). Samples were dissolved in chloroform, and select phospholipids were separated with a Shimadzu Prominence HPLC using a 150 × 4.6 mm Luna 5 μm NH2 column (Phenomenex) with a mobile phase gradient of H2O (increasing from 5% to 50%) and acetonitrile (decreasing from 95% to 50%) at 30°C. Phosphatidylethanolamine (PE), phosphatidylcholine (PC), and

sphingomyelin (SM) fractions were collected by UV detection at 202 nm, and the acyl chain composition of each fraction was further analyzed by GC as previously shown (150). The rationale for selecting these phospholipids was to address the most abundant lipids of the outer (PC, SM) and inner (PE) leaflets and to allow direct comparison with other studies (128).

^{2}H NMR spectroscopy

Sample preparation, NMR spectroscopy, and analysis were as previously described (198). The PC phospholipid (1-[$^2H_{31}$] palmitoyl-2-docosahexaenoylphosphatidylcholine,16:0-22:2PC-d_{31}) used for this study was perdeuterated in the sn-1 chain (custom synthesis, Avanti Polar Lipids), and the samples consisted of aqueous multilamellar dispersions of 50 wt% lipid in 50 mM Tris buffer (pH 7.5). Briefly, lipid mixtures of 16:0-22:6PC-d_{31}/SM (1:1) and 16:0-22:6PC-d_{31}/ SM/cholesterol (1:1:1) were codissolved in chloroform. The solvent was removed, the lipids were hydrated with buffer, and the pH was adjusted. After three lyophilizations with deuterium-depleted water (Sigma), samples were transferred to a 5 mm NMR tube. Stringent precautions were taken to prevent oxidation during sample preparation and data acquisition. NMR experiments were performed on a homebuilt spectrometer operating at 7.05 T using a phase-alternated quadrupolar echo sequence (199, 204).

Lipid raft cross-linking and total internal reflection fluorescence imaging

Cells were fluorescently stained for lipid rafts by cross-linking CTx-B (Invitrogen) and then imaged using total internal reflection fluorescence (TIRF) microscopy. For select experiments, GM1 levels were measured by staining with primary with no secondary antibody for cross-linking. TIRF was performed on an Olympus IX-71

microscope with excitation at 488 nm by a 20 mW Sapphire laser and a 60× 1.45NA oil-immersion TIRF objective. Fluorescence emission was filtered through a LF-488/561-A-OMF filter cube (Semrock) and detected by a Hamamatsu ORCA-R2 progressive scan interline CCD camera. For all imaging experiments, 9 or 10 cells per diet were analyzed per experiment, and image analysis was performed as previously described (150).

Live cell imaging of DiIC$_{18}$

To assess changes in nonraft organization, we measured uptake of the nonraft probe 1,1'-dioctadecyl-3,3,3′,3′-tetramthylindocarbocyanine perchlorate (DiIC$_{18}$, Invitrogen) (205). The approach was similar to our previous report where we used FAST-DiI (187). However, FAST-DiI uptake was extremely rapid under live cell imaging conditions; therefore, we relied on DiIC$_{18}$. A total of 1 × 10^6 B cells were washed with RPMI 1640 without phenol red at 37°C and resuspended in 1 ml of the same media and placed into Delta T dishes (Bioptechs Inc.). We added 0.2 μl of a 1 mg/ml stock of DiIC$_{18}$ to the dishes and imaged. Live cell, wide-field microscopy was conducted with an Olympus IX-70 microscope using an oil 100× objective and a Hamamatsu CCD camera, equipped with stage and objective heaters (Bioptechs Inc.). Imaging was started at 1 min after addition of the fluorescent probe at 37°C. Images were acquired with MetaMorph software and analyzed with NIH ImageJ. All settings were kept constant between experiments.

Generalized polarization imaging

Generalized polarization (GP) was calculated to determine the molecular order of the B and EL4 cell plasma membrane (206). Cells were stained with 4 μM di-4-ANEPPDHQ (Invitrogen) for 30 min at 37°C, washed twice with PBS, and fixed with 4%

paraformaldehyde (207). For some experiments, as an additional control, B cells were treated with 10 μM methyl-β-cyclodextrin (Sigma-Aldrich) for 15 min at 37°C to deplete cholesterol. Imaging was conducted on a Zeiss LSM-510 confocal microscope using a 100x objective with excitation at 488 nm and fluorescence emission detected in two channels: 505–545 nm for ordered regions and 650–750 nm for disordered regions. Quantification of fluorescence intensity (I), after background subtraction for the two channels, was performed using NIH ImageJ. GP was calculated using the formula: GP = $(I_{505–545} – (G)I_{650–750})/(I_{505–545} + (G)I_{650–750})$, where G is the G-factor and I is fluorescence intensity (206).

B cell activation with lipopolysaccharide (LPS)

B cells were stimulated with 1 μg/ml of LPS for 24 h, and the secreted cytokine profiles were measured from supernatants using a Multi-Analyte ELISArray kit (SA Biosciences) as previously demonstrated (160). In addition, B cells were analyzed for surface expression of activation markers using fluorescently labeled anti-MHC class II M5/114.15 (Bio X Cell), anti-CD69 H1.2F3 (BD Biosciences), and anti-CD80 16-10A1 (Bio X Cell) on a BD LSR II flow cytometer. Antibodies for MHC class II and CD80 were conjugated with fluorophores using a kit (GE Healthcare).

B cell activation of naive $CD4^+$ T cells

B cells were peptide loaded with $OVA_{323–339}$ (GenScript) at various concentrations in serum-free media for 1 h at 37°C and then washed with fresh media. A total of 1×10^5 B cells were then plated with 3×10^5 nondiet modified OT-II transgenic T cells, spun quickly, and incubated for 24 h at 37°C in 96-well plates. After 24 h, the supernatant was collected to analyze secreted IFN (interferon)-γ and IL-2 with an ELISArray kit (SA

Biosciences) following the manufacturer's protocol. The cells were stained with fluorescently labeled anti-CD4-PE (Miltenyi Biotech), anti-CD69-FITC (BD Biosciences), and anti-CD25-PE-Cy7 (BD Biosciences) and analyzed by flow cytometry on a BD LSR II. In all flow cytometry experiments, SYTOX Blue (Invitrogen) was used to discriminate dead cells, and at least 10,000 live events were collected for analyses. Control experiments were routinely conducted in the absence of peptide and with T cells only (no B cells) to ensure T-cell activation was driven by peptide-loaded B cells.

Statistical analyses

All ex vivo and in vitro data are from several independent experiments, with each ex vivo experiment representing one mouse per diet. The only exception was the ex vivo DRM/DSM analysis, in which two mice were pooled per experiment. Data were first analyzed for normality using a Kolmogorov-Smirnov test (GraphPad Prism). For a few select experiments with nonparametric distributions, we relied on paired Wilcoxon t-tests. Pairing was required due to differences in experimental settings between experiments as previously described (187). For the majority of animal experiments, statistical significance was established using an unpaired one-tailed or two-tailed Student's t-test. One-tailed unpaired t-tests were used to analyze the GC data from animals because before experimentation we predicted an increase in n-3 PUFA levels (128). In vitro studies relied on one-way ANOVAs followed by a Dunnett's post hoc t-test (160). P values less than 0.05 were considered significant. The NMR data were not analyzed for statistical significance because they were obtained on model membranes of well defined and controlled composition for which a reproducibility of ±1% applies to multiple acquisitions. This approach is standard for model membrane studies using

NMR spectroscopy (198, 199).

Results

Body weights, food intake, and cellularity

The FO diet, relative to CD, had no effect on the rate of body weight gain (Supplementary Figure 4.1A) or food intake per day (Supplementary Figure 4.1B). Spleen weight (Supplementary Figure 4.1C) was significantly elevated for mice on the FO diet but did not affect the steady-state number of B cells (data not shown). Given that we recently reported n-3 PUFAs at high doses can lower energy expenditure (208), we verified that the FO diet had no impact on whole body energy expenditure using metabolic cages (data not shown).

FO promoted uptake of EPA/DHA into DSMs and DHA into PC of DRMs

The first objective was to biochemically determine if the physiologically relevant dose of FO manipulated the molecular composition of B cell “raft”-like DRMs. We used detergent extraction followed by HPLC-GC to determine the acyl chain composition of PE, PC, and SM ex vivo (Figure 4.1). The relative proportion of PC, PE, and SM in DRM and DSM fractions was not changed by FO (Figure 4.1A). Relative PC and SM levels were generally higher in DRMs than in DSMs. SM was the smallest fraction of PE/PC/SM, consistent with studies in other cell types (177).

In PE, EPA (20:5) and DHA (22:6) did not incorporate into DRMs but were significantly increased in DSMs (Figure 4.1B). FO also increased 22:5 and lowered arachidonic acid (20:4) in PE DSMs (Figure 4.1B). In PC, 20:5 was lowered and 22:6 increased with FO in DRMs ($P = 0.06$) (Figure 4.1C). In DSMs of PC, 20:5 and 22:6 did not significantly increase (Figure 4.1C). In SM, 20:5 and 22:6 did not change in DRMs

Figure 4.1

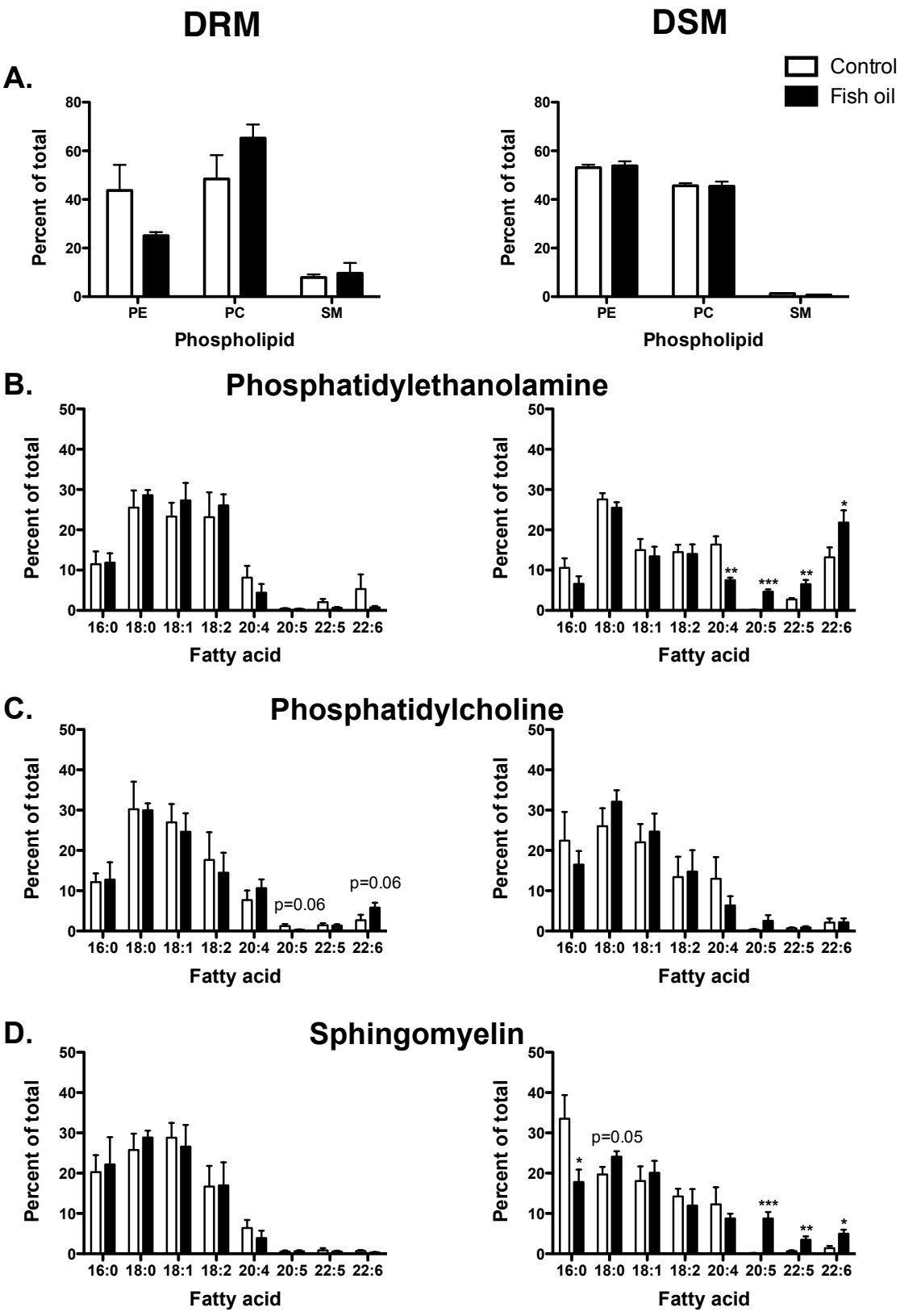
DRM
DSM
A.
Control
Fish oil
Percent of total
Phospholipid
PE
PC
SM
B.
Phosphatidylethanolamine
C.
Phosphatidylcholine
D.
Sphingomyelin
Fatty acid
16:0 18:0 18:1 18:2 20:4 20:5 22:5 22:6
p=0.06
p=0.05

Figure 4.1: FO promoted uptake of EPA/DHA into DSMs and DHA into PC of DRMs. (A) Relative levels of B-cell PE, PC, and SM of DRM (left) and DSM (right) fractions. Acyl chain composition of B-cell DRM or DSM fractions of (B) PE, (C) PC, and (D) SM. B cells were isolated from mice fed control or FO-enriched diets. Data are means ± SEM (n = 4, with two mice pooled per experiment). Asterisks indicate different from control: *P < 0.05; **P < 0.01; ***P < 0.001.

(Figure 4.1D). In DSMs of SM, FO significantly decreased palmitic acid (16:0) and increased stearic acid (18:0), 20:5, 22:5, and 22:6 (Figure 4.1D). Because we did not quantify the exact levels of EPA and DHA, we conducted a few select experiments to approximate the levels EPA and DHA incorporating into DRMs and DSMs (data not shown). On average, ~5–8% of the total n-3 PUFA were localized to DRMs with the remaining amount in DSMs, consistent with another study (209).

Cholesterol levels in DRM and DSM fractions were not changed with FO (Supplementary Table 4.2). We also analyzed the ratio of DRM to DSM cholesterol based on a very recent study that reported that DHA treatment in vitro increased cholesterol into DSMs when analyzed as a ratio (200). FO had no effect on the ratio (Supplementary Table 4.2).

Overall, the data were highly consistent with predictions from detergent-free model membrane studies in which PCs containing DHA were found to have higher solubility for cholesterol, and by implication to have more favorable interactions with rafts, than PEs containing DHA (152). We confirmed this by comparing the order of cholesterol on the perdeuterated sn-1 chain on a DHA-containing PC (16:0-22:6PC-d_{31}) vs. a DHA-containing PE (16:0-22:2PE-d_{31}) in mixtures with SM (1:1) and SM/ cholesterol (1:1:1), mimicking rafts, using ^{2}H NMR spectroscopy (Table 4.2) (198). The increase in order due to cholesterol (reflecting proximity), measured for the PC-containing DHA, was more than twice that for the PE-containing DHA (Table 4.2). This observation was consistent with the ex vivo biochemical data that suggest DHA infiltrated into PCs of DRMs and PEs of DSMs.

FO increased B cell lipid raft size induced by cross-linking GM1

Table 4.2: DHA-containing PC displayed increased molecular order in the presence of lipid raft molecules relative to PE. Average order parameter values were calculated from 2H NMR spectra collected at 40°C for mixtures of 16:0-22:6PC-d31 with sphingomyelin (1:1), and with sphingomyelin and cholesterol (1:1:1). Values for 16:0-22:6PE-d31 were from previously published data (198). Data were collected by Williams, J. and Wassall, S. R.

Lipid mixture	Order parameter value	Percent increase in order
16:0-22:6PC-d_{31}/Sphingomyelin	0.115	68.7%
16:0-22:6PC-d_{31}/Sphingomyelin/Cholesterol	0.194	
16:0-22:6PE-d_{31}/Sphingomyelin	0.150	26.0%
16:0-22:6PE-d_{31}/Sphingomyelin/Cholesterol	0.189	

The next objective was to measure changes in raft organization with the FO diet relative to the CD using microscopy. This was essential because biochemical approaches are a useful predictive tool but also have limitations due to the use of detergent (158, 159). TIRF imaging of B cells from FO- and CD-fed mice showed a significant difference in the spatial distribution of GM1 molecules cross-linked with CTx-B (Figure 4.2A). TIRF image analysis, confirmed with confocal image analysis (data not shown), revealed the Feret's diameter was increased by 79% with FO relative to CD (Figure 4.2B). The binding of CTx-B to GM1 in the presence of cross-linking, measured in terms of fluorescence intensity, showed on average a 36% increase with FO, but this failed to reach statistical significance with TIRF analysis (Figure 4.2C). To determine if the propensity for an increase in CTx-B intensity was due to increased surface levels of GM1, the binding of CTx-B in the absence of cross-linking was measured, which revealed a 49% increase in intensity with FO (Figure 4.2D). To ensure the observed effects were FO specific, we also measured raft size and binding of CTx-B with a safflower oil-enriched diet and found no evidence of raft disruption with this diet (Supplementary Figure 4.2). We also ensured the effects were specific for rafts. Changes in nonraft organization were measured in terms of uptake of the nonraft probe $DiIC_{18}$ (205). Live cell imaging revealed that $DiIC_{18}$ uptake was identical between cells isolated from CD- and FO-fed mice (Supplementary Figure 4.3). The imaging results provided the first evidence that a physiologically relevant dose of FO disrupted raft, but not nonraft, organization.

FO increased membrane order upon cross-linking rafts relative to the absence of cross-linking

Figure 4.2

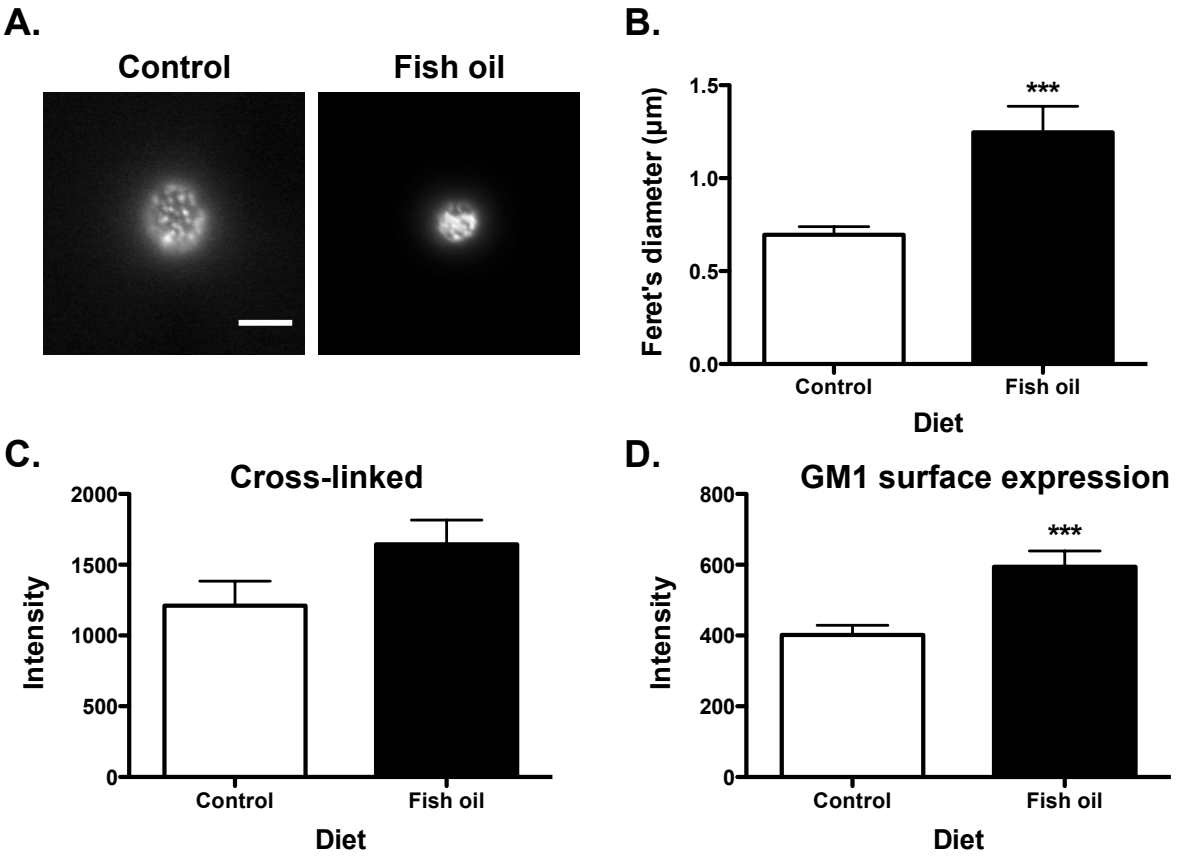

Figure 4.2: FO increased the size of rafts induced by CTxB cross-linking. (A) Sample fluorescence images of B cells isolated from control or FO-fed mice and cross-linked to induce raft clustering. Images are from TIRF microscopy (bar, 5 μm). (B) Lipid raft size in terms of Feret's diameter for B cells. (C) CTxB fluorescence intensity after cross-linking. (D) GM1 surface levels. Values are means ± SEM (n = 6 from 65 total cells analyzed per diet in A–C; n = 4 from 86-90 cells analyzed per diet in D). Asterisks indicate different from control: ***$P < 0.001$.

We subsequently determined if the aforementioned changes with FO on raft organization affected membrane molecular order. This directly addressed two opposing models in which n-3 PUFAs in response to stimulation increase membrane order ex vivo versus a decrease in membrane order in vitro (140, 177). To measure molecular order, we used di-4-ANEPPDHQ, an environmental sensing fluorescent dye that can shift its emission spectra 30 nm depending on the degree of packing in the surrounding lipid chains (Figure 4.3A) (210). As an initial control, B cells were treated with 10 μM methyl-β-cyclodextrin to remove cholesterol from the membrane. GP significantly decreased upon cholesterol depletion (data not shown). In the absence of cross-linking, FO, compared with CD, significantly decreased the average GP by 25% (Figure 4.3B). This decrease was consistent with data showing that n-3 PUFAs exert a disordering effect on membrane microviscosity in the absence of inducing raft formation (105). Although there was no difference in GP values between CD and FO diets upon cross-linking (Figure 4.3C), GP values for FO were elevated to a greater extent than CD relative to no cross-linking (Figure 4.3D). Analysis of the differences in GP values between cross-linking and no cross-linking showed FO had a greater ordering effect by 65% compared with CD (Figure 4.3D). These results supported the ex vivo model that FO is capable of exerting an ordering effect on the membrane upon stimulation (140).

EPA and DHA incorporated into DRMs/DSMs and did not increase GM1 surface expression in vitro

We previously reported that treatment of EL4 cells with DHA, but not EPA, increased raft size (150). Therefore, we conducted comparative biochemical and imaging studies to determine if the in vivo and in vitro modes of raft disruption were

Figure 4.3

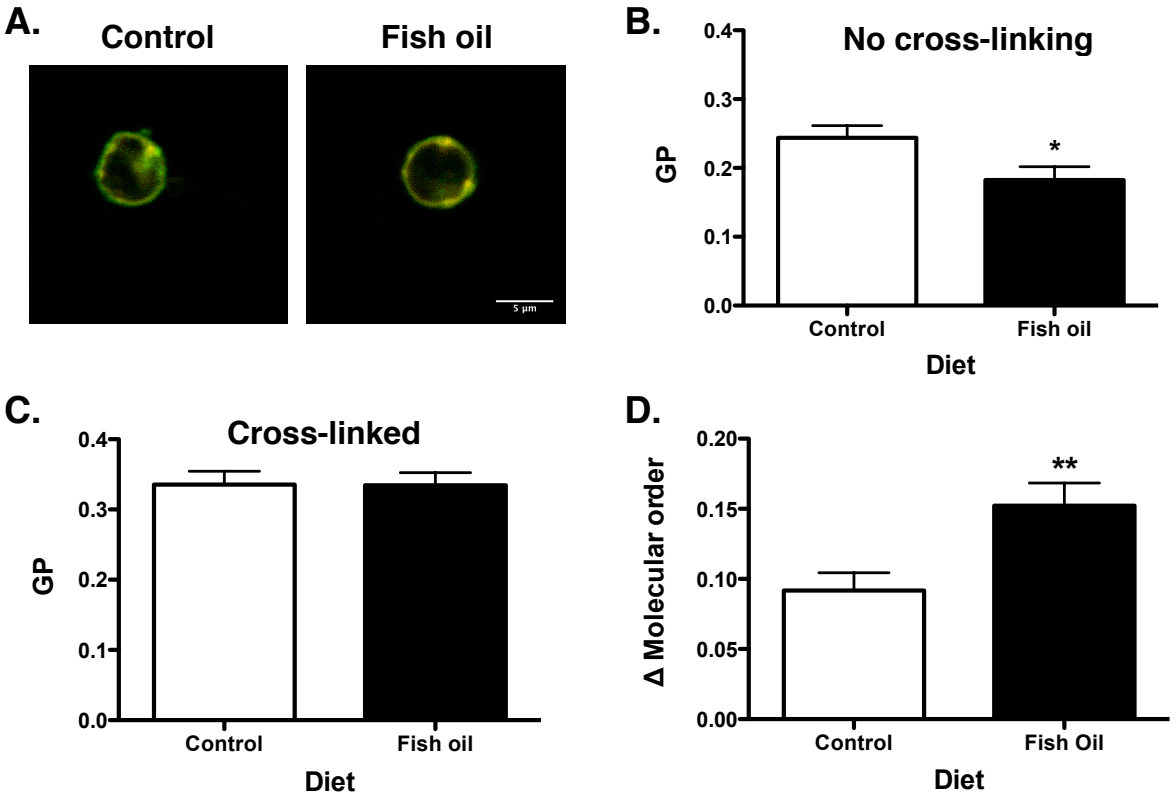

Figure 4.3: FO increased B-cell membrane molecular upon cross-linking relative to no cross-linking. (A) Sample merged intensity images of B cells, stained with di-4-ANEPPDHQ, isolated from control or fish oil enriched diets. Ordered (green) and disordered (red) channels are merged to illustrate the ratio between channels. B: Plasma membrane GP values from B cells isolated from control and FO-fed mice without CTxB cross-linking. C: GP analysis of B cells cross-linked with CTxB. D: Change in GP values upon cross-linking CTxB relative to no cross-linking. Values are means ± SEM (n = 4 from 40 total cells analyzed per diet). Asterisks indicate different from control: *$P < 0.05$; **$P < 0.01$.

similar in addition to discriminating differences in bioactivity of EPA vs. DHA.

Similar to ex vivo measurements, relative PC and SM levels were higher in DRMs than in DSMs and were not affected by EPA or DHA (Figure 4.4A). In PE, EPA treatment increased 20:5 and 22:5 in DRMs. DHA treatment had no significant effect on 22:6 in DRMs of PE (Figure 4.4B). In PE DSMs, EPA and DHA treatment lowered 20:4 and DHA increased 22:6 (Figure 4.4B). In PCs, EPA and DHA treatment did not significantly increase 20:5 or 22:6 in DRMs (Figure 4.4C). In PC DSMs, EPA and DHA treatment, respectively, increased 20:5/22:5 and 22:6 levels. EPA and DHA treatment lowered 18:1 in DRMs and DSMs of PC. In SM, EPA and DHA, respectively, increased 20:5 and 22:6 in DRMs (Figure 4.4D). In DSMs of SM, EPA and DHA lowered 18:1 and, respectively, increased 20:5/22:5 and 22:6. Similar to the ex vivo studies, we did not quantify exact levels of EPA and DHA in DRM/DSM. Based on a few select studies (data not shown), ~30% of the added EPA/DHA was localized to DRMs with the remaining amount in DSMs, consistent with our previous work (150).

Cholesterol levels in the DRM and DSM fractions were not significantly changed with EPA or DHA treatment (Supplementary Table 4.2). There was a tendency for EPA treatment to lower DRM cholesterol relative to BSA when analyzed as a t-test ($P < 0.05$). The ratio of cholesterol in DRM to DSM also had a tendency to be lowered with EPA and DHA treatment ($P = 0.08$) (Supplementary Table 4.2). Finally, we measured GM1 surface levels using microscopy before and after cross-linking and found no effect of EPA or DHA treatment (Supplementary Figure 4.4). These results showed that in vitro treatment with EPA/DHA, consistent with most other in vitro studies, changed DRM composition (128, 154); however, we did not measure an increase in GM1 levels in vitro

Figure 4.4

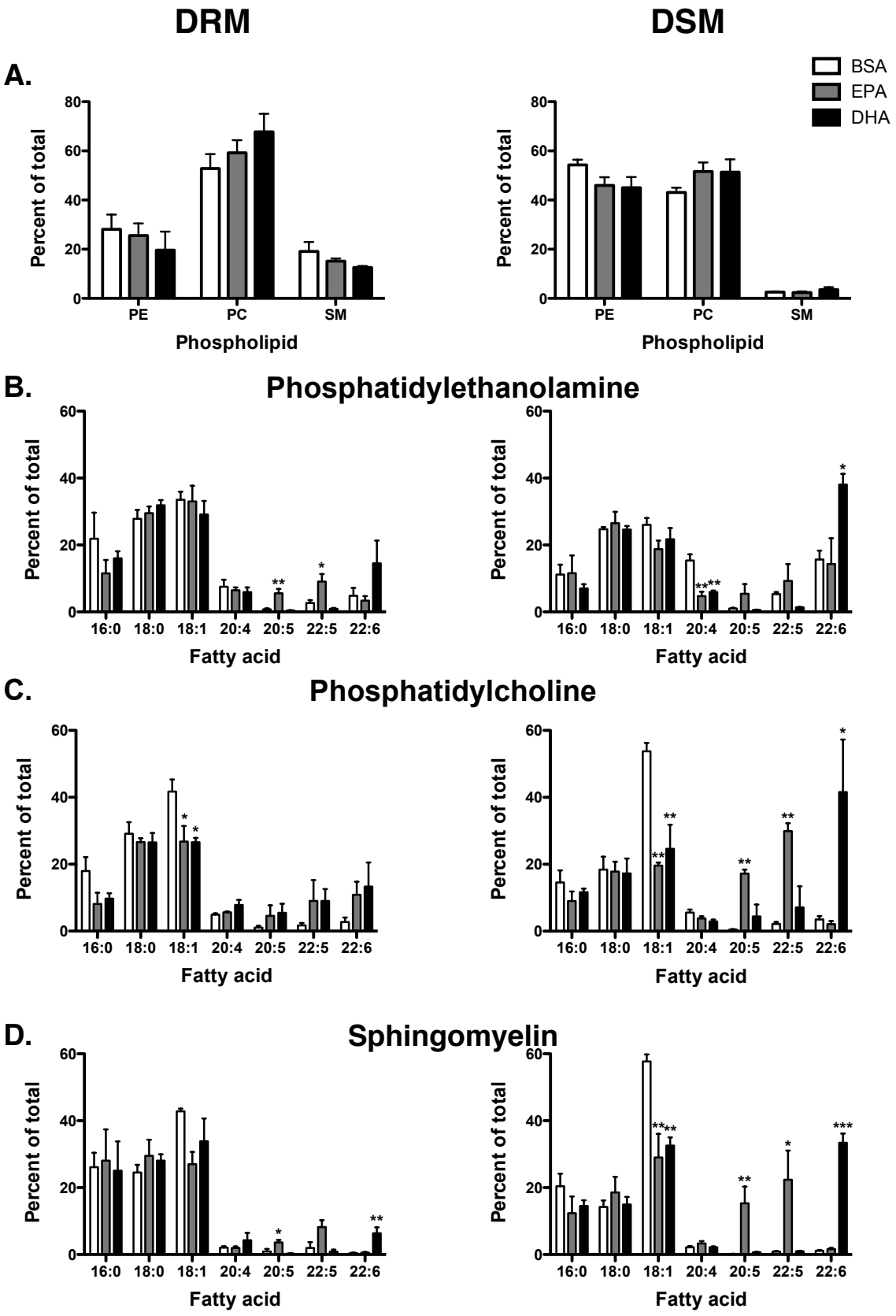
DRM
DSM
A.
BSA
EPA
DHA
Percent of total
PE
PC
SM
Phospholipid
B.
Phosphatidylethanolamine
C.
Phosphatidylcholine
D.
Sphingomyelin
Fatty acid
16:0
18:0
18:1
20:4
20:5
22:5
22:6

Figure 4.4: EPA and DHA treatment targeted DRM and DSM composition of EL4 cells. (A) Relative levels of PE, PC, and SM of EL4 DRM (left) and DSM (right) fractions. Acyl chain composition of DRM or DSM fractions from (B) PE, (C) PC, and (D) SM. EL4 cells were treated with BSA, 25 μM EPA, or DHA. Values are means ± SEM (n = 4). Asterisks indicate different from control: *P < 0.05; **P < 0.01; ***P < 0.001.

with EPA or DHA treatment as observed ex vivo.

DHA, but not EPA, increased membrane order with cross-linking relative to the absence of cross-linking in vitro

We next determined if EPA and DHA treatment increased membrane order as measured ex vivo. In the absence of cross-linking, EPA and DHA, respectively, compared with BSA, decreased GP by 32% and 75% (Figure 4.5A). Upon cross-linking, EPA showed no difference in molecular order relative to BSA; however, DHA treatment lowered GP by 27% (Figure 4.5B). Analysis of the differences in GP values between cross-linking relative to no cross-linking showed DHA, but not EPA, had a greater ordering effect by 60% compared with BSA (Figure 4.5C). These results supported the emerging ex vivo model that an n-3 PUFA exerts an ordering effect upon induction of raft formation (140).

FO enhanced B cell activation in response to LPS stimulation but suppressed B cell stimulation of naive $CD4^+$ T cells

The next set of experiments tested the hypothesis that disruption of lipid raft organization with FO would be accompanied by suppressive effects on downstream innate and adaptive B cell function, as reported for T cells, macrophages, and splenocytes (140, 142, 143). Two different B cell functional studies were conducted. First, we measured the activation of B cells after 24 h of LPS stimulation as a measure of an innate response (Figure 4.6). We found the physiologically relevant dose of FO enhanced B cell activation. The number of B cells activated was the same between the CD and FO diets (data not shown). CD69 surface levels were increased by 22% with FO, whereas MHC class II and CD80 surface expression were not affected by FO

Figure 4.5

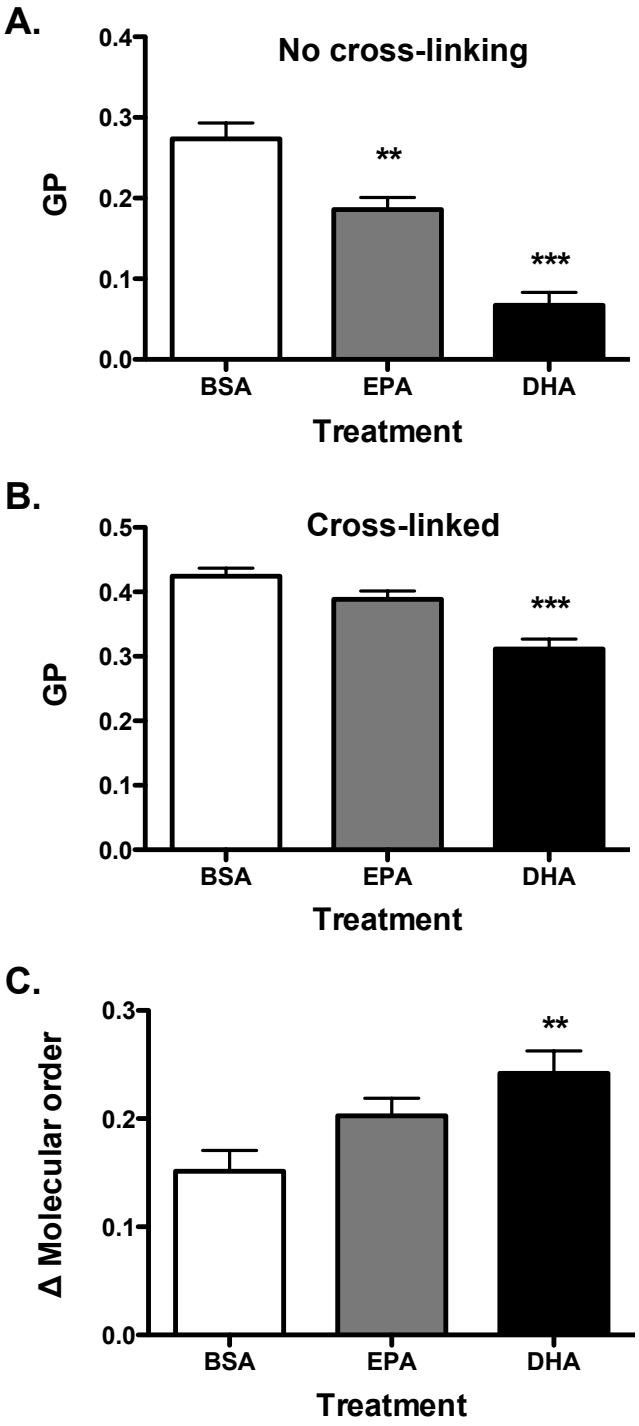
A.
No cross-linking
GP
0.4
0.3
0.2
0.1
0.0
**
***
BSA
EPA
DHA
Treatment
B.
Cross-linked
GP
0.5
0.4
0.3
0.2
0.1
0.0
***
BSA
EPA
DHA
Treatment
C.
Δ Molecular order
0.3
0.2
0.1
0.0
**
BSA
EPA
DHA
Treatment

Figure 4.5: DHA, but not EPA, increased membrane molecular order upon cross-linking relative to no cross-linking in vitro. (A) Plasma membrane GP values from EL4 cells treated with BSA, EPA, or DHA without CTxB cross-linking. (B) GP analysis of EL4 cells cross- linked with CTxB. (C) Change in GP values upon cross-linking CTxB relative to no cross-linking. Values are means ± SEM (n = 3 from 36 cells analyzed per treatment). Asterisks indicate different from control: **$P < 0.01$; ***$P < 0.001$.

(Figure 4.6A). Secretion of IL-6, TNF-α, and IFN-γ were increased compared with FO relative to the CD by 43, 87, and 182% (Figure 4.6B). IL-10 secretion was unaffected with the FO diet (Figure 4.6B).

To determined if the immune enhancing effect of the FO diet on B cells was specific to the innate response or applicable to an adaptive immune response, we tested the ability of B cells isolated from FO-fed mice to stimulate transgenic naive $CD4^+$ T cells that were not from FO-fed mice (Figure 4.7). The concentration of $OVA_{323–339}$ peptide loaded into B cells was optimized for maximal activation at $10^{–5}$ M with no activation at 0 M (data not shown). FO had no impact on the percentage of $CD4^+CD69^+CD25^+$ T cells activated (data not shown). In addition, the surface expression of the activation markers CD69 and CD25 on $CD4^+$ T cells was unchanged with FO (Figure 4.7A). Analysis of secreted cytokines revealed that IFN-γ levels were not significantly decreased with FO, but IL-2 secretion was decreased by 42% with the FO diet relative to CD (Figure 4.7B). These results supported the notion that raft disruption with FO was accompanied by changes in B cell function.

Discussion

In this study, we focused on B cells, a cell type underrepresented in experiments with n-3 PUFAs, especially at the animal level. The results demonstrated several significant advancements. First, the data showed that a relevant dose of FO increased the size of B cell rafts. Next, data integrated from animals, cell culture, and model membranes challenged some models on how n-3 PUFAs disrupted raft molecular organization. Third, the data highlighted differences between EPA and DHA on membrane organization. Finally, we discovered that a physiologically relevant dose of

Figure 4.6

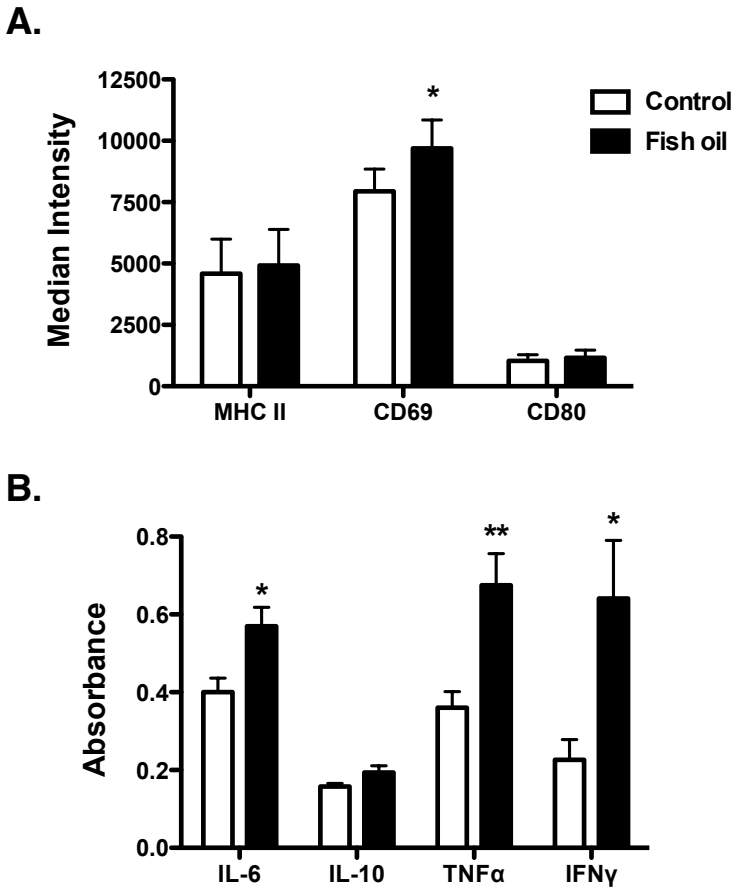

Figure 4.6: FO increased B-cell CD69 expression and cytokine secretion upon activation with LPS. (A) Median fluorescence intensity for B cells stained with anti-MHC class II, anti-CD80, or anti-CD69 after 24 h of LPS activation. B cells were isolated from mice fed a control or FO diet. (B) Cytokine secretion after 24 h of LPS activation. Values are means ± SEM (n = 6). Asterisks indicate different from control: *$P < 0.05$; **$P < 0.01$. Data were collected by Teague, H.

Figure 4.7

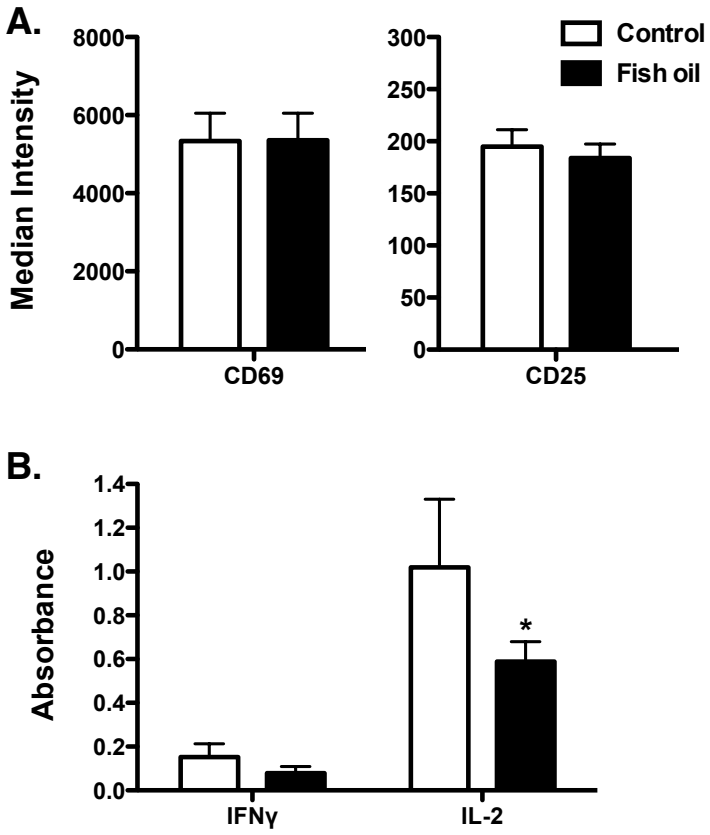

Figure 4.7: FO suppressed B-cell stimulated IL-2 secretion from naive CD4⁺ T cells. A: Median fluorescence intensity of CD4⁺ T cells stained with anti-CD69 and anti-CD25 after 24 h. CD4⁺ T cells were stimulated with B cells isolated from mice fed a control or FO diet. B: Cytokine secretion after 24 h of activation. Values are means ± SEM (n = 6). Asterisk indicates different from control: *P < 0.05. Data were collected by Teague, H.

FO enhanced an innate immune response but suppressed an adaptive response. Therefore, the data also challenged the paradigm that modification of rafts with FO exerts global immunosuppressive effects but overall supported the notion that manipulation of immune cell rafts with FO was accompanied by changes in function.

Biochemical measurements revealed some differences between ex vivo and in vitro measurements

The biochemical data from B cells (Figure 4.1) were generally in agreement with ex vivo studies, with a few exceptions (143, 211). Fan et al. demonstrated biochemically that n-3 PUFAs infiltrated DRMs and DSMs differentially depending on the type of headgroup (155). Their data showed the majority of n-3 PUFAs displayed a preference for inner leaflet lipids such as PEs. We also found greater incorporation of n-3 PUFAs into PEs over PCs. However, Fan et al. reported that n-3 PUFAs incorporated in PE DRMs, whereas we observed the majority of n-3 PUFAs in DSMs of PEs (Figure 4.1) (155). We also found DHA in PC DRMs, whereas they found no n-3 PUFAs in PC DRMs. Finally, we observed an increase in surface levels of GM1, a sphingolipid, whereas the same group reported a decrease in SM in a subsequent study (211). The differences between the studies could be cell specific or due to differences in diet compositions.

The B cell biochemical data showing DHA incorporated more into DRM PC than PE were consistent with model membrane experiments on lipid mixtures containing raft molecules (SM and cholesterol). They showed a DHA-containing PC underwent a greater increase in molecular order upon adding cholesterol compared with a DHA-containing PE (Table 4.2). These results were in agreement with previous studies to

show cholesterol was more soluble in n-3 PUFAs containing PCs than PEs (152). It is also important to note that the DHA-containing PC underwent a substantial increase in molecular order when exposed to cholesterol in the mixture with SM, which was consistent with the increase in membrane molecular order observed ex vivo when comparing cross-linked rafts with the absence of cross-linking with FO (Figure 4.3). Although n-3 PUFA acyl chains are highly disordered, very recent data from Mihailescu et al. revealed that cholesterol could raise the order of a PC-containing DHA (212). Thus, the model membrane data suggest that a PC-containing DHA undergoing an ordering effect upon interaction with cholesterol would allow the PC-containing DHA to favorably incorporate into rafts.

Our ex vivo and in vitro data did not concur with some in vitro measurements from other labs on cholesterol lateral distribution in DRMs and DSMs. Grimm et al. reported that treatment of SH-SY5Y cells with 100 μM DHA increased the normalized DSM/DRM ratio (200). We did not observe differences in cholesterol levels between DRM and DSMs in B cells or EL4 cells; however, the DRM/DSM ratio tended to be lowered in EL4 cells (Supplementary Table 4.2). More work is clearly needed in this area because a very recent study reported that treatment of hepatocytes with EPA increased raft cholesterol levels, opposite of the findings reported by Grimm and coworkers (201).

There were a few differences between the B cell biochemical data compared with the in vitro studies using EL4 cells. The first major difference was that GM1 levels were increased ex vivo with FO but not in vitro. The second major difference was that EPA/DHA did not dramatically infiltrate DRMs ex vivo compared with in vitro. Our in vitro data

were in agreement with cell culture studies from other labs (128, 154). For example, Stulnig and coworkers showed that treatment of Jurkat T cells with EPA resulted in significant incorporation into DRMs and DSMs of SM, PC, and PEs (128). We also observed some uptake of n-3 PUFAs into the SM fraction in both cell types, similar to Stulnig's lab; however, it is possible that the SM fraction could contain some small contaminants from other phospholipids, such as phosphatidylinositols and phosphatidylserines.

Overall, we hypothesize that the differences between our ex vivo and in vitro studies were due to differences in cell type (primary vs. immortal) and methods of lipid delivery (diet vs. exogenous addition of EPA or DHA). Furthermore, the levels of fatty acids (data not shown) and cholesterol (Supplementary Table 4.2) in EL4 cells were much higher than B cells, which was not surprising because EL4 cells are dramatically larger than primary B cells. Based on a few select experiments, we observed that ~30% of the total n-3 PUFAs incorporated into DRMs of EL4 cells, whereas ~5–8% of the total n-3 PUFAs were in DRMs of primary B cells, generally consistent with previous work from our lab and others (150, 209). The significant incorporation of EPA/DHA into DRMs in EL4 cells was not due to the dose of fatty acid in culture because even low levels of EPA or DHA (5–20 μM) showed the same distribution within error into DRMs and DSMs (data not shown).

Imaging demonstrated that FO increased membrane order upon cross-linking

Detergent extraction is a predictive tool but can induce artifacts (158, 159). An alternative method would have been to conduct studies with detergent-free methods to isolate rafts (119); however, this was beyond the scope of the study. We discovered,

consistent with other studies, that detergent-free methods required a very large number of cells (>100 × 106) to isolate rafts (93). Therefore, we relied heavily on imaging to determine how FO disrupted raft organization upon CTx-B cross-linking.

The ex vivo imaging data (Figure 4.2, 4.3) were highly consistent with ex vivo data to show that fat-1 mice, which express high endogenous levels of n-3 PUFAs, displayed increased molecular order within the $CD4^+$ T-cell immunological synapse upon activation with a cognate hybridoma cell relative to nonsynapse regions (140). Similarly, we observed that cross-linking GM1 molecules of B cells from FO-fed mice had a greater increase in molecular order relative to no cross-linking (Figure 4.3). Supporting in vitro studies showed DHA, but not EPA, increased membrane molecular order upon cross-linking relative to no cross-linking (Figure 4.5). These results were novel because very little is known about the differences in bioactivity between EPA and DHA on membrane organization.

The ex vivo and in vitro imaging data were in agreement with our previous studies. We showed previously that treatment of EL4 cells with DHA, but not EPA, diminished CTx-B-induced clustering of EL4 cells (150). We also discovered administration of a very high dose of a fish/flaxseed oil-enriched diet to mice disrupted B cell raft organization with no impact on nonraft organization (187). The data in this study provide the first evidence for changes in B cell raft organization with a physiologically relevant dose of FO.

Emerging model by which FO increases raft size

We propose the following working model to explain the ex vivo and in vitro data. In the absence of cross-linking, n-3 PUFA incorporation into the membrane, either

through the diet or in culture, decreased membrane order due to the highly disordered nature of the n-3 PUFA acyl chains (105). In vivo, FO also enhanced GM1 surface levels, which could be due to targeting of GM1 biosynthesis and/or trafficking to the plasma membrane. Although the GM1 molecules were poised to form rafts in the absence of cross-linking, they were not in a state where large-scale phase separation could be observed (213, 214).

Upon cross-linking CTx-B, the membrane became more ordered as lipid molecules were forced together and micron-scale domains became visible with FO. We speculate that FO administration resulted in the trapping of n-3 PUFAs into the large-scale raft domains. Cholesterol was not displaced out of the rafts in either model system. Instead, the mixing of cholesterol with n-3 PUFAs had an ordering effect on the membrane, as demonstrated with model membrane studies. In vitro studies demonstrated that the effects on membrane order were driven by DHA rather than by EPA. Overall, our data supported the model that FO can exert an ordering effect as opposed to the other models discussed above (140).

Disruption of rafts with FO was accompanied by differential effects on innate and adaptive B cell functions

The previous work on how FO disrupts rafts and the subsequent impact on immune cell function has centered on $CD4^+$ T cells, macrophages, and splenocytes (140, 142, 143). Generally, manipulation of lipid microdomain organization (which may have utility as a biomarker of n-3 PUFA manipulation) with n-3 PUFAs was reported to be accompanied by immunosuppression. Here we discovered that LPS stimulation of B cells increased cytokine secretion (Figure 4.6). The data were similar to a few studies

showing that activation of splenic macrophages with LPS resulted in increased cytokine secretion with FO (73, 215, 216). The data were also in agreement with our previous report showing that very long-term administration of a high–fat, fish/flaxseed oil-enriched diet enhanced activation of B cells (160). We had previously suggested that the increase in B cell activation was due to body weight gain, which we now know is not the driving factor.

The functional data (Figure 4.6) were not entirely in agreement with some in vitro studies showing that DHA suppressed LPS activation of macrophages and dendritic cells (68, 217, 218). This could be due to aforementioned differences (e.g., cell type, diet vs. in vitro treatment, etc.). Increased proinflammatory cytokine secretion does not allow us to conclude that FO is proinflammatory. It is possible that increased B cell activation could have potential clinical utility, especially in terms of antibody production. A few labs have studied the impact of FO on antibody production with mixed results (219-222). Altogether, these data highlighted the notion that FO is not universally immunosuppressive.

The antigen presentation data were the first to demonstrate that dietary manipulation of B cells with FO suppressed naive T-cell activation (Figure 4.7). Our data confirmed several in vitro studies that showed EPA and/or DHA treatment of B cells, dendritic cells, and monocytes/macrophages diminished antigen presentation to cognate T cells (162, 223). The data were also consistent with one ex vivo study demonstrating a mixture of antigen-presenting cells (B cells, macrophages, dendritic cells) isolated from a DHA-enriched diet suppressed the proliferation of naive $CD4^+$ T cells from mice fed control diets (224).

The functional data open the door to a wide range of new targets and mechanisms by which FO differentially affects B cell function. The mechanisms downstream of the plasma membrane by which n-3 PUFAs enhance B cell activation will require studying complex signaling pathways and their impact on gene activation. In the case of the antigen presentation studies, we now for the first time raise the possibility that lipid manipulation of the B cell side of the immunological synapse may be a major contributing factor by which T-cell activation was suppressed with n-3 PUFAs. It will be interesting to determine how manipulation of lipid microdomains can lead to an immune-enhancing effect with LPS and to a suppression of function when interacting with a T cell. It was beyond the scope of this study to address this, but it is something we aim to pursue in order to develop FO as a therapeutic agent for chronic inflammation.

Conclusion

We demonstrated that a physiologically relevant dose of FO increased the size of B cell rafts, GM1 surface expression, and membrane molecular order upon cross-linking CTx-B. Supporting in vitro studies suggested that the effects on membrane order were driven by DHA but not EPA. Furthermore, the B cell data supported an emerging model that increasing raft size with FO was accompanied by changes in innate and adaptive function. Overall, the results established the utility of using a relevant dose of FO for the first time to target B cell microdomain clustering and cellular function.

CHAPTER 5: MHC CLASS II ORGANIZATION ON THE B CELL SIDE OF THE MURINE IMMUNOLOGICAL SYNAPSE IS DISRUPTED BY DIETARY N-3 POLYUNSATURATED FATTY ACIDS

Introduction

n-3 PUFAs are unique bioactive molecules with emerging health benefits and clinical applications for treating acute and chronic inflammatory diseases (1). In particular, EPA and DHA, the major n-3 PUFAs of fish oil, are increasingly recognized as regulators of both innate and adaptive immunity (2). EPA and DHA exert their functional effects on immunity at a cellular level through several mechanisms. One central but poorly studied mechanism of these fatty acids is to disrupt the lateral organization of plasma membrane lipid-protein molecules that facilitate efficient intracellular signaling or cell-cell communication (225). In this study, we focused on the mechanistic effects of fish oil on the immunological synapse, a highly organized membrane domain formed between APCs and T cells that is critical for immune responses (131, 133).

A series of studies over the past decade have established that n-3 fatty acids in fish oil disrupt lipid microdomain composition and protein lateral distribution of naïve $CD4^+$ T cells in order to suppress downstream activation. For example, administration of dietary fish oil to mice suppressed recruitment of T cell PKCθ into lipid raft microdomains and subsequent IL-2 secretion when activated with anti-CD3/28 antibodies (211). Likewise, *in vitro* treatment of Jurkat T cells with EPA diminished recruitment of signaling proteins to the immunological synapse when mixed with untreated antigen loaded APCs (139). Similar results were also reported with *ex vivo* studies using $CD4^+$ T cells from *fat-1* transgenic mice that endogenously produce n-3

PUFAs (140, 141). In contrast, very little is known about the effects of fish oil on the molecular organization of proteins on the APC side of the immunological synapse.

B cells can serve as APCs in addition to their canonical role as antibody producing cells (84, 85). MHC class II proteins on the surface of B cells present antigens to $CD4^+$ T cells by clustering at the site of the immunological synapse (226). Our lab has previously shown that B cells, isolated from mice fed a physiologically relevant dose of fish oil, suppressed IL-2 secretion from $CD4^+$ T cells compared to a control diet (227). Furthermore, the functional changes were accompanied by diminished clustering of cholera-toxin induced GM1 microdomains with fish oil on the B cell plasma membrane. Our functional data were highly consistent with other studies that show fish oil administration to mice can indirectly suppress naïve $CD4^+$ T cell activation by targeting accessory cells including macrophages, dendritic cells and B cells (72, 224, 228).

In this study, we tested the hypothesis that dietary fish oil disrupts B cell MHC class II clustering and localization to the immunological synapse, a potential mechanism by which fish oil suppresses $CD4^+$ T cell activation. We studied the impact of fish oil on murine MHC class II lateral organization in the absence and presence of the formation of the immunological synapse using a combination of imaging methods. We compared the magnitude of the effects of fish oil with two well-described pharmacological reagents known to disrupt protein lateral organization (229, 230). We used methyl-beta-cyclodextrin (MβCD) to deplete cellular cholesterol and cytochalasin D to prevent actin polymerization. Our data reveal a novel mechanism of fish oil and show for the first time that dietary lipids manipulated the APC side of the immunological synapse.

Experimental Procedures

Mice and cells

Male C57BL/6 mice (Charles River), 4–6 weeks old, were fed for 3 weeks a purified 5% total fat by weight control or fish oil diet (Harlan-Teklad) as previously described (227). The mouse fish oil diet models human intake of approximately 4 grams of fish oil per day, which is in use clinically for treating elevated triglycerides (52). Mice were euthanized using CO_2 inhalation and cervical dislocation. $B220^+$ B cells were isolated from the spleens of the C57BL/6 mice and $CD4^+$ T cells were isolated from OT-II transgenic mice as previously shown (227). All of the experiments with mice fulfilled the guidelines established by the East Carolina University Brody School of Medicine for euthanasia and humane treatment.

GC

Total lipids were extracted from B cells and the fatty acid composition was analyzed by GC as previously described (160). Areas of identified peaks were summed and each peak area is expressed as the percentage of total peak area for each sample. Only the major fatty acids are reported for simplicity.

Reagents and antibodies

M5/114 MHC class II antibody (BioXCell) was conjugated to either Cy3 or Cy5 using a standard fluorophore conjugation kit (GE Healthcare). For some experiments, B cells were treated for 15 min with 10 mM MβCD (Sigma) or 2 μg/mL cytochalasin D (Sigma). α-FITC-CD3ε molecular complex (BD Biosciences), goat-α-PKCθ (Santa Cruz), and α-goat Alexa Fluor 633 (Invitrogen) were used for immunological synapse staining.

TIRF microscopy and analysis

6.25 x 10^5 $B220^+$ B cells were adhered to glass cover slips (Corning) coated with poly-D-lysine (Sigma) and then fixed with 4% paraformaldehyde (Electron Microscopy Sciences). For cells treated with MβCD and cytochalasin D, cells were first adhered and then treated. Cells were stained with anti-MHC class II antibody and mounted onto slides. TIRF microscopy was preformed as shown in a recent study by our lab (227). TIRF images were acquired at a penetration depth of 100 nanometers. Approximately 10 cells per experiment were analyzed for each treatment or diet using NIH ImageJ (http://rsbweb.nih.gov/ij/). The number of clusters and average cluster size was determined by creating a region of interest within a cell, confirmed by DIC, followed by setting a threshold to analyze particles.

FRET microscopy and analysis

MHC class II FRET was measured in terms of the efficiency of energy transfer from donor (Cy3) to acceptor (Cy5) fluorophores as previously described (187). Briefly, B cells were fixed with 4% paraformaldehyde and then stained with separately labeled Cy3 and Cy5 MHC class II antibodies. Cells were imaged on a Zeiss LSM 510 before and after photobleaching the acceptor fluorophore. All images were analyzed using NIH ImageJ and the FRET calc plugin for acceptor photobleaching FRET (172). Positive control images were generated using a single antibody dual labeled with both donor and acceptor. Negative control images were generated to optimize photobleaching time by using only single colors.

Immunological synapse staining and analysis

To form immunological synapses, B cells were first incubated with 10^{-5} M OVA_{323-}

$_{339}$ peptide (GenScript) for 1 hour at 37°C. Peptide loaded B cells from C57BL/6 mice (either from diet modified mice or treated with pharmacological agents) and $CD4^+$ T cells from OT-II transgenic mice were then mixed (1:2) and briefly spun down on a bench-top centrifuge. Cell-cell conjugates were subsequently transferred to poly-D-lysine coated coverslips and incubated at 37°C for 30 min. Additional time points were tested for select experiments. The cells were then fixed with 4% paraformaldehyde, permeabilized with 0.2% Triton X-100 (Sigma) and blocked overnight in PBS with 2% fatty acid free BSA at 4°C. Cells were stained for key immunological synapse markers.

Images were acquired on a Zeiss LSM 510 or an Olympus IX-81 FV1000 confocal microscope. Scoring of protein patching at the immunological synapse was performed as described by others (140, 231, 232). The cells were scored by BDR and SRS. The percentage of B cells forming B-T conjugates was also calculated from the same set of images.

Statistics

Reported values are means ± SEM from several independent experiments. All statistical analyses were calculated using GraphPad Prism (GraphPad Software). Select experiments for measuring the recruitment of molecules into the immunological synapse were performed blinded to ensure lack of bias. All the data sets were verified for normality. For experiments when two treatments were performed compared to a control, significance was determined by a one-way ANOVA followed by Dunnett's post-hoc t test. For all other experiments, significance was established by a two-tailed t test. P-values < 0.05 were considered significant.

Results

Fish oil increases B cell EPA and DHA levels

Prior to initiating studies on MHC class II organization, we first ensured that the fish oil diet increased murine B cell levels of EPA and DHA. GC analysis revealed the fish oil diet significantly increased 16:1 levels by 75% compared to the control. EPA, 20:5 n-3, and its elongation production 22:5 n-3 were both increased relative to the control by 760% and 260%, respectively (Table 5.1). DHA, 22:6 n-3, levels increased by 66% with the fish oil diet compared to the control. This resulted in a 124% increase of total n-3 PUFA fatty acid levels with the fish oil diet. Conversely, there was a 36% decrease in 20:4 (n-6) and a 27% decrease in total n-6 PUFA fatty acid levels with the fish oil diet compared to the control (Table 5.1). The n-6/n-3 ratio was significantly decreased from 4.1 for the control diet to 1.5 for the fish oil diet (Table 5.1). These data are in agreement with our previous findings to show fish oil increases total B cell n-3 PUFA levels at the expense of n-6 fatty acids (227).

Fish oil has no impact on B cell MHC class II organization in the absence of an immunological synapse

MHC class II is expressed in clusters on the plasma membrane surface of B cells (233, 234). Therefore, we addressed if dietary fish oil disrupts B cell MHC class II IAb clustering prior to the formation of the immunological synapse. Using TIRF microscopy, we visualized MHC class II protein clustering on the plasma membrane surface (Figure 5.1A). B cells isolated from mice fed the fish oil diet showed no change in average cluster quantity compared to the control (Figure 5.1B). We also measured MHC class II protein distribution on the nanoscale using acceptor photobleaching FRET microscopy. Again, there was no significant difference in FRET efficiency of MHC class II molecules

Table 5.1: Fatty acid analysis of B cells

Fatty Acid	Control	Fish Oil
14:0	0.6 ± 0.2	1.0 ± 0.2
16:0	26.9 ± 0.9	28.2 ± 0.9
16:1	1.2 ± 0.1	2.1 ± 0.2***
18:0	26.2 ± 3.8	24.9 ± 2.6
18:1 trans	0.5 ± 0.2	0.6 ± 0.2
18:1 cis	11.8 ± 1.8	10.9 ± 1.5
18:2 (n-6)	13.4 ± 2.8	8.3 ± 2.5
18:3 (n-6)	1.3 ± 0.4	4.3 ± 2.3
18:3 (n-3)	1.2 ± 0.4	0.9 ± 0.3
20:4 (n-6)	10.6 ± 1.0	6.7 ± 0.4**
20:5 (n-3)	0.5 ± 0.4	4.3 ± 0.6***
22:5 (n-3)	0.8 ± 0.1	2.9 ± 0.3***
22:6 (n-3)	3.5 ± 0.4	5.8 ± 0.7*
∑SFA	53.7 ± 3.9	54.0 ± 3.2
∑MUFA	13.5 ± 1.9	13.5 ± 1.6
∑PUFA (n-6)	25.2 ± 2.0	18.3 ± 2.3*
∑PUFA (n-3)	6.2 ± 0.4	13.9 ± 1.4***
n-6/n-3	4.1 ± 0.3	1.5 ± 0.4***

Fatty acids were extracted from the diets and analyzed with gas chromatography. Values are the percentage of total fatty acids. Values less than 0.5 are omitted for clarity. Asterisks indicate different from control: *P < 0.05; **P < 0.01; ***P < 0.001.

Figure 5.1

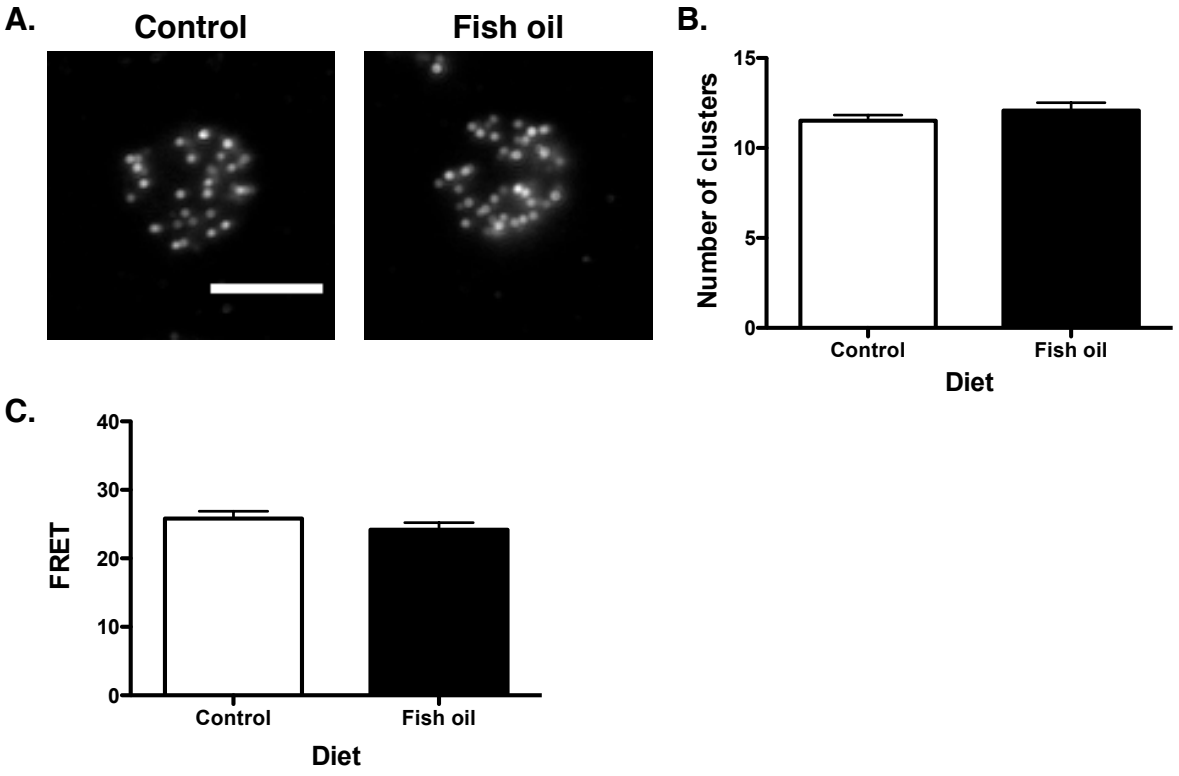

Figure 5.1: Fish oil diet has no effect on B cell MHC class II lateral organization prior to synapse formation. A) Representative TIRF images of MHC class II molecules on B cells isolated from mice fed control (left) or fish oil (right) diets. Scale bar represents 5 microns. B) Quantification of the number of B cell MHC class II clusters in a given region of interest from control (white) and fish oil (black) fed mice. C) FRET efficiency for MHC class II molecules from control (white) and fish oil (black). Values in B are means ± SEM (n = 5 with 110 - 111 cells analyzed per diet). Values in C are means ± SEM (n = 4 with 39-40 cells analyzed per diet). Data in A-B were collected by Melton, M.

on the B cell surface between the fish oil diet compared to the control (Figure 5.1C). There was also no change in the surface expression of MHC class II molecules on B cells from the fish oil diet as measured with microscopy and flow cytometry (data not shown).

Pharmacological agents disrupt B cell MHC class II organization in the absence of an immunological synapse

We next tested the sensitivity of MHC class II organization by treating B cells with pharmacological agents known to disrupt protein organization (233, 235-237). We again used TIRF microscopy to visualize MHC class II protein clustering. Figure 5.2A shows representative images of B cell MHC class II clustering from control cells and those treated with MβCD or cytochalasin D. The number of MHC class II clusters was decreased by 42% with MβCD treatment (Figure 5.2B). In contrast, cytochalasin D treatment had no effect on the average number of clusters per region of interest. On the nanometer scale, MβCD treatment did not modify FRET efficiency (Figure 5.2C). However, cytochalasin D treatment of B cells decreased FRET efficiency between MHC class II molecules by 20% compared to the control. Treatment of B cells with MβCD or cytochalasin D was not associated with any change in the surface expression of MHC class II molecules (data not shown). Taken together, the micron and nanoscale measurements revealed that the B cell plasma membrane MHC class II organization was sensitive to changes in lateral organization with pharmacological agents, albeit in different ways.

Naïve B and naïve T cells form a stable immunological synapse after 30 minutes of conjugation

Figure 5.2

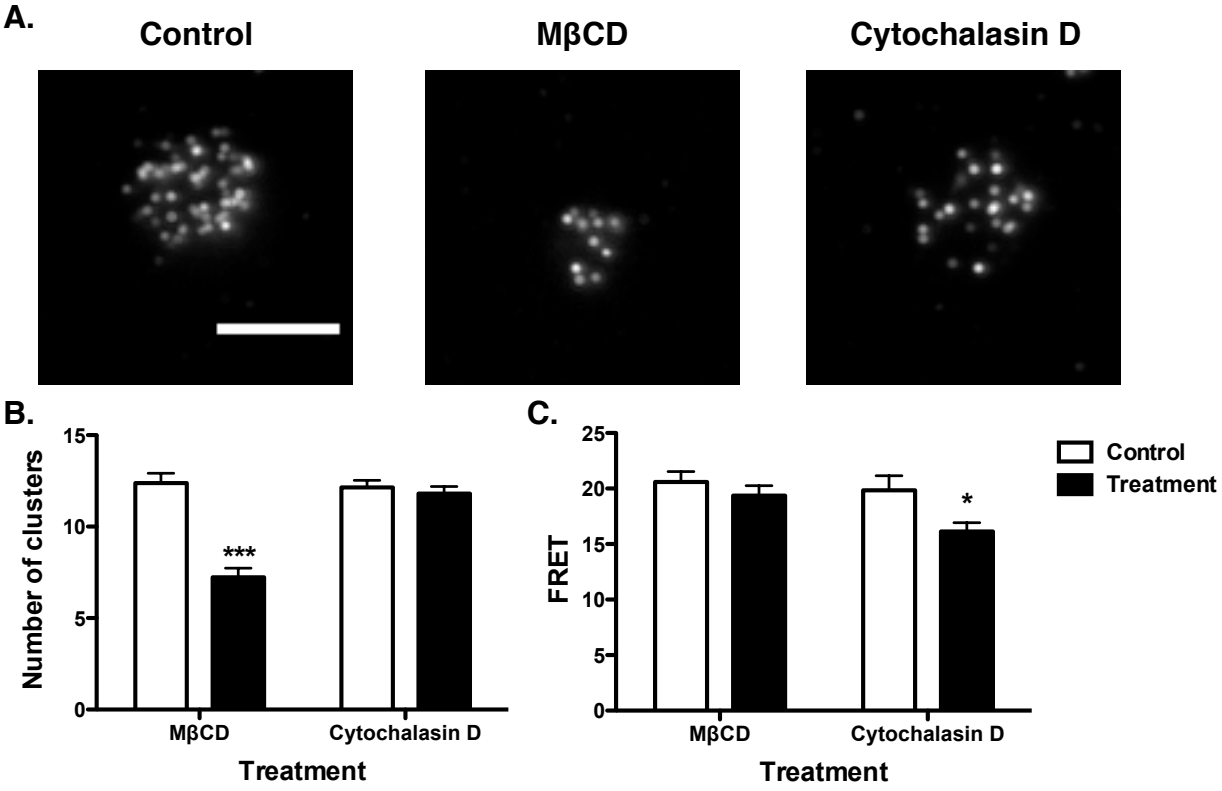

Figure 5.2: Cholesterol depletion and actin disruption reveal differential effects on MHC class II clustering. A) Representative TIRF images of MHC class II from control, MβCD, or cytochalasin D treated B cells. Scale bar represents 5 microns. B) Quantification of the number of MHC class II clusters in a region of interest from TIRF microscopy for control (white) and treatment (black). C) FRET efficiency for MHC class II molecules from control (white) and treatment (black). Values are means ± SEM (n = 3 with 30 - 50 cells analyzed per treatment). Asterisks indicate different from control: *P < 0.05; ***P < 0.001. Data in A-B were collected by Melton, M.

The next goal was to determine the effect of fish oil and pharmacological agents on MHC class II lateral organization in the immunological synapse. Due to the novelty of investigating murine naïve B-naïve T synapse formation, the kinetics of synapse formation within this model system were first determined. We measured the patching of key proteins at the immunological synapse as a function of conjugation time. Representative images were acquired for B cell MHC class II and T cell CD3ε and PKCθ over time (Figure 5.3A). There was a 90% increase in MHC class II patching after 30 minutes, as well as a 100% increase at 45 minutes of conjugation compared to 5 minutes (Figure 5.3B). CD3ε patching peaked at 30 minutes, increasing by 250% compared to 5 minutes (Figure 5.3C). PKCθ patching plateaued at 30-45 minutes, increasing by 100% compared to 5 minutes (Figure 5.3C). Therefore, we selected 30 minutes of conjugation time for the next set of experiments since this time point provided the highest percentage of patching for all markers tested.

Fish oil decreases B cell MHC class II and cognate CD4$^+$ T cell PKCθ recruitment to the immunological synapse independent of changes in cell-cell adhesion

We next tested the hypothesis that in the immunological synapse, fish oil would disrupt MHC class II recruitment. B cells from mice fed fish oil or control diets were loaded with peptide and mixed with CD4$^+$ T cells to stimulate formation of immunological synapses. Representative images of MHC class II, CD3ε and PKCθ staining are shown in Figure 5.4A. MHC class II patching in the synapse was decreased by 15% with the fish oil diet compared to the control (Figure 5.4B). In addition, FRET microscopy revealed a trend (P=0.07) in lowering FRET efficiency for MHC class II molecules (Figure 5.4C).

Figure 5.3

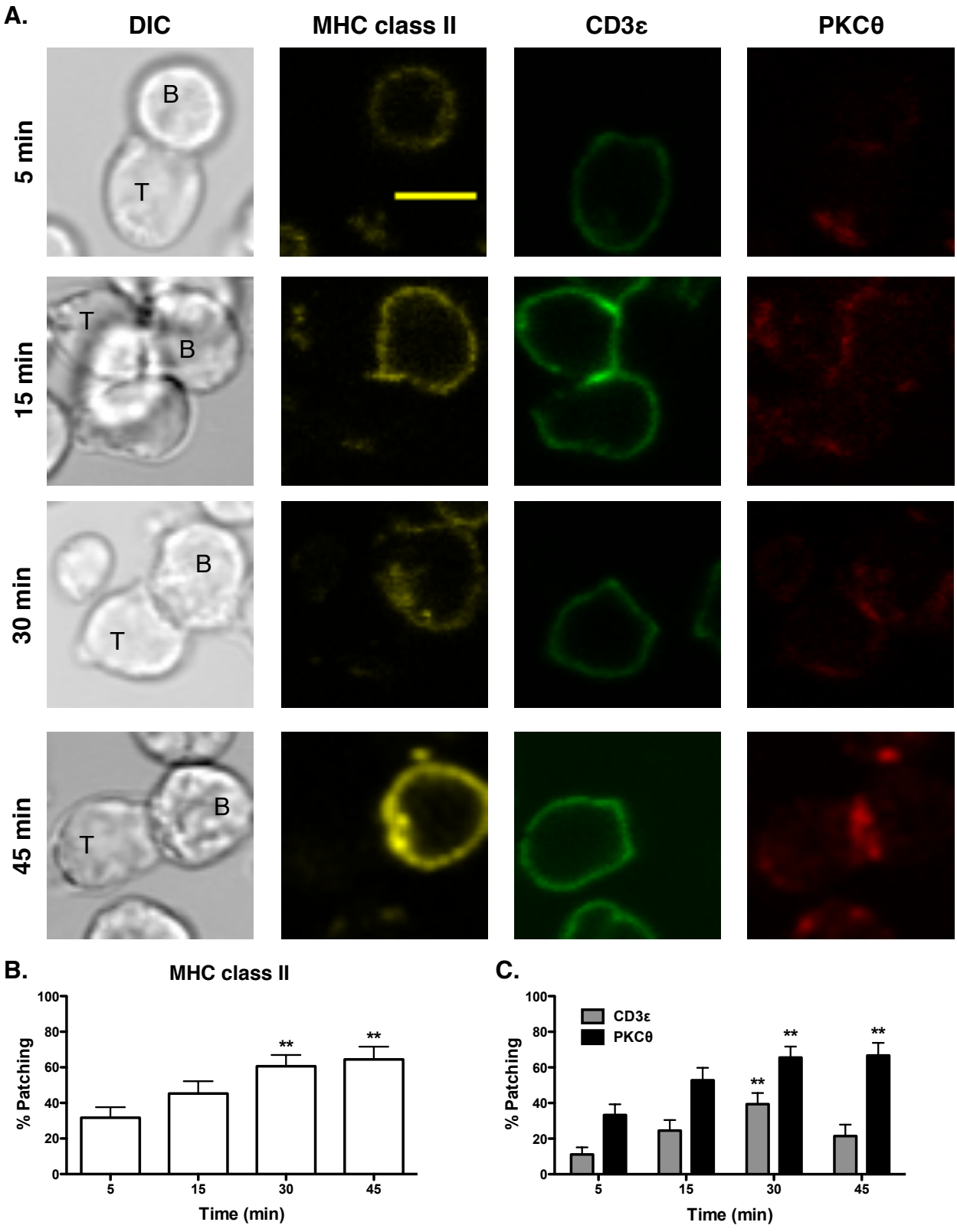
A.
DIC
MHC class II
CD3ε
PKCθ
5 min
15 min
30 min
45 min
B
T
B.
MHC class II
% Patching
Time (min)
C.
CD3ε
PKCθ
% Patching
Time (min)

Figure 5.3: Localization of B and T cell molecules at the immunological synapse as a function of conjugation time. A) Representative DIC (left) and immunofluorescent confocal images of MHC class II (yellow), CD3ε (green), and PKCθ (red) at the immunological synapse after 5, 15, 30, and 45 min of incubation. Scale bar represents 5 microns. B) Quantification of the percentage of conjugated B and T cells displaying patching of MHC class II at the immunological synapse over time. C) Percent patching of CD3ε (grey) and PKCθ (black) at the immunological synapse over time. Values are means ± SEM (n = 3 - 4 with 42 - 63 cells analyzed per diet). Asterisks indicate different from 5 min: **$P < 0.01$.

Figure 5.4

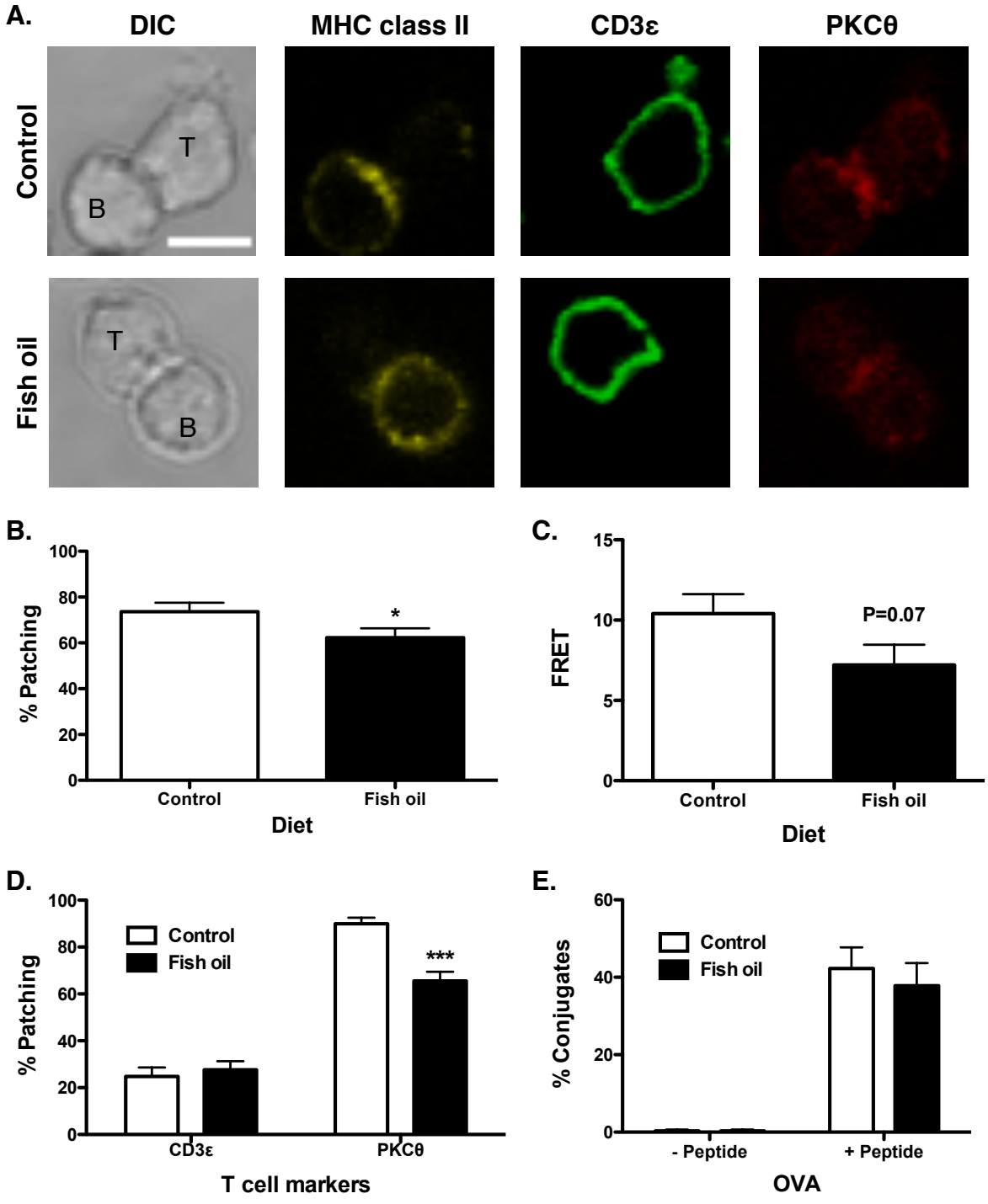
A.
DIC
MHC class II
CD3ε
PKCθ
Control
Fish oil
T
B
T
B
B.
% Patching
100
80
60
40
20
0
*
Control
Fish oil
Diet
C.
FRET
15
10
5
0
P=0.07
Control
Fish oil
Diet
D.
% Patching
100
80
60
40
20
0
Control
Fish oil
***
CD3ε
PKCθ
T cell markers
E.
% Conjugates
60
40
20
0
Control
Fish oil
- Peptide
+ Peptide
OVA

Figure 5.4: Fish oil disrupts the B-T cell immunological synapse. A) Representative DIC (left) and immunofluorescent confocal images of MHC class II (yellow), CD3ε (green), and PKCθ (red) at the immunological synapse. B cells were isolated from mice fed a control (top) or fish oil (bottom) diet. Scale bar represents 5 microns. B) Percent patching of MHC class II at the immunological synapse for B cells from control or fish oil fed mice. C) FRET efficiency for MHC class II molecules at the site of the immunological synapse from control and fish oil fed mice. D) Percent patching of CD3ε and PKCθ at the immunological synapse. The B cells are from control or fish oil fed mice and T cells are from OT-II transgenic mice fed a standard chow. E) Percentage of B cells from control or fish oil fed mice that conjugate with $CD4^+$ T cells. Values in B, D - E are means ± SEM (n = 4 with 129 - 146 cells analyzed per diet). Values in C are means ± SEM (n = 4 with 35 cells analyzed per diet). Asterisks indicate different from control: *$P < 0.05$; ***$P < 0.001$.

To address the impact of the change in MHC class II organization with fish oil on the T cell side, we measured patching of CD3ε and PKCθ at the immunological synapse. CD3ε organization was unmodified by the fish oil diet. However, PKCθ patching decreased 27% with fish oil (Figure 5.4D). We confirmed the percentage patching data by also measuring the fluorescent intensity values of the staining for each marker inside the synapse region compared to the non-synapse region (Supplemental Figure 5.1 A,C). We then computed the ratio of the staining synapse/non-synapse (Supplemental Figure 5.1B,D). These changes in protein localization were not a consequence of decreased conjugate formation, as there was no significant difference in the percentage of B cells forming conjugates with T cells (Figure 5.4E).

Given that previous studies have shown that EPA and/or DHA treatment can suppress cell-cell adhesion *in vitro*, we performed a static cell adhesion assay on B cells from the control and fish oil fed mice (139, 162). The ability of B cells to bind immunological synapse adhesion proteins VCAM-1, ICAM-1, ADAM28, and the extracellular matrix protein fibronectin was not modified by the fish oil diet (data not shown). Overall, these data show fish oil can modify MHC class II lateral organization and indirectly manipulate PKCθ lateral organization in the synapse.

Pharmacological agents disrupt B and T cell protein organization in the immunological synapse similar to fish oil

Finally, we compared the effects of fish oil on the formation of the immunological synapse with MβCD and cytochalasin D treatment to B cells. Representative immunofluorescence images of MHC class II, CD3ε, and PKCθ are shown in Figure 5.5A. MβCD treatment of B cells decreased MHC class II patching by 23% (Figure

Figure 5.5

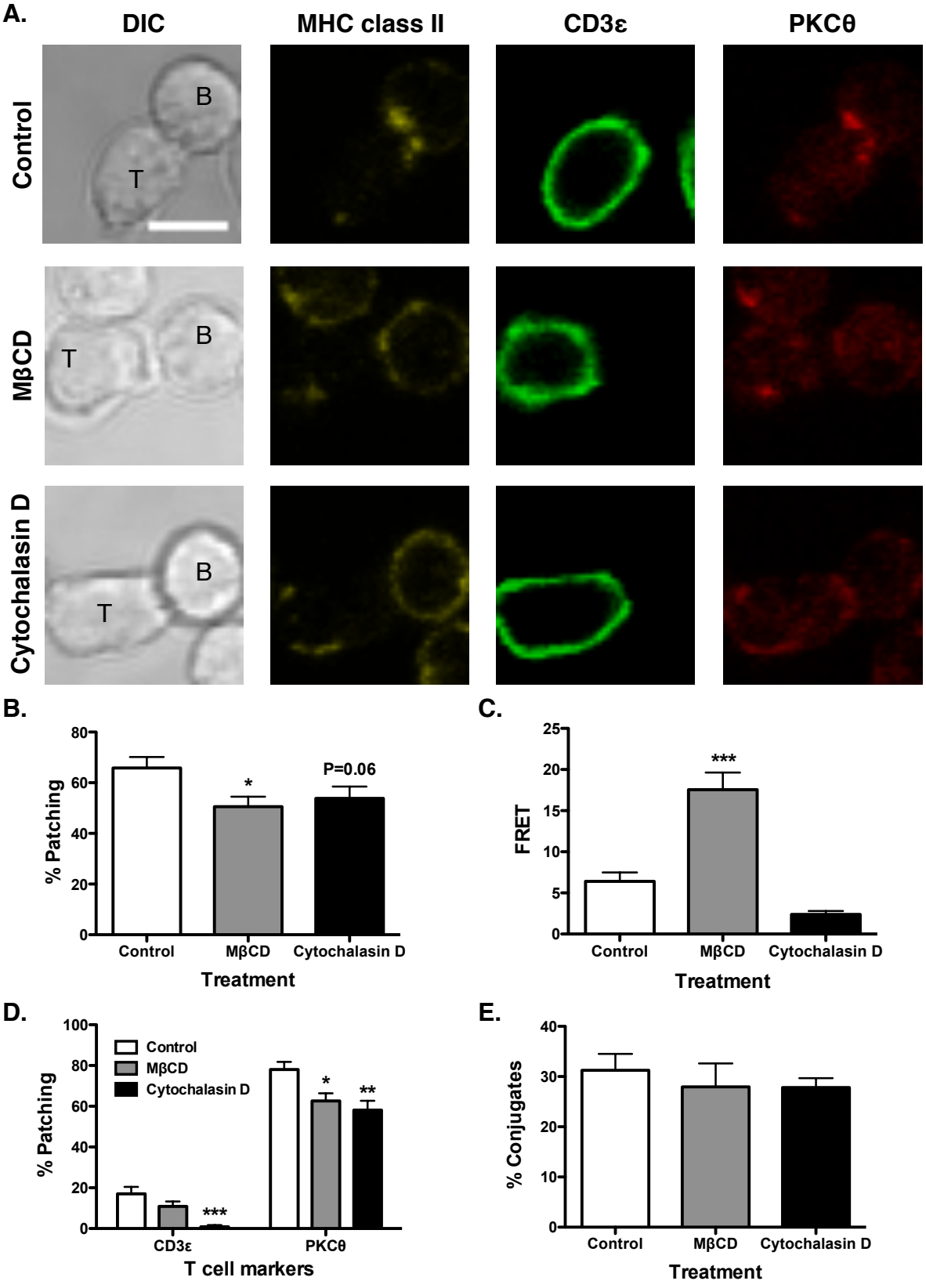
A.
DIC
MHC class II
CD3ε
PKCθ
Control
MβCD
Cytochalasin D
B
T
B.
% Patching
P=0.06
Control
MβCD
Cytochalasin D
Treatment
C.
FRET
Control
MβCD
Cytochalasin D
Treatment
D.
% Patching
Control
MβCD
Cytochalasin D
CD3ε
PKCθ
T cell markers
E.
% Conjugates
Control
MβCD
Cytochalasin D
Treatment

Figure 5.5: Pharmacological agents disrupt the B-T cell immunological synapse. A) Representative DIC (left) and immunofluorescent confocal images of MHC class II (yellow), CD3ε (green), and PKCθ (red) at the immunological synapse from control (top), MβCD (middle), or cytochalasin D (bottom) treated B cells. Scale bar represents 5 microns. B) Percent patching of MHC class II at the immunological synapse for control (white), MβCD (grey), or cytochalasin D (black) treated B cells. C) FRET efficiency for MHC class II molecules from control, MβCD, or cytochalasin D treated B cells. D) Percent patching of CD3ε and PKCθ at the immunological synapse for control, MβCD, or cytochalasin D treated B cells. E) Percentage of control, MβCD, or cytochalasin D treated B cells that conjugate with $CD4^+$ T cells. Values in B, D-E are means ± SEM (n = 3 with 117 - 166 cells analyzed per treatment). Values in C are means ± SEM (n = 3 with 30 cells analyzed per treatment). Asterisks indicate different from control: *$P < 0.05$; **$P < 0.01$; ***$P < 0.001$.

5.5B). Cytochalasin D treatment showed a trend in the reduction in MHC class II patching (P=0.06) (Figure 5.5B). We next measured FRET efficiency of MHC class II molecules at the synapse. Interestingly, despite lower localization at the synapse, MβCD treatment increased MHC class II FRET efficiency by 174% compared to the control (Figure 5.5C). Cytochalasin D treatment did not impact FRET efficiency at the synapse (Figure 5.5C).

Similar to fish oil, treatment of B cells with MβCD and cytochalasin D also diminished protein patching on the T cell side of the immunological synapse. CD3ε patching was unchanged by MβCD treatment (Figure 5.5D). However, cytochalasin D treatment of B cells decreased CD3ε patching by 95% compared to control (Figure 5.5D). MβCD and cytochalasin D treatment both reduced patching of PKCθ at the synapse by 20% and 26% respectively (Figure 5.5D). We also confirmed the percentage patching data here also by measuring the fluorescent intensity values of the staining for each marker inside the synapse region compared to the non-synapse region (Supplemental Figure 5.2 A,C). We then computed the ratio of the staining synapse/ non-synapse (Supplemental Figure 5.2 B,D). Although protein localization was disrupted, the percent of cells that formed conjugates was not modified by either treatment (Figure 5.5E). These data reveal that pharmacological treatment of B cells disrupts the organization of immunological synapse proteins on both the B and T cell side of the immunological synapse, similar to the fish oil diet.

Discussion

In this study we establish that fish oil-mediated disruption of B cell MHC class II organization at the immunological synapse can translate into an effect on T-cell

membrane organization. Our data show for the first time that fish oil can target the APC side of the immunological synapse in a manner similar to that reported for the effects of fish oil on T cells (139-141, 211). This work significantly expands our understanding of how fish oil, compared to other pharmacological agents, can target the molecular organization of B cells. Furthermore, our data establish a role for dietary lipids on the APC side of the synapse.

The APC side of the immunological synapse

Although the literature is replete with investigations on how fish oil modulates the organization of the synapse, the work-to-date has focused on the T cell side and far less is known about the molecular organization of the APC side, in particular the B cell component (238). Our findings underscore the impact of manipulating specifically B cells through dietary means on the formation of the immunological synapse. Our rationale for focusing on B cells was driven by our previous data to show that administration of fish oil to mice suppressed B cell mediated activation of naïve T cells. We did pursue select studies with $CD11c^{+}$ dendritic cells (DC) and discovered that activated DCs did not affect on naïve T cell activation; furthermore, fish oil had no effect on DC lipid-protein microdomain organization (data not shown, manuscript in review).

Peptide loaded clusters of MHC class II complexes are critical for initiating T cell activation (233). Even a single MHC–peptide complex can trigger a Ca^{2+} signal and a mature synapse can be formed when approximately 10 complexes are present (239). However, what is unclear is how the underlying lipid composition controls MHC class II organization and its impact on the formation of the synapse on the T cell side. To date, a few other studies have previously suggested that membrane lipids have a role in

disrupting the APC side of the synapse (162, 240). For example, Fooksman et al. showed that the concentration of $PI(4,5)P_2$ at the synapse regulated APC function (240). Sequestration of PI(4,5)P2 upon transfection with specific constructs in mouse and human B cells prevented the APCs from effective recognition by cognate T cells. These effects were likely tied to changes in the organization of the cytoskeleton. Recently, myosin 1c was identified to be co-localized with MHC class II molecules and recruited on the B cell side of the synapse (241). Our data demonstrate that dietary composition influences the APC side of the synapse, and indirectly alters the T cell side by targeting MHC class II.

Some studies suggest that naïve B cells do not efficiently activate naïve T cells or do so only under certain circumstances (242, 243). Due to this limitation, we felt that it was imperative to establish the time course of naïve B-naïve T cell synapse formation. In our model system, we found the maximum amount of MHC class II and PKCθ localized at the synapse after 30 minutes of conjugation. Watson et al. also found maximal PKCθ localization at 30 minutes with naïve APCs and naïve T cells in a similar transgenic system with BALB/c mice (231). However, the population of APCs used in their study was splenocytes and not purified B cells. Another study also reported the formation of a mature synapse using human naïve B and naïve T cells, but the kinetics were not reported (138).

Fish oil versus pharmacological disruption of the lateral organization of MHC class II in the absence of the synapse

MHC class II organization is critical for immunological synapse formation and its function is dependent on the residing lipid environment (244). MHC class II molecules

reside in lipid raft-like domains to enhance antigen presentation to T cells (245, 246). Some have even proposed that newly synthesized MHC class II molecules are trafficked to lipid raft domains prior to antigen loading (247). Since we previously demonstrated that fish oil diminished B cell lipid microdomain clustering induced by cholera toxin cross-linking (227), we expected MHC class II organization would be disrupted with n-3 fatty acids (in the absence of a synapse). However, contrary to our expectation, our data showed no effect of fish oil on the lateral organization of MHC class II molecules prior to the formation of an immunological synapse. Perhaps, we were unable to detect subtle changes considering that a fraction of MHC class II molecules are pre-clustered on the B cell surface (248). However, another study showed that primary B cells displayed MHC class II clustering upon exposure to antigen (234). Our data support this notion, as we observed no changes in MHC class II lateral organization in the absence of antigen.

Given that little is known about the molecular organization of the APC side of the synapse, we compared the effects of fish oil to known disrupters of membrane organization. Treatment of B cells with pharmacological agents provided varying results on MHC class II organization. Previously, Vrljic et al. showed that removal of cholesterol with MβCD decreased MHC class II diffusion (235). Our TIRF data appear to be in agreement with this study. Removing cholesterol from the plasma membrane generates solid-like domains (containing lipids with a high melting temperature) (235). This process slows protein diffusion and limits the number of protein clusters dispersed on the plasma membrane. The actin cytoskeleton also serves a role in clustering or corralling molecules on the plasma membrane surface. It was previously demonstrated

that cytochalasin D treatment of B cells did not change the lateral organization of MHC class II molecules (233). Umemura et al. explains this by showing that MHC class II actually undergoes hop diffusion in the plasma membrane (249). Our data suggest that the cytoskeleton may impact nanoscale spatial distribution of MHC class II molecules but may not completely remodel the surface organization observed at the micron scale. Taken together, our data show that in the absence of the synapse, fish oil and pharmacological agents have distinct effects on B cell MHC class II organization.

Fish oil, similar to pharmacological agents, inhibits the ability of B cells to organize MHC class II molecules at the immunological synapse

Although we previously reported B cells isolated from mice fed a fish oil diet suppressed T cell IL-2 secretion (227), we did not investigate the underlying mechanism at the level of the immunological synapse. Our data suggest the downstream functional effects reported previously by our lab and others are driven, in part, by an inability of MHC class II molecules to recruit to the synapse and thereby prevent recruitment of PKCθ, which is an early marker for stable formation of an immunological synapse (132).

We did not observe an effect of fish oil on B cell adhesion or surface expression of MHC class II (data not shown). It was previously reported that human B lymphoblasts treated with DHA *in vitro* could evade lysis by alloreactive human $CD8^+$ T cells as a result of an inability to conjugate (162). Similarly, Stulnig and co-workers reported that EPA treatment of T cells could suppress the formation of the synapse by diminishing APC-T cell conjugation (128). Furthermore, fish oil supplementation in humans was shown to decrease the expression of adhesion molecules and MHC class II levels in monocytes, which prevented antigen presentation to autologous lymphocytes (70, 250).

Therefore, we conducted extensive studies on B cell adhesion to known ligands (data not shown) and found no effect of fish oil. Furthermore, we conducted select studies in which we treated immortal Raji B cells with n-3 fatty acids and indeed discovered that cell adhesion with Jurkat T cells was suppressed *in vitro* (data not shown). Thus, we reconcile our data with those of others based on differences between treatment in cell culture and administration of dietary fish oil to animals.

We relied on pharmacological agents to disrupt B cells to compare with the effects of fish oil. Although there were differential effects on MHC class II clustering prior to synapse formation, both MβCD treatment and dietary manipulation of B cells resulted in diminished localization of MHC class II and PKCθ at the immunological synapse. This finding is consistent with evidence that treatment of either B or T cells with MβCD results in inhibition of T cell activation (251-253). Likewise, cytoskeletal disruption of B or T cells similarly results in inhibition of T cell activation (252, 254, 255). Although we did not find a statistically significant reduction in MHC class II localization to the synapse with cytochalasin D treatment, we did observe a trend (P=0.06). Pharmacological disruption of membrane organization appears to have a similar functional impact on synapse protein localization to that of fish oil.

Fish oil suppresses T cell activation by targeting both B and T cells

Figure 5.6 shows how fish oil impacts both B and T cells during the formation of the immunological synapse. Shown in red are results from this study (Figure 5.6). Fish oil modifies the composition of the B cell plasma membrane and directly suppresses MHC class II localization and thereby prevents PKCθ recruitment into the immunological synapse (Figure 5.6). Shown in blue are results from previous studies

Figure 5.6

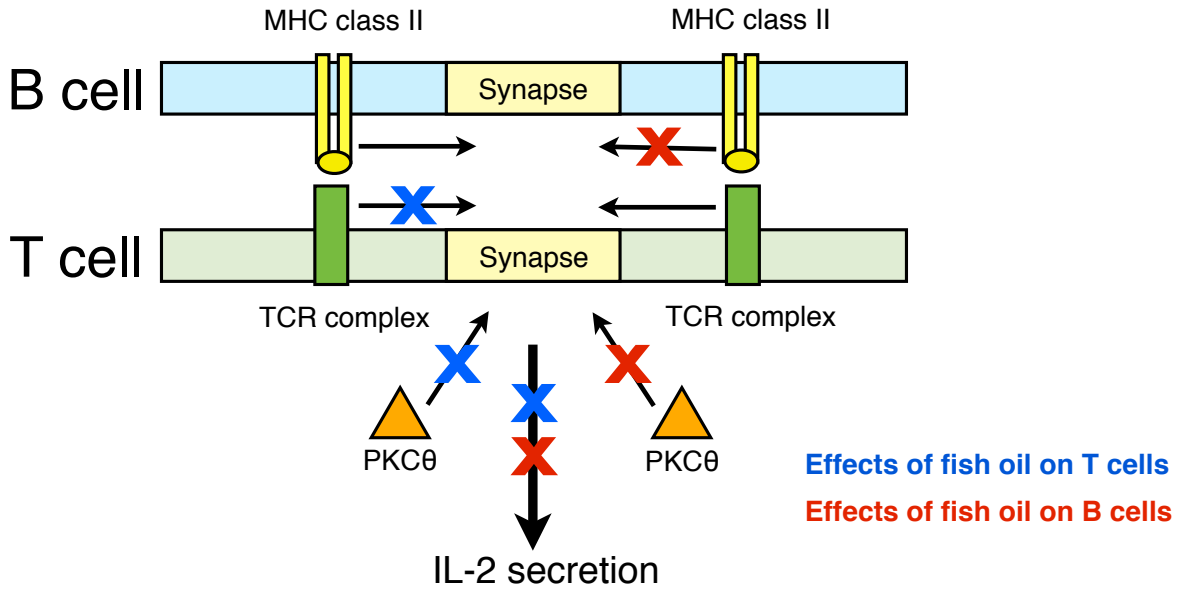

Figure 5.6: Fish oil suppresses CD4⁺ T cell activation by targeting both B and T cells. MHC class II proteins localize to the immunological synapse on the surface of B cells (top) to present antigen to T cells (bottom). CD3ε and PKCθ localize to the immunological synapse in response to antigen stimulation by the APC, ultimately promoting downstream cytokine secretion. The cumulative work from this study and those of others show fish oil can block the process of CD4⁺ T cell activation by targeting molecular organization of both B cells (shown in red) and T cells (shown in blue).

from other labs focusing on the impact of n-3 fatty acids on T cells (Figure 5.6) (139, 140). For instance, Kim et al. show that *fat-1* mouse $CD4^+$ T cells have reduced PKCθ localization to the site of CD3/CD28 binding (140). The same group later showed that mitochondrial localization and subsequent calcium signaling was also impaired by n-3 fatty acids in the same model system (141). Combined with our previous findings of reduced T cell activation by B cells and those of others on the T cell side, we propose that fish oil exerts very similar effects on the both sides of the synapse to suppress T cell activation (Figure 5.6) (139-141).

In summary, our data demonstrate a novel mechanism to explain how fish oil suppresses T cell activation. We specifically demonstrate that fish oil can target MHC class II organization in the synapse, which has an impact on the T cell side. Furthermore, this is the first evidence demonstrating that the molecular organization of the APC side of the immunological synapse is sensitive to dietary fish oil lipids. This work significantly expands our understanding of how fish oil, modeling current clinical use, can exert immunosuppressive effects.

CHAPTER 6: CONCLUSIONS

Overview

Using various high and low fat n-3 PUFA mouse diet models, we have established how n-3 PUFAs can target lipid-protein organization and thereby B cell antigen presentation. In doing so, we have advanced the field of n-3 PUFAs in a number of areas. We demonstrated that a physiologically relevant dose of fish oil dispersed clustering of B cell lipid rafts on a micron scale, and enhanced membrane molecular order upon cross-linking CTx-B. We found that the effects on lipid rafts are primarily driven by DHA and not EPA, and that n-3 PUFAs have a limited influence on non-raft lateral organization. We also demonstrate reduced activity when consuming very high doses of n-3 PUFAs. Finally, we show that fish oil suppresses B cell antigen presentation and subsequent $CD4^+$ T cell IL-2 secretion, by disrupting the B cell side of the immunological synapse. While we have not solved all the mechanisms for how fish oil can exert immunosuppressive effects on B cells, we have demonstrated that plasma membrane lateral organization plays a critical role in this process.

The challenge of studying lipid rafts

A major limitation for studying lipid rafts is the lack of clear evidence for the specific structure and function of these membrane domains (114). Detergent extraction has some success as a predictive tool for which proteins may be localized to lipid raft domains, but this method is also very prone to inducing artifacts because of the harsh nature of detergents (158, 159). In Chapter 4 we used detergent extraction and HPLC/GC methods to determine the alteration in phospholipid acyl chain profile upon fish oil consumption. However, in Chapters 2, 4 and 5, we also relied heavily on a combination

of imaging techniques, such as FRET, TIRF, and generalized polarization, to support our findings from the lipid extraction and biochemical techniques. Mass spectrometry and other advances in lipidomics will give additional details about novel acylation of lipids or proteins by EPA/DHA. These added resources would provide tremendous benefit for finding new targets that may provide better insight into how fish oil disrupts lipid raft clustering. Here our studies provided clear visual evidence that fish oil disrupts plasma membrane domains of B cells, and we have gained some insight into how this disruption occurs.

DHA, a distinct disrupter of raft clustering

EPA and DHA do not behave identically in targeting the plasma membrane. In Figure 4.5, we show that DHA has a much more dramatic effect on plasma membrane molecular order than EPA. We also have previously shown that treatment of EL4 cells with DHA, but not EPA, disrupted lipid raft clustering (150). The Fenton lab has since confirmed this finding in animals through specific mouse diet models (manuscript in preparation). One explanation for this may be that, when DHA is incorporated into PCs, it is twice as likely as EPA to localize in a raft-like domain (256). Inside a raft domain, without a stimulus to preserve the molecular packing and order, the highly dynamic biophysical properties of DHA would displace cholesterol and proteins. However, most DHA and EPA incorporate into PEs, which localize primarily on the inner leaflet of the plasma membrane in non-raft like domains (Figure 4.1). Yet, as we have shown in Chapter 2, non-raft proteins are not as sensitive to disrupted clustering as raft proteins. These findings establish DHA as a potent disrupter of lipid raft clustering, and could

possibly yield functional differences in antigen presentation, compared to EPA, which should be explored in the future.

Raft clustering is dispersed on the sub-micron scale

One of the significant questions we set out to answer was what effect the increased visible raft size has on molecular order and the nanoscale raft environment. Lipid rafts are defined as highly ordered in nature, yet n-3 PUFAs, DHA most of all, are highly disordered in nature, having a high degree of conformational mobility (105, 116). In Chapter 4, we used generalized polarization measurements to test molecular order with a unique florescent probe di-4-ANEPPDHQ. This probe is environmentally sensitive and displays an increased charge separation when excited in polar solvents (257, 258). The charge separation yields an increased dipole moment resulting in a red shift in its fluorescent emission. The calculation of membrane order is dependent on the change in water molecule penetration into the plasma membrane (259). Without a stimulus such as CTx-B cross-linking or immunological synapse formation, molecular order was decreased in B cells from the fish oil diet (Figure 4.3). Since solvent penetration is directly dependent on membrane packing order with this probe, it seems unlikely that this decrease in order was an artifact of just solvent penetration. Once a stimulus like the immunological synapse forms, DHA-PCs, unlike EPA-PCs, can interact with cholesterol, allowing for recovery in molecular order (256). This is exactly what we found in Figure 4.3. The change in order before and after cross-linking was significantly elevated with fish oil.

In Chapter 5 we demonstrate that although synapse formation occurs, the proteins vital for signaling have been displaced from the site of the immunological

synapse. MHC class II shows a trend toward nanoscale disrupted clustering, and a significant decrease in synapse localization (Figure 5.4). Although we did not measure molecular order at the synapse in B cells, there is evidence for n-3 PUFAs to actually enhance molecular order at the T cell side of the immunological synapse (140). Taken together, we propose a model to describe how DHA disrupts lipid raft clustering by creating a network of disrupted nanoscale size raft pieces, which DHA-PCs separate (Figure 6.1A). Disrupting raft clustering also frees GM1 clustering, which would allow for more binding of CTx-B (181). These pieces are now more easily extensively cross-linked generating the increased visualized size. In a model of the immunological synapse, which has raft-like properties, a similar process would occur (Figure 6.2B). EPA and DHA-PEs have little affect on synapse organization. On the other hand, DHA-PC in the synapse recruits cholesterol and slows MHC class II recruitment, disrupting synapse organization and, ultimately, T cell activation.

B cells are critical for autoimmune diseases

We focused our studies on B cells, a cell type underrepresented in experiments with n-3 PUFAs, especially at the animal level. What we discovered in Chapter 5 was B cells are targetable in antigen presentation critical for subsequent $CD4^+$ T cell activation. This is an important finding for autoimmune diseases such as rheumatoid arthritis, lupus, allograft rejection, and chronic allergic lung disease, where directed targeting of B cell antigen presentation would have clinical utility. In addition, n-3 PUFAs have been shown to promote a T helper 2 (Th2) response instead of a T helper 1 (Th1) response (260-264). Th1 cells produce pro-inflammatory cytokines IL-2, IFN-γ, and TNF-α, while Th2 cells produce anti-inflammatory cytokines IL-4, IL-5, IL-6, IL-9, IL-10, and IL-13

Figure 6.1

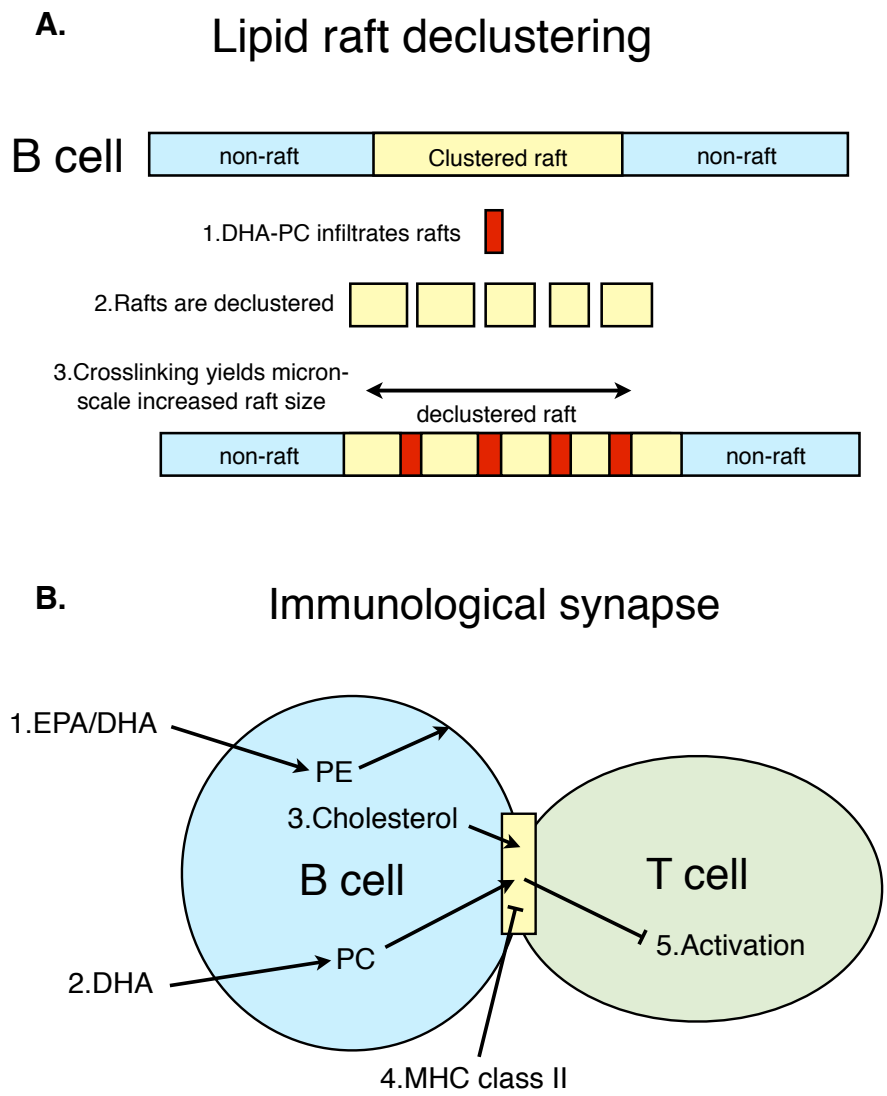
A.
Lipid raft declustering
B cell
non-raft
Clustered raft
non-raft
1.DHA-PC infiltrates rafts
2.Rafts are declustered
3.Crosslinking yields micron-scale increased raft size
declustered raft
non-raft
non-raft
B.
Immunological synapse
1.EPA/DHA
PE
3.Cholesterol
B cell
T cell
5.Activation
PC
2.DHA
4.MHC class II
C.
Fish oil
B cells
?
Th1 T cell response
Th2 T cell response
Beneficial impact:
Rheumatoid arthritis
Allograft rejection
Inflammation
Negative impact:
Allergies
Lung inflammation

Figure 6.1: DHA disrupts lipid raft clustering and the immunological synapse. A) DHA-PC (red) can localize into clustered lipid rafts (yellow). This declusters the raft and when cross-linked the micron scale size appears larger. B) In B cells EPA/DHA can incorporate into the plasma membrane as PEs, but localize outside of the immunological synapse (yellow). DHA incorporated as PC can localize in the synapse along with cholesterol. This displaces signaling proteins such as MHC class II for the site of the immunological synapse, diminishing T cell activation. C) Overview of potential positive and negative affect of fish oil consumption on cell mediated and humoral immune response.

(265). Th2 cells are protective in diseases such as rheumatoid arthritis, type 1 diabetes, and multiple sclerosis, whereas Th1 cells are pathogenic (266). However, promoting Th2 immunity may not be universally beneficial. For example, in the case of lung inflammation disorders like allergic asthma, a Th2 response enhances progression of the disease (267-269). Though not fully investigated, this study demonstrates that fish oil in B cells may contribute to Th2/Th1 as evidenced by the reduced IL-2 secretion though disrupted antigen presentation (Figure 4.7B). While there are many important potential pathways to which fish oil can contribute, the implications of membrane disruption could lead to breakthroughs in other disease models. In Figure 6.1C is an outline describing these implications. A shift from Th1 to Th2 would decrease cell mediated immune response and increase the humoral immune response. This would not be universally beneficial for all diseases. In addition, studies looking at the other functions of B cells such as antibody production will further determine the utility of fish oil supplementation.

Precaution for high doses of fish oil

Once the mechanisms are better established, moving fish oil into the clinic will still have other considerations. One of these is the dosing necessary for clinical efficacy. The dose of fish oil used in many other studies varies widely, and dosing remains one of the larger challenges for strengthening our understanding of how fish oil exerts its effects (52). Our novel findings of body weight gain and energy expenditure reductions shown in Chapter 3 raise questions that must be addressed for proper clinical and dietary recommendations. Although fish oil is a source of EPA and DHA, these fatty acids only make up a modest percentage of the total fatty acid profile of fish oil. Analysis

of our fish oil diets shows a full fatty acid profile (Supplemental Table 2.1). In addition, there are some additional contaminants from consuming fish or fish oil including: methylmercury, dioxins, polychlorinated biphenyls, and organic pollutants from industrial processing (270). Monitoring the metabolic implications and dietary formulation for fish oil supplementation should be done in combination with any clinical studies moving forward.

Conclusion

Taken together, this work highlights the utility of fish oil, more specifically DHA, as a tool for disrupting plasma membrane lateral organization. We add to the biochemical understanding of how these fatty acids may disrupt various downstream signaling events and cell-cell interactions. It also emphasizes the importance of the plasma membrane as a target for suppressing other cellular functions mediated through lipid raft domains. Finally, these studies add B cells as key targets for suppression of antigen presentation in diseases such as rheumatoid arthritis.

REFERENCES

1. Tur, J. A., Bibiloni, M. M., Sureda, A., and Pons, A. (2012) Dietary sources of omega 3 fatty acids: public health risks and benefits. *Br J Nutr* **107 Suppl 2**, S23–52.
2. Galli, C., and Calder, P. C. (2009) Effects of fat and fatty acid intake on inflammatory and immune responses: a critical review. *Ann Nutr Metab* **55**, 123–139.
3. Kromann, N., and Green, A. (1980) Epidemiological studies in the Upernavik district, Greenland. Incidence of some chronic diseases 1950-1974. *Acta Med Scand* **208**, 401–406.
4. Dyerberg, J., Bang, H. O., and Hjorne, N. (1975) Fatty acid composition of the plasma lipids in Greenland Eskimos. *Am J Clin Nutr* **28**, 958–966.
5. Bang, H. O., Dyerberg, J., and Sinclair, H. M. (1980) The composition of the Eskimo food in north western Greenland. *Am J Clin Nutr* **33**, 2657–2661.
6. Feskens, E. J., and Kromhout, D. (1993) Epidemiologic studies on Eskimos and fish intake. *Ann N Y Acad Sci* **683**, 9–15.
7. Nagata, C., Takatsuka, N., and Shimizu, H. (2002) Soy and fish oil intake and mortality in a Japanese community. *Am. J. Epidemiol.* **156**, 824–831.
8. Okuyama, H., Kobayashi, T., and Watanabe, S. (1996) Dietary fatty acids--the N-6/N-3 balance and chronic elderly diseases. Excess linoleic acid and relative N-3 deficiency syndrome seen in Japan. *Prog Lipid Res* **35**, 409–457.
9. Breslow, J. L. (2006) n-3 fatty acids and cardiovascular disease. *Am J Clin Nutr* **83**, 1477S–1482S.
10. Harris, W. S. (2005) Extending the cardiovascular benefits of omega-3 Fatty acids. *Curr Atheroscler Rep* **7**, 375–380.

11. Kris-Etherton, P. M., Harris, W. S., Appel, L. J., Nutrition Committee (2003) Fish consumption, fish oil, omega-3 fatty acids, and cardiovascular disease. *Arterioscler. Thromb. Vasc. Biol.* **23**, e20–30.

12. Harper, C. R., and Jacobson, T. A. (2001) The fats of life: the role of omega-3 fatty acids in the prevention of coronary heart disease. *Arch. Intern. Med.* **161**, 2185–2192.

13. Delgado-Lista, J., Perez-Martinez, P., Lopez-Miranda, J., and Perez-Jimenez, F. (2012) Long chain omega-3 fatty acids and cardiovascular disease: a systematic review. *Br J Nutr* **107 Suppl 2**, S201–13.

14. Larsson, S. C., Kumlin, M., Ingelman-Sundberg, M., and Wolk, A. (2004) Dietary long-chain n-3 fatty acids for the prevention of cancer: a review of potential mechanisms. *Am J Clin Nutr* **79**, 935–945.

15. Turk, H. F., and Chapkin, R. S. (2012) Membrane lipid raft organization is uniquely modified by n-3 polyunsaturated fatty acids. *Prostaglandins Leukot Essent Fatty Acids.* Article in press, doi:10.1016/j.plefa.2012.03.008.

16. Gerber, M. (2012) Omega-3 fatty acids and cancers: a systematic update review of epidemiological studies. *Br J Nutr* **107 Suppl 2**, S228–39.

17. Calder, P. C. (2006) n-3 polyunsaturated fatty acids, inflammation, and inflammatory diseases. *Am J Clin Nutr* **83**, 1505S–1519S.

18. Cleland, L. G., James, M. J., and Proudman, S. M. (2003) The role of fish oils in the treatment of rheumatoid arthritis. *Drugs* **63**, 845–853.

19. Miles, E. A., and Calder, P. C. (2012) Influence of marine n-3 polyunsaturated fatty acids on immune function and a systematic review of their effects on clinical

outcomes in rheumatoid arthritis. *Br J Nutr* **107 Suppl 2**, S171–84.

20. Cabré, E., Mañosa, M., and Gassull, M. A. (2012) Omega-3 fatty acids and inflammatory bowel diseases - a systematic review. *Br J Nutr* **107 Suppl 2**, S240–52.
21. Dangour, A. D., Andreeva, V. A., Sydenham, E., and Uauy, R. (2012) Omega 3 fatty acids and cognitive health in older people. *Br J Nutr* **107 Suppl 2**, S152–8.
22. Campoy, C., Escolano-Margarit, M. V., Anjos, T., Szajewska, H., and Uauy, R. (2012) Omega 3 fatty acids on child growth, visual acuity and neurodevelopment. *Br J Nutr* **107 Suppl 2**, S85–S106.
23. Ortega, R. M., Rodríguez-Rodríguez, E., and López-Sobaler, A. M. (2012) Effects of omega 3 fatty acids supplementation in behavior and non-neurodegenerative neuropsychiatric disorders. *Br J Nutr* **107 Suppl 2**, S261–70.
24. Calder, P. C. (1997) N-3 polyunsaturated fatty acids and immune cell function. *Adv Enzyme Regul* **37**, 197–237.
25. Nakamura, M. T., and Nara, T. Y. (2004) Structure, function, and dietary regulation of delta6, delta5, and delta9 desaturases. *Annu Rev Nutr* **24**, 345–376.
26. Ferdinandusse, S., Denis, S., Dacremont, G., and Wanders, R. J. A. (2003) Studies on the metabolic fate of n-3 polyunsaturated fatty acids. *J Lipid Res* **44**, 1992–1997.
27. Poumès-Ballihaut, C., Langelier, B., Houlier, F., Alessandri, J. M., Durand, G., Latge, C., and Guesnet, P. (2001) Comparative bioavailability of dietary alpha-linolenic and docosahexaenoic acids in the growing rat. *Lipids* **36**, 793–800.
28. Cunnane, S. C., and Anderson, M. J. (1997) The majority of dietary linoleate in

growing rats is beta-oxidized or stored in visceral fat. *J Nutr* **127**, 146–152.

29. Giltay, E. J., Gooren, L. J. G., Toorians, A. W. F. T., Katan, M. B., and Zock, P. L. (2004) Docosahexaenoic acid concentrations are higher in women than in men because of estrogenic effects. *Am J Clin Nutr* **80**, 1167–1174.

30. Pawlosky, R. J., Hibbeln, J. R., Novotny, J. A., and Salem, N. (2001) Physiological compartmental analysis of alpha-linolenic acid metabolism in adult humans. *J Lipid Res* **42**, 1257–1265.

31. Barceló-Coblijn, G., Collison, L. W., Jolly, C. A., and Murphy, E. J. (2005) Dietary alpha-linolenic acid increases brain but not heart and liver docosahexaenoic acid levels. *Lipids* **40**, 787–798.

32. Barceló-Coblijn, G., and Murphy, E. J. (2009) Alpha-linolenic acid and its conversion to longer chain n-3 fatty acids: benefits for human health and a role in maintaining tissue n-3 fatty acid levels. *Prog Lipid Res* **48**, 355–374.

33. Mohrhauer, H., Christiansen, K., Gan, M. V., Deubig, M., and Holman, R. T. (1967) Chain elongation of linoleic acid and its inhibition by other fatty acids in vitro. *J Biol Chem* **242**, 4507–4514.

34. Brenner, R. R., and Peluffo, R. O. (1966) Effect of saturated and unsaturated fatty acids on the desaturation in vitro of palmitic, stearic, oleic, linoleic, and linolenic acids. *J Biol Chem* **241**, 5213–5219.

35. Spychalla, J. P., Kinney, A. J., and Browse, J. (1997) Identification of an animal omega-3 fatty acid desaturase by heterologous expression in Arabidopsis. *Proc Natl Acad Sci USA* **94**, 1142–1147.

36. Kang, J. X., Wang, J., Wu, L., and Kang, Z. B. (2004) Transgenic mice: fat-1 mice

convert n-6 to n-3 fatty acids. *Nature* **427**, 504.

37. Aranceta, J., and Pérez-Rodrigo, C. (2012) Recommended dietary reference intakes, nutritional goals and dietary guidelines for fat and fatty acids: a systematic review. *Br J Nutr* **107 Suppl 2**, S8–S22.
38. Harris, W. S. (2007) International recommendations for consumption of long-chain omega-3 fatty acids. *J Cardiovasc Med* **8 Suppl 1**, S50–2.
39. Molendi-Coste, O., Legry, V., and Leclercq, I. A. (2011) Why and How Meet n-3 PUFA Dietary Recommendations? *Gastroenterol Res Pract* **2011**, 364040.
40. Gebauer, S. K., Psota, T. L., Harris, W. S., and Kris-Etherton, P. M. (2006) n-3 fatty acid dietary recommendations and food sources to achieve essentiality and cardiovascular benefits. *Am J Clin Nutr* **83**, 1526S–1535S.
41. Lauritzen, L., and Hansen, H. S. (2003) Which of the n-3 FA should be called essential? *Lipids* **38**, 889–891.
42. Arterburn, L. M., Hall, E. B., and Oken, H. (2006) Distribution, interconversion, and dose response of n-3 fatty acids in humans. *Am J Clin Nutr* **83**, 1467S–1476S.
43. Moghadasian, M. H. (2008) Advances in dietary enrichment with n-3 fatty acids. *Crit Rev Food Sci Nutr* **48**, 402–410.
44. *Omega-3 Foods and Beverages in the U.S.* (2011) *Omega-3 Foods and Beverages in the U.S.*, 3rd Ed, Packaged Facts [online] http://www.packagedfacts.com/Omega-Foods-Beverages-6168781/.
45. Valenzuela, A., Valenzuela, V., Sanhueza, J., and Nieto, S. (2005) Effect of supplementation with docosahexaenoic acid ethyl ester and sn-2 docosahexaenyl monoacylglyceride on plasma and erythrocyte fatty acids in rats.

Ann Nutr Metab **49**, 49–53.

46. Ikeda, I., Sasaki, E., Yasunami, H., Nomiyama, S., Nakayama, M., Sugano, M., Imaizumi, K., and Yazawa, K. (1995) Digestion and lymphatic transport of eicosapentaenoic and docosahexaenoic acids given in the form of triacylglycerol, free acid and ethyl ester in rats. *Biochim Biophys Acta* **1259**, 297–304.
47. Yang, L. Y., Kuksis, A., and Myher, J. J. (1990) Intestinal absorption of menhaden and rapeseed oils and their fatty acid methyl and ethyl esters in the rat. *Biochem. Cell Biol.* **68**, 480–491.
48. Yang, L. Y., Kuksis, A., and Myher, J. J. (1990) Lipolysis of menhaden oil triacylglycerols and the corresponding fatty acid alkyl esters by pancreatic lipase in vitro: a reexamination. *J Lipid Res* **31**, 137–147.
49. Qi, K., Fan, C., Jiang, J., Zhu, H., Jiao, H., Meng, Q., and Deckelbaum, R. J. (2008) Omega-3 fatty acid containing diets decrease plasma triglyceride concentrations in mice by reducing endogenous triglyceride synthesis and enhancing the blood clearance of triglyceride-rich particles. *Clin Nutr* **27**, 424–430.
50. Davidson, M. H., Stein, E. A., Bays, H. E., Maki, K. C., Doyle, R. T., Shalwitz, R. A., Ballantyne, C. M., Ginsberg, H. N., and COMBination of prescription Omega-3 with Simvastatin COMBOS Investigators (2007) Efficacy and tolerability of adding prescription omega-3 fatty acids 4 g/d to simvastatin 40 mg/d in hypertriglyceridemic patients: an 8-week, randomized, double-blind, placebo-controlled study. *Clin Ther* **29**, 1354–1367.
51. Hoy, S. M., and Keating, G. M. (2009) Omega-3 Ethylester Concentrate. *Drugs* **69**, 1077–1105

52. Kim, W., McMurray, D. N., and Chapkin, R. S. (2010) n-3 polyunsaturated fatty acids-physiological relevance of dose. *Prostaglandins Leukot Essent Fatty Acids* **82**, 155–158.

53. Sijben, J. W. C., and Calder, P. C. (2007) Differential immunomodulation with long-chain n-3 PUFA in health and chronic disease. *Proc Nutr Soc* **66**, 237–259.

54. Calder, P. C. (2007) Immunomodulation by omega-3 fatty acids. *Prostaglandins Leukot Essent Fatty Acids* **77**, 327–335.

55. Akhtar Khan, N. (2010) Polyunsaturated fatty acids in the modulation of T-cell signalling. *Prostaglandins Leukot Essent Fatty Acids* **82**, 179–187.

56. Kaushansky, K. (2006) Lineage-specific hematopoietic growth factors. *N Engl J Med* **354**, 2034–2045.

57. Schmid-Schönbein, G. W. (2006) Analysis of inflammation. *Annu Rev Biomed Eng* **8**, 93–131.

58. Freund, A., Orjalo, A. V., Desprez, P.-Y., and Campisi, J. (2010) Inflammatory networks during cellular senescence: causes and consequences. *Trends Mol Med* **16**, 238–246.

59. Tipping, P. G. (2006) Toll-like receptors: the interface between innate and adaptive immunity. *J. Am. Soc. Nephrol.* **17**, 1769–1771.

60. Hoebe, K., Janssen, E., and Beutler, B. (2004) The interface between innate and adaptive immunity. *Nat Immunol* **5**, 971–974.

61. Virella, G., Fourspring, K., Hyman, B., Haskill-Stroud, R., Long, L., Virella, I., La Via, M., Gross, A. J., and Lopes-Virella, M. (1991) Immunosuppressive effects of fish oil in normal human volunteers: correlation with the in vitro effects of

eicosapentanoic acid on human lymphocytes. *Clin. Immunol. Immunopathol.* **61**, 161–176.

62. Calder, P. C., and Newsholme, E. A. (1992) Polyunsaturated fatty acids suppress human peripheral blood lymphocyte proliferation and interleukin-2 production. *Clin Sci* **82**, 695–700.

63. Yaqoob, P., Newsholme, E. A., and Calder, P. C. (1994) The effect of dietary lipid manipulation on rat lymphocyte subsets and proliferation. *Immunology* **82**, 603–610.

64. Jolly, C. A., Jiang, Y. H., Chapkin, R. S., and McMurray, D. N. (1997) Dietary (n-3) polyunsaturated fatty acids suppress murine lymphoproliferation, interleukin-2 secretion, and the formation of diacylglycerol and ceramide. *J Nutr* **127**, 37–43.

65. Tricon, S., Burdge, G. C., Kew, S., Banerjee, T., Russell, J. J., Grimble, R. F., Williams, C. M., Calder, P. C., and Yaqoob, P. (2004) Effects of cis-9,trans-11 and trans-10,cis-12 conjugated linoleic acid on immune cell function in healthy humans. *Am J Clin Nutr* **80**, 1626–1633.

66. Kelley, D. S., and Erickson, K. L. (2003) Modulation of body composition and immune cell functions by conjugated linoleic acid in humans and animal models: benefits vs. risks. *Lipids* **38**, 377–386.

67. Yaqoob, P., and Calder, P. (1995) Effects of dietary lipid manipulation upon inflammatory mediator production by murine macrophages. *Cell Immunol* **163**, 120–128.

68. Zeyda, M., Säemann, M. D., Stuhlmeier, K. M., Mascher, D. G., Nowotny, P. N., Zlabinger, G. J., Waldhäusl, W., and Stulnig, T. M. (2005) Polyunsaturated fatty

acids block dendritic cell activation and function independently of NF-kappa B activation. *J Biol Chem* **280**, 14293–14301.

69. Fujikawa, M., Yamashita, N., Yamazaki, K., Sugiyama, E., Suzuki, H., and Hamazaki, T. (1992) Eicosapentaenoic acid inhibits antigen-presenting cell function of murine splenocytes. *Immunology* **75**, 330–335.
70. Hughes, D. A., and Pinder, A. C. (2000) n-3 polyunsaturated fatty acids inhibit the antigen-presenting function of human monocytes. *Am J Clin Nutr* **71**, 357S–60S.
71. Kim, W., Khan, N. A., McMurray, D. N., Prior, I. A., Wang, N., and Chapkin, R. S. (2010) Regulatory activity of polyunsaturated fatty acids in T-cell signaling. *Prog Lipid Res* **49**, 250–261.
72. Pompos, L. J., and Fritsche, K. L. (2002) Antigen-driven murine $CD4^+$ T lymphocyte proliferation and interleukin-2 production are diminished by dietary (n-3) polyunsaturated fatty acids. *J Nutr* **132**, 3293–3300.
73. Petursdottir, D. H., and Hardardottir, I. (2007) Dietary fish oil increases the number of splenic macrophages secreting TNF-alpha and IL-10 but decreases the secretion of these cytokines by splenic T cells from mice. *J Nutr* **137**, 665–670.
74. Kantor, A. B., and Herzenberg, L. A. (1993) Origin of murine B cell lineages. *Annu Rev Immunol* **11**, 501–538.
75. LeBien, T. W., and Tedder, T. F. (2008) B lymphocytes: how they develop and function. *Blood* **112**, 1570–1580.
76. Briles, D. E., Nahm, M., Schroer, K., Davie, J., Baker, P., Kearney, J., and Barletta, R. (1981) Antiphosphocholine antibodies found in normal mouse serum are protective against intravenous infection with type 3 streptococcus pneumoniae. *J*

Exp Med **153**, 694–705.

77. Haas, K. M., Poe, J. C., Steeber, D. A., and Tedder, T. F. (2005) B-1a and B-1b cells exhibit distinct developmental requirements and have unique functional roles in innate and adaptive immunity to S. pneumoniae. *Immunity* **23**, 7–18.
78. Petro, J. B., Gerstein, R. M., Lowe, J., Carter, R. S., Shinners, N., and Khan, W. N. (2002) Transitional type 1 and 2 B lymphocyte subsets are differentially responsive to antigen receptor signaling. *J Biol Chem* **277**, 48009–48019.
79. Martin, F., and Kearney, J. F. (2002) Marginal-zone B cells. *Nat Rev Immunol* **2**, 323–335.
80. Takahashi, Y., Dutta, P. R., Cerasoli, D. M., and Kelsoe, G. (1998) In situ studies of the primary immune response to (4-hydroxy-3-nitrophenyl)acetyl. V. Affinity maturation develops in two stages of clonal selection. *J Exp Med* **187**, 885–895.
81. McHeyzer-Williams, L. J., and McHeyzer-Williams, M. G. (2005) Antigen-specific memory B cell development. *Annu Rev Immunol* **23**, 487–513.
82. Crawford, A., Macleod, M., Schumacher, T., Corlett, L., and Gray, D. (2006) Primary T cell expansion and differentiation in vivo requires antigen presentation by B cells. *J Immunol* **176**, 3498–3506.
83. Linton, P.-J., Bautista, B., Biederman, E., Bradley, E. S., Harbertson, J., Kondrack, R. M., Padrick, R. C., and Bradley, L. M. (2003) Costimulation via OX40L expressed by B cells is sufficient to determine the extent of primary CD4 cell expansion and Th2 cytokine secretion in vivo. *J Exp Med* **197**, 875–883.
84. Constant, S., Schweitzer, N., West, J., Ranney, P., and Bottomly, K. (1995) B lymphocytes can be competent antigen-presenting cells for priming CD4+ T cells

to protein antigens in vivo. *J Immunol* **155**, 3734–3741.

85. Kurt-Jones, E. A., Liano, D., HayGlass, K. A., Benacerraf, B., Sy, M. S., and Abbas, A. K. (1988) The role of antigen-presenting B cells in T cell priming in vivo. Studies of B cell-deficient mice. *J Immunol* **140**, 3773–3778.

86. Takemura, S., Klimiuk, P. A., Braun, A., Goronzy, J. J., and Weyand, C. M. (2001) T cell activation in rheumatoid synovium is B cell dependent. *J Immunol* **167**, 4710–4718.

87. Chan, O. T., Hannum, L. G., Haberman, A. M., Madaio, M. P., and Shlomchik, M. J. (1999) A novel mouse with B cells but lacking serum antibody reveals an antibody-independent role for B cells in murine lupus. *J Exp Med* **189**, 1639–1648.

88. Noorchashm, H., Reed, A. J., Rostami, S. Y., Mozaffari, R., Zekavat, G., Koeberlein, B., Caton, A. J., and Naji, A. (2006) B cell-mediated antigen presentation is required for the pathogenesis of acute cardiac allograft rejection. *J Immunol* **177**, 7715–7722.

89. Lindell, D. M., Berlin, A. A., Schaller, M. A., and Lukacs, N. W. (2008) B cell antigen presentation promotes Th2 responses and immunopathology during chronic allergic lung disease. *PLoS ONE* **3**, e3129.

90. Reff, M. E., Carner, K., Chambers, K. S., Chinn, P. C., Leonard, J. E., Raab, R., Newman, R. A., Hanna, N., and Anderson, D. R. (1994) Depletion of B cells in vivo by a chimeric mouse human monoclonal antibody to CD20. *Blood* **83**, 435–445.

91. Cohen, S. B., Emery, P., Greenwald, M. W., Dougados, M., Furie, R. A., Genovese,

M. C., Keystone, E. C., Loveless, J. E., Burmester, G.-R., Cravets, M. W., Hessey, E. W., Shaw, T., Totoritis, M. C., REFLEX Trial Group (2006) Rituximab for rheumatoid arthritis refractory to anti-tumor necrosis factor therapy: Results of a multicenter, randomized, double-blind, placebo-controlled, phase III trial evaluating primary efficacy and safety at twenty-four weeks. *Arthritis Rheum.* **54**, 2793–2806.

92. Tak, P. P., Rigby, W. F., Rubbert-Roth, A., Peterfy, C. G., van Vollenhoven, R. F., Stohl, W., Hessey, E., Chen, A., Tyrrell, H., Shaw, T. M., IMAGE Investigators (2011) Inhibition of joint damage and improved clinical outcomes with rituximab plus methotrexate in early active rheumatoid arthritis: the IMAGE trial. *Ann. Rheum. Dis.* **70**, 39–46.

93. Kheirallah, S., Caron, P., Gross, E., Quillet-Mary, A., Bertrand-Michel, J., Fournié, J.-J., Laurent, G., and Bezombes, C. (2010) Rituximab inhibits B-cell receptor signaling. *Blood* **115**, 985–994.

94. Christensen, J. P., Kauffmann, S. Ø., and Thomsen, A. R. (2003) Deficient CD4+ T cell priming and regression of CD8+ T cell functionality in virus-infected mice lacking a normal B cell compartment. *J Immunol* **171**, 4733–4741.

95. Jump, D. B., and Clarke, S. D. (1999) Regulation of gene expression by dietary fat. *Annu Rev Nutr* **19**, 63–90.

96. Xu, H. E., Lambert, M. H., Montana, V. G., Parks, D. J., Blanchard, S. G., Brown, P. J., Sternbach, D. D., Lehmann, J. M., Wisely, G. B., Willson, T. M., Kliewer, S. A., and Milburn, M. V. (1999) Molecular recognition of fatty acids by peroxisome proliferator-activated receptors. *Mol Cell* **3**, 397–403.

97. Oh, D. Y., Talukdar, S., Bae, E. J., Imamura, T., Morinaga, H., Fan, W., Li, P., Lu, W. J., Watkins, S. M., and Olefsky, J. M. (2010) GPR120 is an omega-3 fatty acid receptor mediating potent anti-inflammatory and insulin-sensitizing effects. *Cell* **142**, 687–698.

98. Oh, D. Y., and Olefsky, J. M. (2012) Omega 3 fatty acids and GPR120. *Cell Metab.* **15**, 564–565.

99. Serhan, C. N., Hong, S., Gronert, K., Colgan, S. P., Devchand, P. R., Mirick, G., and Moussignac, R.-L. (2002) Resolvins: a family of bioactive products of omega-3 fatty acid transformation circuits initiated by aspirin treatment that counter proinflammation signals. *J Exp Med* **196**, 1025–1037.

100. Levy, B. D., Clish, C. B., Schmidt, B., Gronert, K., and Serhan, C. N. (2001) Lipid mediator class switching during acute inflammation: signals in resolution. *Nat Immunol* **2**, 612–619.

101. Serhan, C. N., Clish, C. B., Brannon, J., Colgan, S. P., Chiang, N., and Gronert, K. (2000) Novel functional sets of lipid-derived mediators with antiinflammatory actions generated from omega-3 fatty acids via cyclooxygenase 2-nonsteroidal antiinflammatory drugs and transcellular processing. *J Exp Med* **192**, 1197–1204.

102. Malkowski, M. G., Thuresson, E. D., Lakkides, K. M., Rieke, C. J., Micielli, R., Smith, W. L., and Garavito, R. M. (2001) Structure of eicosapentaenoic and linoleic acids in the cyclooxygenase site of prostaglandin endoperoxide H synthase-1. *J Biol Chem* **276**, 37547–37555.

103. Jump, D. B. (2002) The biochemistry of n-3 polyunsaturated fatty acids. *J Biol Chem* **277**, 8755–8758.

104. Serhan, C. N., and Petasis, N. A. (2011) Resolvins and protectins in inflammation resolution. *Chem. Rev.* **111**, 5922–5943.

105. Stillwell, W., and Wassall, S. R. (2003) Docosahexaenoic acid: membrane properties of a unique fatty acid. *Chem Phys Lipids* **126**, 1–27.

106. Feller, S. E., Gawrisch, K., and MacKerell, A. D. (2002) Polyunsaturated fatty acids in lipid bilayers: intrinsic and environmental contributions to their unique physical properties. *J Am Chem Soc* **124**, 318–326.

107. Shaikh, S. R., and Edidin, M. (2006) Polyunsaturated fatty acids, membrane organization, T cells, and antigen presentation. *Am J Clin Nutr* **84**, 1277–1289.

108. Singer, S. J., and Nicolson, G. L. (1972) The fluid mosaic model of the structure of cell membranes. *Science* **175**, 720–731.

109. Lindner, R., and Naim, H. Y. (2009) Domains in biological membranes. *Exp Cell Res* **315**, 2871–2878.

110. Simons, K., and Ikonen, E. (1997) Functional rafts in cell membranes. *Nature* **387**, 569–572.

111. Pike, L. J. (2006) Rafts defined: a report on the Keystone symposium on lipid rafts and cell function. *J Lipid Res* **47,** 1597–1598.

112. Brown, D. A., and London, E. (1998) Functions of lipid rafts in biological membranes. *Annu Rev Cell Dev Biol* **14**, 111–136.

113. Pike, L. J. (2003) Lipid rafts: bringing order to chaos. *J Lipid Res* **44**, 655–667.

114. Munro, S. (2003) Lipid rafts: elusive or illusive? *Cell* **115**, 377–388.

115. Leslie, M. (2011) Mysteries of the cell. Do lipid rafts exist? *Science* **334**, 1046–1047.

116. Pike, L. J. (2009) The challenge of lipid rafts. *J Lipid Res* **50 Suppl**, S323–8.

117. Simons, K., and Gerl, M. J. (2010) Revitalizing membrane rafts: new tools and insights. *Nat Rev Mol Cell Biol* **11**, 688–699.

118. Kenworthy, A. K. (2008) Have we become overly reliant on lipid rafts? Talking Point on the involvement of lipid rafts in T-cell activation. *EMBO Rep* **9**, 531–535.

119. Macdonald, J. L., and Pike, L. J. (2005) A simplified method for the preparation of detergent-free lipid rafts. *J Lipid Res* **46**, 1061–1067.

120. Ishitsuka, R., Sato, S. B., and Kobayashi, T. (2005) Imaging lipid rafts. *J Biochem* **137**, 249–254.

121. Marks, D. L., Bittman, R., and Pagano, R. E. (2008) Use of Bodipy-labeled sphingolipid and cholesterol analogs to examine membrane microdomains in cells. *Histochem Cell Biol* **130**, 819–832.

122. Radhakrishnan, A., Anderson, T. G., and McConnell, H. M. (2000) Condensed complexes, rafts, and the chemical activity of cholesterol in membranes. *Proc Natl Acad Sci USA* **97**, 12422–12427.

123. Sharma, P., Varma, R., Sarasij, R. C., Ira, Gousset, K., Krishnamoorthy, G., Rao, M., and Mayor, S. (2004) Nanoscale organization of multiple GPI-anchored proteins in living cell membranes. *Cell* **116**, 577–589.

124. Lingwood, D., and Simons, K. (2010) Lipid rafts as a membrane-organizing principle. *Science* **327**, 46–50.

125. Suzuki, K. G. N., Kasai, R. S., Hirosawa, K. M., Nemoto, Y. L., Ishibashi, M., Miwa, Y., Fujiwara, T. K., and Kusumi, A. (2012) Transient GPI-anchored protein homodimers are units for raft organization and function. *Nat Chem Biol* **9**, 774–

783.

126. Shaikh, S. R., Cherezov, V., Caffrey, M., Stillwell, W., and Wassall, S. R. (2003) Interaction of cholesterol with a docosahexaenoic acid-containing phosphatidylethanolamine: trigger for microdomain/raft formation? *Biochemistry* **42**, 12028–12037.

127. Stulnig, T. M., Berger, M., Sigmund, T., Raederstorff, D., Stockinger, H., and Waldhausl, W. (1998) Polyunsaturated fatty acids inhibit T cell signal transduction by modification of detergent-insoluble membrane domains. *J Cell Biol* **143**, 637–644.

128. Stulnig, T. M., Huber, J., Leitinger, N., Imre, E. M., Angelisova, P., Nowotny, P., and Waldhausl, W. (2001) Polyunsaturated eicosapentaenoic acid displaces proteins from membrane rafts by altering raft lipid composition. *J Biol Chem* **276**, 37335–37340.

129. Stillwell, W., Shaikh, S. R., Zerouga, M., Siddiqui, R., and Wassall, S. R. (2005) Docosahexaenoic acid affects cell signaling by altering lipid rafts. *Reprod Nutr Dev* **45**, 559–579.

130. Wassall, S. R., and Stillwell, W. (2008) Docosahexaenoic acid domains: the ultimate non-raft membrane domain. *Chem Phys Lipids* **153**, 57–63.

131. Dykstra, M., Cherukuri, A., Sohn, H. W., Tzeng, S.-J., and Pierce, S. K. (2003) Location is everything: lipid rafts and immune cell signaling. *Annu Rev Immunol* **21**, 457–481.

132. Bromley, S. K., Burack, W. R., Johnson, K. G., Somersalo, K., Sims, T. N., Sumen, C., Davis, M. M., Shaw, A. S., Allen, P. M., and Dustin, M. L. (2001) The

immunological synapse. *Annu Rev Immunol* **19**, 375–396.

133. Fooksman, D. R., Vardhana, S., Vasiliver-Shamis, G., Liese, J., Blair, D. A., Waite, J., Sacristán, C., Victora, G. D., Zanin-Zhorov, A., and Dustin, M. L. (2010) Functional anatomy of T cell activation and synapse formation. *Annu Rev Immunol* **28**, 79–105.

134. Friedl, P., Boer, den, A. T., and Gunzer, M. (2005) Tuning immune responses: diversity and adaptation of the immunological synapse. *Nat Rev Immunol* **5**, 532–545.

135. McKeithan, T. W. (1995) Kinetic proofreading in T-cell receptor signal transduction. *Proc Natl Acad Sci USA* **92**, 5042–5046.

136. Rachmilewitz, J. (2008) Serial triggering model. *Adv. Exp. Med. Biol.* **640**, 95–102.

137. Freiberg, B. A., Kupfer, H., Maslanik, W., Delli, J., Kappler, J., Zaller, D. M., and Kupfer, A. (2002) Staging and resetting T cell activation in SMACs. *Nat Immunol* **3**, 911–917.

138. Reichardt, P., Dornbach, B., Rong, S., Beissert, S., Gueler, F., Loser, K., and Gunzer, M. (2007) Naive B cells generate regulatory T cells in the presence of a mature immunologic synapse. *Blood* **110**, 1519–1529.

139. Geyeregger, R., Zeyda, M., Zlabinger, G. J., Waldhäusl, W., and Stulnig, T. M. (2005) Polyunsaturated fatty acids interfere with formation of the immunological synapse. *J Leukoc Biol* **77**, 680–688.

140. Kim, W., Fan, Y.-Y., Barhoumi, R., Smith, R., McMurray, D. N., and Chapkin, R. S. (2008) n-3 polyunsaturated fatty acids suppress the localization and activation of signaling proteins at the immunological synapse in murine CD4+ T cells by

affecting lipid raft formation. *J Immunol* **181**, 6236–6243.

141. Yog, R., Barhoumi, R., McMurray, D. N., and Chapkin, R. S. (2010) n-3 polyunsaturated fatty acids suppress mitochondrial translocation to the immunologic synapse and modulate calcium signaling in T cells. *J Immunol* **184**, 5865–5873.

142. Bonilla, D. L., Ly, L. H., Fan, Y.-Y., Chapkin, R. S., and McMurray, D. N. (2010) Incorporation of a dietary omega 3 fatty acid impairs murine macrophage responses to Mycobacterium tuberculosis. *PLoS ONE* **5**, e10878.

143. Ruth, M. R., Proctor, S. D., and Field, C. J. (2009) Feeding long-chain n-3 polyunsaturated fatty acids to obese leptin receptor-deficient JCR:LA- cp rats modifies immune function and lipid-raft fatty acid composition. *Br J Nutr* **101**, 1341–1350.

144. Fetterman, J. W., and Zdanowicz, M. M. (2009) Therapeutic potential of n-3 polyunsaturated fatty acids in disease. *Am J Health Syst Pharm* **66**, 1169–1179.

145. Kris-Etherton, P. M., Harris, W. S., Appel, L. J., American Heart Association. Nutrition Committee (2002) Fish consumption, fish oil, omega-3 fatty acids, and cardiovascular disease. *Circulation* **106**, 2747–2757.

146. Fedor, D., and Kelley, D. S. (2009) Prevention of insulin resistance by n-3 polyunsaturated fatty acids. *Curr Opin Clin Nutr Metab Care* **12**, 138–146.

147. Kabir, M., Skurnik, G., Naour, N., Pechtner, V., Meugnier, E., Rome, S., Quignard-Boulangé, A., Vidal, H., Slama, G., Clément, K., Guerre-Millo, M., and Rizkalla, S. W. (2007) Treatment for 2 mo with n 3 polyunsaturated fatty acids reduces adiposity and some atherogenic factors but does not improve insulin sensitivity in

women with type 2 diabetes: a randomized controlled study. *Am J Clin Nutr* **86**, 1670–1679.

148. Chapkin, R. S., Seo, J., McMurray, D. N., and Lupton, J. R. (2008) Mechanisms by which docosahexaenoic acid and related fatty acids reduce colon cancer risk and inflammatory disorders of the intestine. *Chem Phys Lipids* **153**, 14–23.

149. Yaqoob, P., and Shaikh, S. R. (2010) The nutritional and clinical significance of lipid rafts. *Curr Opin Clin Nutr Metab Care* **13**, 156–166.

150. Shaikh, S. R., Rockett, B. D., Salameh, M., and Carraway, K. (2009) Docosahexaenoic acid modifies the clustering and size of lipid rafts and the lateral organization and surface expression of MHC class I of EL4 cells. *J Nutr* **139**, 1632–1639.

151. Shaikh, S. R., and Edidin, M. (2006) Membranes are not just rafts. *Chem Phys Lipids* **144**, 1–3.

152. Shaikh, S. R., Cherezov, V., Caffrey, M., Soni, S. P., LoCascio, D., Stillwell, W., and Wassall, S. R. (2006) Molecular organization of cholesterol in unsaturated phosphatidylethanolamines: X-ray diffraction and solid state ^{2}H NMR reveal differences with phosphatidylcholines. *J Am Chem Soc* **128**, 5375–5383.

153. Shaikh, S. R., Locascio, D. S., Soni, S. P., Wassall, S. R., and Stillwell, W. (2009) Oleic- and docosahexaenoic acid-containing phosphatidylethanolamines differentially phase separate from sphingomyelin. *Biochim Biophys Acta* **1788**, 2421–2426.

154. Schley, P. D., Brindley, D. N., and Field, C. J. (2007) (n-3) PUFA alter raft lipid composition and decrease epidermal growth factor receptor levels in lipid rafts of

human breast cancer cells. *J Nutr* **137**, 548–553.

155. Fan, Y.-Y., McMurray, D. N., Ly, L. H., and Chapkin, R. S. (2003) Dietary (n-3) polyunsaturated fatty acids remodel mouse T-cell lipid rafts. *J Nutr* **133**, 1913–1920.

156. Li, Q., Tan, L., Wang, C., Li, N., Li, Y., Xu, G., and Li, J. (2006) Polyunsaturated eicosapentaenoic acid changes lipid composition in lipid rafts. *Eur J Nutr* **45**, 144–151.

157. Lichtenberg, D., Goñi, F. M., and Heerklotz, H. (2005) Detergent-resistant membranes should not be identified with membrane rafts. *Trends Biochem Sci* **30**, 430–436.

158. Heerklotz, H. (2002) Triton promotes domain formation in lipid raft mixtures. *Biophys J* **83**, 2693–2701.

159. Lingwood, D., and Simons, K. (2007) Detergent resistance as a tool in membrane research. *Nat Protoc* **2**, 2159–2165.

160. Rockett, B. D., Salameh, M., Carraway, K., Morrison, K., and Shaikh, S. R. (2010) n-3 PUFA improves fatty acid composition, prevents palmitate-induced apoptosis, and differentially modifies B cell cytokine secretion in vitro and ex vivo. *J Lipid Res* **51**, 1284–1297.

161. Reeves, P. G. (1997) Components of the AIN-93 diets as improvements in the AIN-76A diet. *J Nutr* **127**, 838S–841S.

162. Shaikh, S. R., and Edidin, M. (2007) Immunosuppressive effects of polyunsaturated fatty acids on antigen presentation by human leukocyte antigen class I molecules. *J Lipid Res* **48**, 127–138.

163. Gómez-Moutón, C., Lacalle, R. A., Mira, E., Jiménez-Baranda, S., Barber, D. F., Carrera, A. C., Martínez-A, C., and Mañes, S. (2004) Dynamic redistribution of raft domains as an organizing platform for signaling during cell chemotaxis. *J Cell Biol* **164**, 759–768.

164. Seveau, S., Eddy, R. J., Maxfield, F. R., and Pierini, L. M. (2001) Cytoskeleton-dependent membrane domain segregation during neutrophil polarization. *Mol Biol Cell* **12**, 3550–3562.

165. Bowness, P., Caplan, S., and Edidin, M. (2009) MHC molecules lead many lives: Workshop on MHC Class I Molecules at the interface between Biology & Medicine. *EMBO Rep* **10**, 30–34.

166. Edidin, M. (2010) Class I MHC molecules as probes of membrane patchiness: from biophysical measurements to modulation of immune responses. *Immunol. Res.* **47**, 265–272.

167. Goebel, J., Forrest, K., Flynn, D., Rao, R., and Roszman, T. L. (2002) Lipid rafts, major histocompatibility complex molecules, and immune regulation. *Hum Immunol* **63**, 813–820.

168. Kenworthy, A. K., Petranova, N., and Edidin, M. (2000) High-resolution FRET microscopy of cholera toxin B-subunit and GPI-anchored proteins in cell plasma membranes. *Mol Biol Cell* **11**, 1645–1655.

169. Kenworthy, A. K., and Edidin, M. (1998) Distribution of a glycosylphosphatidylinositol-anchored protein at the apical surface of MDCK cells examined at a resolution of <100 Å Using Imaging Fluorescence Resonance Energy Transfer. *J Cell Biol* **142**, 69–84.

170. Wu, P., and Brand, L. (1994) Resonance energy transfer: methods and applications. *Anal. Biochem.* **218**, 1–13.

171. Bastiaens, P. I., and Jovin, T. M. (1996) Microspectroscopic imaging tracks the intracellular processing of a signal transduction protein: fluorescent-labeled protein kinase C beta I. *Proc Natl Acad Sci USA* **93**, 8407–8412.

172. Stepensky, D. (2007) FRETcalc plugin for calculation of FRET in non-continuous intracellular compartments. *Biochem Biophys Res Commun* **359**, 752–758.

173. Thumser, A. E., and Storch, J. (2007) Characterization of a BODIPY-labeled fluorescent fatty acid analogue. Binding to fatty acid-binding proteins, intracellular localization, and metabolism. *Mol Cell Biochem* **299**, 67–73.

174. Verlengia, R., Gorjão, R., Kanunfre, C. C., Bordin, S., de Lima, T. M., Martins, E. F., Newsholme, P., and Curi, R. (2004) Effects of EPA and DHA on proliferation, cytokine production, and gene expression in Raji cells. *Lipids* **39**, 857–864.

175. Mannini, A., Kerstin, N., Calorini, L., Mugnai, G., and Ruggieri, S. (2009) Dietary n-3 polyunsaturated fatty acids enhance metastatic dissemination of murine T lymphoma cells. *Br J Nutr* **102**, 958–961.

176. Lyons, A. B. (2000) Analysing cell division in vivo and in vitro using flow cytometric measurement of CFSE dye dilution. *J. Immunol. Methods* **243**, 147–154.

177. Zech, T., Ejsing, C. S., Gaus, K., de Wet, B., Shevchenko, A., Simons, K., and Harder, T. (2009) Accumulation of raft lipids in T-cell plasma membrane domains engaged in TCR signalling. *EMBO J* **28**, 466–476.

178. Rogers, K. R., Kikawa, K. D., Mouradian, M., Hernandez, K., McKinnon, K. M., Ahwah, S. M., and Pardini, R. S. (2010) Docosahexaenoic acid alters epidermal

growth factor receptor-related signaling by disrupting its lipid raft association. *Carcinogenesis* **31**, 1523–1530.

179. Chen, W., Jump, D. B., Esselman, W. J., and Busik, J. V. (2007) Inhibition of cytokine signaling in human retinal endothelial cells through modification of caveolae/lipid rafts by docosahexaenoic acid. *Invest Ophthalmol Vis Sci* **48**, 18–26.

180. Chapkin, R. S., Wang, N., Fan, Y.-Y., Lupton, J. R., and Prior, I. A. (2008) Docosahexaenoic acid alters the size and distribution of cell surface microdomains. *Biochim Biophys Acta* **1778**, 466–471.

181. Shi, J., Yang, T., Kataoka, S., Zhang, Y., Diaz, A. J., and Cremer, P. S. (2007) GM1 clustering inhibits cholera toxin binding in supported phospholipid membranes. *J Am Chem Soc* **129**, 5954–5961.

182. Wong, S. W., Kwon, M.-J., Choi, A. M. K., Kim, H.-P., Nakahira, K., and Hwang, D. H. (2009) Fatty acids modulate Toll-like receptor 4 activation through regulation of receptor dimerization and recruitment into lipid rafts in a reactive oxygen species-dependent manner. *J Biol Chem* **284**, 27384–27392.

183. Altenburg, J. D., and Siddiqui, R. A. (2009) Omega-3 polyunsaturated fatty acids down-modulate CXCR4 expression and function in MDA-MB-231 breast cancer cells. *Mol Cancer Res* **7**, 1013–1020.

184. Cunnane, S. C., Ganguli, S., Menard, C., Liede, A. C., Hamadeh, M. J., Chen, Z. Y., Wolever, T. M., and Jenkins, D. J. (1993) High alpha-linolenic acid flaxseed (Linum usitatissimum): some nutritional properties in humans. *Br J Nutr* **69**, 443–453.

185. Burns, C. P., Halabi, S., Clamon, G., Kaplan, E., Hohl, R. J., Atkins, J. N., Schwartz, M. A., Wagner, B. A., and Paskett, E. (2004) Phase II study of high-dose fish oil capsules for patients with cancer-related cachexia. *Cancer* **101**, 370–378.

186. Kremer, J. M., Lawrence, D. A., Petrillo, G. F., Litts, L. L., Mullaly, P. M., Rynes, R. I., Stocker, R. P., Parhami, N., Greenstein, N. S., and Fuchs, B. R. (1995) Effects of high-dose fish oil on rheumatoid arthritis after stopping nonsteroidal antiinflammatory drugs. Clinical and immune correlates. *Arthritis Rheum.* **38**, 1107–1114.

187. Rockett, B. D., Franklin, A., Harris, M., Teague, H., Rockett, A., and Shaikh, S. R. (2011) Membrane raft organization is more sensitive to disruption by (n-3) PUFA than nonraft organization in EL4 and B cells. *J Nutr* **141**, 1041–1048.

188. Kim, J.-Y., van de Wall, E., Laplante, M., Azzara, A., Trujillo, M. E., Hofmann, S. M., Schraw, T., Durand, J. L., Li, H., Li, G., Jelicks, L. A., Mehler, M. F., Hui, D. Y., Deshaies, Y., Shulman, G. I., Schwartz, G. J., and Scherer, P. E. (2007) Obesity-associated improvements in metabolic profile through expansion of adipose tissue. *J Clin Invest* **117**, 2621–2637.

189. Barber, M. D., McMillan, D. C., Preston, T., Ross, J. A., and Fearon, K. C. (2000) Metabolic response to feeding in weight-losing pancreatic cancer patients and its modulation by a fish-oil-enriched nutritional supplement. *Clin Sci* **98**, 389–399.

190. Bortolotti, M., Tappy, L., and Schneiter, P. (2007) Fish oil supplementation does not alter energy efficiency in healthy males. *Clin Nutr* **26**, 225–230.

191. Jones, P. J. H., Jew, S., and AbuMweis, S. (2008) The effect of dietary oleic,

linoleic, and linolenic acids on fat oxidation and energy expenditure in healthy men. *Metab Clin Exp* **57**, 1198–1203.

192. Macallan, D. C., Noble, C., Baldwin, C., Jebb, S. A., Prentice, A. M., Coward, W. A., Sawyer, M. B., McManus, T. J., and Griffin, G. E. (1995) Energy expenditure and wasting in human immunodeficiency virus infection. *N Engl J Med* **333**, 83–88.

193. Kosmiski, L. A., Kuritzkes, D. R., Lichtenstein, K. A., Glueck, D. H., Gourley, P. J., Stamm, E. R., Scherzinger, A. L., and Eckel, R. H. (2001) Fat distribution and metabolic changes are strongly correlated and energy expenditure is increased in the HIV lipodystrophy syndrome. *AIDS* **15**, 1993–2000.

194. Grinspoon, S., and Carr, A. (2005) Cardiovascular risk and body-fat abnormalities in HIV-infected adults. *N Engl J Med* **352**, 48–62.

195. Duda, M. K., O'Shea, K. M., Tintinu, A., Xu, W., Khairallah, R. J., Barrows, B. R., Chess, D. J., Azimzadeh, A. M., Harris, W. S., Sharov, V. G., Sabbah, H. N., and Stanley, W. C. (2009) Fish oil, but not flaxseed oil, decreases inflammation and prevents pressure overload-induced cardiac dysfunction. *Cardiovasc Res* **81**, 319–327.

196. Harris, W. S., Mozaffarian, D., Lefevre, M., Toner, C. D., Colombo, J., Cunnane, S. C., Holden, J. M., Klurfeld, D. M., Morris, M. C., and Whelan, J. (2009) Towards establishing dietary reference intakes for eicosapentaenoic and docosahexaenoic acids. *J Nutr* **139**, 804S–19S.

197. Calder, P. C. (2008) The relationship between the fatty acid composition of immune cells and their function. *Prostaglandins Leukot Essent Fatty Acids* **79**, 101–108.

198. Shaikh, S. R., Dumaual, A. C., Castillo, A., LoCascio, D., Siddiqui, R. A., Stillwell,

W., and Wassall, S. R. (2004) Oleic and docosahexaenoic acid differentially phase separate from lipid raft molecules: a comparative NMR, DSC, AFM, and detergent extraction study. *Biophys J* **87**, 1752–1766.

199. Soni, S. P., Locascio, D. S., Liu, Y., Williams, J. A., Bittman, R., Stillwell, W., and Wassall, S. R. (2008) Docosahexaenoic acid enhances segregation of lipids between raft and nonraft domains: ^{2}H-NMR study. *Biophys J* **95**, 203–214.

200. Grimm, M. O. W., Kuchenbecker, J., Grösgen, S., Burg, V. K., Hundsdörfer, B., Rothhaar, T. L., Friess, P., de Wilde, M. C., Broersen, L. M., Penke, B., Péter, M., Vigh, L., Grimm, H. S., and Hartmann, T. (2011) Docosahexaenoic acid reduces amyloid beta production via multiple pleiotropic mechanisms. *J Biol Chem* **286**, 14028–14039.

201. Aliche-Djoudi, F., Podechard, N., Chevanne, M., Nourissat, P., Catheline, D., Legrand, P., Dimanche-Boitrel, M.-T., Lagadic-Gossmann, D., and Sergent, O. (2011) Physical and chemical modulation of lipid rafts by a dietary n-3 polyunsaturated fatty acid increases ethanol-induced oxidative stress. *Free Radic Biol Med* **51**, 2018–2030.

202. Winer, D. A., Winer, S., Shen, L., Wadia, P. P., Yantha, J., Paltser, G., Tsui, H., Wu, P., Davidson, M. G., Alonso, M. N., Leong, H. X., Glassford, A., Caimol, M., Kenkel, J. A., Tedder, T. F., McLaughlin, T., Miklos, D. B., Dosch, H.-M., and Engleman, E. G. (2011) B cells promote insulin resistance through modulation of T cells and production of pathogenic IgG antibodies. *Nature Medicine* **17**, 610–617.

203. Hikada, M., and Zouali, M. (2010) Multistoried roles for B lymphocytes in

autoimmunity. *Nat Immunol* **11**, 1065-1068.

204. Davis, J. H., Jeffrey, K. R., Bloom, M., and Valic, M. I. (1976) Quadrupolar echo deuteron magnetic resonance spectroscopy in ordered hydrocarbon chains. *Chem. Phys. Lett.* **42**, 390–394.

205. Bacia, K., Scherfeld, D., Kahya, N., and Schwille, P. (2004) Fluorescence correlation spectroscopy relates rafts in model and native membranes. *Biophys J* **87**, 1034–1043.

206. Parasassi, T., De Stasio, G., d'Ubaldo, A., and Gratton, E. (1990) Phase fluctuation in phospholipid membranes revealed by Laurdan fluorescence. *Biophys J* **57**, 1179–1186.

207. Miguel, L., Owen, D. M., Lim, C., Liebig, C., Evans, J., Magee, A. I., and Jury, E. C. (2011) Primary human $CD4^+$ T cells have diverse levels of membrane lipid order that correlate with their function. *J Immunol* **186**, 3505–3516.

208. Rockett, B. D., Harris, M., and Shaikh, S. R. (2012) High dose of an n-3 polyunsaturated fatty acid diet lowers activity of C57BL/6 mice. *Prostaglandins Leukot Essent Fatty Acids* **86**, 137–140.

209. Switzer, K. C., Fan, Y.-Y., Wang, N., McMurray, D. N., and Chapkin, R. S. (2004) Dietary n-3 polyunsaturated fatty acids promote activation-induced cell death in Th1-polarized murine CD4+ T-cells. *J Lipid Res* **45**, 1482–1492.

210. Jin, L., Millard, A. C., Wuskell, J. P., Dong, X., Wu, D., Clark, H. A., and Loew, L. M. (2006) Characterization and application of a new optical probe for membrane lipid domains. *Biophys J* **90**, 2563–2575.

211. Fan, Y.-Y., Ly, L. H., Barhoumi, R., McMurray, D. N., and Chapkin, R. S. (2004)

Dietary docosahexaenoic acid suppresses T cell protein kinase Cθ lipid raft recruitment and IL-2 production. *J Immunol* **173**, 6151–6160.

212. Mihailescu, M., Soubias, O., Worcester, D., White, S. H., and Gawrisch, K. (2011) Structure and dynamics of cholesterol-containing polyunsaturated lipid membranes studied by neutron diffraction and NMR. *J Membrane Biol* **239**, 63–71.

213. Lingwood, D., Ries, J., Schwille, P., and Simons, K. (2008) Plasma membranes are poised for activation of raft phase coalescence at physiological temperature. *Proc Natl Acad Sci USA* **105**, 10005–10010.

214. van Zanten, T. S., Gómez, J., Manzo, C., Cambi, A., Buceta, J., Reigada, R., and Garcia-Parajo, M. F. (2010) Direct mapping of nanoscale compositional connectivity on intact cell membranes. *Proc Natl Acad Sci USA* **107**, 15437–15442.

215. Hsu, C.-S., Chiu, W.-C., Yeh, C.-L., Hou, Y.-C., Chou, S.-Y., and Yeh, S.-L. (2006) Dietary fish oil enhances adhesion molecule and interleukin-6 expression in mice with polymicrobial sepsis. *Br J Nutr* **96**, 854–860.

216. Blok, W. L., de Bruijn, M. F., Leenen, P. J., Eling, W. M., van Rooijen, N., Stanley, E. R., Buurman, W. A., and van der Meer, J. W. (1996) Dietary n-3 fatty acids increase spleen size and postendotoxin circulating TNF in mice; role of macrophages, macrophage precursors, and colony-stimulating factor-1. *J Immunol* **157**, 5569–5573.

217. Weldon, S. M., Mullen, A. C., Loscher, C. E., Hurley, L. A., and Roche, H. M. (2007) Docosahexaenoic acid induces an anti-inflammatory profile in

lipopolysaccharide-stimulated human THP-1 macrophages more effectively than eicosapentaenoic acid. *J Nutr Biochem* **18**, 250–258.

218. Weatherill, A. R., Lee, J. Y., Zhao, L., Lemay, D. G., Youn, H. S., and Hwang, D. H. (2005) Saturated and polyunsaturated fatty acids reciprocally modulate dendritic cell functions mediated through TLR4. *J Immunol* **174**, 5390–5397.

219. Beli, E., Li, M., Cuff, C., and Pestka, J. J. (2008) Docosahexaenoic acid-enriched fish oil consumption modulates immunoglobulin responses to and clearance of enteric reovirus infection in mice. *J Nutr* **138**, 813–819.

220. Weise, C., Hilt, K., Milovanovic, M., Ernst, D., Rühl, R., and Worm, M. (2011) Inhibition of IgE production by docosahexaenoic acid is mediated by direct interference with STAT6 and NFκB pathway in human B cells. *J Nutr Biochem* **22**, 269–275.

221. Lauritzen, L., Kjær, T. M. R., Porsgaard, T., Fruekilde, M. B., Mu, H., and Frøkiær, H. (2011) Maternal intake of fish oil but not of linseed oil reduces the antibody response in neonatal mice. *Lipids* **46**, 171–178.

222. Selvaraj, R. K., and Cherian, G. (2004) Dietary n-3 fatty acids reduce the delayed hypersensitivity reaction and antibody production more than n-6 fatty acids in broiler birds. *Eur J Lipid Sci Technol* **106**, 3–10.

223. Sanderson, P., MacPherson, G. G., Jenkins, C. H., and Calder, P. C. (1997) Dietary fish oil diminishes the antigen presentation activity of rat dendritic cells. *J Leukoc Biol* **62**, 771–777.

224. Chapkin, R. S., Arrington, J. L., Apanasovich, T. V., Carroll, R. J., and McMurray, D. N. (2002) Dietary n-3 PUFA affect TcR-mediated activation of purified murine T

cells and accessory cell function in co-cultures. *Clin Exp Immunol* **130**, 12–18.

225. Calder, P. C. (2012) Mechanisms of action of (n-3) fatty acids. *J Nutr* **142**, 592S–599S.

226. Gottschalk, R. A., Hathorn, M. M., Beuneu, H., Corse, E., Dustin, M. L., Altan-Bonnet, G., and Allison, J. P. (2012) Distinct influences of peptide-MHC quality and quantity on in vivo T-cell responses. *Proc Natl Acad Sci USA* **109**, 881–886.

227. Rockett, B. D., Teague, H., Harris, M., Melton, M., Williams, J., Wassall, S. R., and Shaikh, S. R. (2012) Fish oil increases raft size and membrane order of B cells accompanied by differential effects on function. *J Lipid Res* **53**, 674–685.

228. Petursdottir, D. H., and Hardardottir, I. (2009) Dietary fish oil decreases secretion of T helper (Th) 1-type cytokines by a direct effect on murine splenic T cells but enhances secretion of a Th2-type cytokine by an effect on accessory cells. *Br J Nutr* **101**, 1040–1046.

229. Zidovetzki, R., and Levitan, I. (2007) Use of cyclodextrins to manipulate plasma membrane cholesterol content: evidence, misconceptions and control strategies. *Biochim Biophys Acta* **1768**, 1311–1324.

230. Schliwa, M. (1982) Action of cytochalasin D on cytoskeletal networks. *J Cell Biol* **92**, 79–91.

231. Watson, A. R. O., and Lee, W. T. (2004) Differences in signaling molecule organization between naive and memory CD4+ T lymphocytes. *J Immunol* **173**, 33–41.

232. Antón, O. M., Andrés-Delgado, L., Reglero-Real, N., Batista, A., and Alonso, M. A. (2011) MAL protein controls protein sorting at the supramolecular activation

cluster of human T lymphocytes. *J Immunol* **186**, 6345–6356.

233. Gombos, I., Detre, C., Vámosi, G., and Matkó, J. (2004) Rafting MHC-II domains in the APC (presynaptic) plasma membrane and the thresholds for T-cell activation and immunological synapse formation. *Immunol. Lett.* **92**, 117–124.

234. Narayan, K., Perkins, E. M., Murphy, G. E., Dalai, S. K., Edidin, M., Subramaniam, S., and Sadegh-Nasseri, S. (2009) Staphylococcal enterotoxin A induces small clusters of HLA-DR1 on B cells. *PLoS ONE* **4**, e6188.

235. Vrljic, M., Nishimura, S. Y., Moerner, W. E., and McConnell, H. M. (2005) Cholesterol depletion suppresses the translational diffusion of class II major histocompatibility complex proteins in the plasma membrane. *Biophys J* **88**, 334–347.

236. la Fuente, de, H., Mittelbrunn, M., Sánchez-Martín, L., Vicente-Manzanares, M., Lamana, A., Pardi, R., Cabañas, C., and Sánchez-Madrid, F. (2005) Synaptic clusters of MHC class II molecules induced on DCs by adhesion molecule-mediated initial T-cell scanning. *Mol Biol Cell* **16**, 3314–3322.

237. Khandelwal, S., and Roche, P. A. (2010) Distinct MHC class II molecules are associated on the dendritic cell surface in cholesterol-dependent membrane microdomains. *J Biol Chem* **285**, 35303–35310.

238. Rodríguez-Fernández, J. L., Riol-Blanco, L., and Delgado-Martín, C. (2010) What is the function of the dendritic cell side of the immunological synapse? *Sci Signal* **3**, re2.

239. Irvine, D. J., Purbhoo, M. A., Krogsgaard, M., and Davis, M. M. (2002) Direct observation of ligand recognition by T cells. *Nature* **419**, 845–849.

240. Fooksman, D. R., Shaikh, S. R., Boyle, S., and Edidin, M. (2009) Cutting edge: phosphatidylinositol 4,5-bisphosphate concentration at the APC side of the immunological synapse is required for effector T cell function. *J Immunol* **182**, 5179–5182.

241. Maravillas-Montero, J. L., Gillespie, P. G., Patiño-López, G., Shaw, S., and Santos-Argumedo, L. (2011) Myosin 1c participates in B cell cytoskeleton rearrangements, is recruited to the immunologic synapse, and contributes to antigen presentation. *J Immunol* **187**, 3053–3063.

242. Lassila, O., Vainio, O., and Matzinger, P. (1988) Can B cells turn on virgin T cells? *Nature* **334**, 253–255.

243. Morris, S. C., Lees, A., and Finkelman, F. D. (1994) In vivo activation of naive T cells by antigen-presenting B cells. *J Immunol* **152**, 3777–3785.

244. Zilber, M.-T., Setterblad, N., Vasselon, T., Doliger, C., Charron, D., Mooney, N., and Gelin, C. (2005) MHC class II/CD38/CD9: a lipid-raft-dependent signaling complex in human monocytes. *Blood* **106**, 3074–3081.

245. Anderson, H. A., Hiltbold, E. M., and Roche, P. A. (2000) Concentration of MHC class II molecules in lipid rafts facilitates antigen presentation. *Nat Immunol* **1**, 156–162.

246. Hiltbold, E. M., Poloso, N. J., and Roche, P. A. (2003) MHC class II-peptide complexes and APC lipid rafts accumulate at the immunological synapse. *J Immunol* **170**, 1329–1338.

247. Poloso, N. J., Muntasell, A., and Roche, P. A. (2004) MHC class II molecules traffic into lipid rafts during intracellular transport. *J Immunol* **173**, 4539–4546.

248. Jenei, A., Varga, S., Bene, L., Mátyus, L., Bodnár, A., Bacsó, Z., Pieri, C., Gáspár, R., Farkas, T., and Damjanovich, S. (1997) HLA class I and II antigens are partially co-clustered in the plasma membrane of human lymphoblastoid cells. *Proc Natl Acad Sci USA* **94**, 7269–7274.

249. Umemura, Y. M., Vrljic, M., Nishimura, S. Y., Fujiwara, T. K., Suzuki, K. G. N., and Kusumi, A. (2008) Both MHC class II and its GPI-anchored form undergo hop diffusion as observed by single-molecule tracking. *Biophys J* **95**, 435–450.

250. Hughes, D. A., Pinder, A. C., Piper, Z., Johnson, I. T., and Lund, E. K. (1996) Fish oil supplementation inhibits the expression of major histocompatibility complex class II molecules and adhesion molecules on human monocytes. *Am J Clin Nutr* **63**, 267–272.

251. Marwali, M. R., Rey-Ladino, J., Dreolini, L., Shaw, D., and Takei, F. (2003) Membrane cholesterol regulates LFA-1 function and lipid raft heterogeneity. *Blood* **102**, 215–222.

252. Setterblad, N., Bécart, S., Charron, D., and Mooney, N. (2004) B cell lipid rafts regulate both peptide-dependent and peptide-independent APC-T cell interaction. *J Immunol* **173**, 1876–1886.

253. Wang, S.-H., Yuan, S.-G., Peng, D.-Q., and Zhao, S.-P. (2012) HDL and ApoA-I inhibit antigen presentation-mediated T cell activation by disrupting lipid rafts in antigen presenting cells. *Atherosclerosis*. Article in press, 10.1016/ j.atherosclerosis.2012.07.029.

254. Barois, N., Forquet, F., and Davoust, J. (1998) Actin microfilaments control the MHC class II antigen presentation pathway in B cells. *J Cell Sci* **111 (Pt 13)**,

1791–1800.

255. Holsinger, L. J., Graef, I. A., Swat, W., Chi, T., Bautista, D. M., Davidson, L., Lewis, R. S., Alt, F. W., and Crabtree, G. R. (1998) Defects in actin-cap formation in Vav-deficient mice implicate an actin requirement for lymphocyte signal transduction. *Curr Biol* **8**, 563–572.

256. Williams, J. A., Batten, S. E., Harris, M., Rockett, B. D., Shaikh, S. R., Stillwell, W., and Wassall, S. R. (2012) Docosahexaenoic and Eicosapentaenoic Acids Segregate Differently between Raft and Nonraft Domains. *Biophys J* **103**, 228–237.

257. Jin, L., Millard, A. C., Wuskell, J. P., Clark, H. A., and Loew, L. M. (2005) Cholesterol-enriched lipid domains can be visualized by di-4-ANEPPDHQ with linear and nonlinear optics. *Biophys J* **89**, L04–6.

258. Owen, D. M., and Gaus, K. (2010) Optimized time-gated generalized polarization imaging of Laurdan and di-4-ANEPPDHQ for membrane order image contrast enhancement. *Microsc Res Tech* **73**, 618–622.

259. Gaus, K., Zech, T., and Harder, T. (2006) Visualizing membrane microdomains by Laurdan 2-photon microscopy. *Mol Membr Biol* **23**, 41–48.

260. Mizota, T., Fujita-Kambara, C., Matsuya, N., Hamasaki, S., Fukudome, T., Goto, H., Nakane, S., Kondo, T., and Matsuo, H. (2009) Effect of dietary fatty acid composition on Th1/Th2 polarization in lymphocytes. *JPEN J Parenter Enteral Nutr* **33**, 390–396.

261. Sierra, S., Lara-Villoslada, F., Comalada, M., Olivares, M., and Xaus, J. (2006) Dietary fish oil n-3 fatty acids increase regulatory cytokine production and exert

anti-inflammatory effects in two murine models of inflammation. *Lipids* **41**, 1115–1125.

262. Arrington, J. L., Chapkin, R. S., Switzer, K. C., Morris, J. S., and McMurray, D. N. (2001) Dietary n-3 polyunsaturated fatty acids modulate purified murine T-cell subset activation. *Clin Exp Immunol* **125**, 499–507.

263. Wallace, F. A., Miles, E. A., Evans, C., Stock, T. E., Yaqoob, P., and Calder, P. C. (2001) Dietary fatty acids influence the production of Th1- but not Th2-type cytokines. *J Leukoc Biol* **69**, 449–457.

264. Kleemann, R., Scott, F. W., Wörz-Pagenstert, U., Nimal Ratnayake, W. M., and Kolb, H. (1998) Impact of dietary fat on Th1/Th2 cytokine gene expression in the pancreas and gut of diabetes-prone BB rats. *J. Autoimmun.* **11**, 97–103.

265. Mosmann, T. R., and Sad, S. (1996) The expanding universe of T-cell subsets: Th1, Th2 and more. *Immunol. Today* **17**, 138–146.

266. Liblau, R. S., Singer, S. M., and McDevitt, H. O. (1995) Th1 and Th2 CD4+ T cells in the pathogenesis of organ-specific autoimmune diseases. *Immunol. Today* **16**, 34–38.

267. Leigh, R., Ellis, R., Wattie, J. N., Hirota, J. A., Matthaei, K. I., Foster, P. S., O'Byrne, P. M., and Inman, M. D. (2004) Type 2 cytokines in the pathogenesis of sustained airway dysfunction and airway remodeling in mice. *Am. J. Respir. Crit. Care Med.* **169**, 860–867.

268. Larché, M., Robinson, D. S., and Kay, A. B. (2003) The role of T lymphocytes in the pathogenesis of asthma. *J. Allergy Clin. Immunol.* **111**, 450–63.

269. Garlisi, C. G., Falcone, A., Kung, T. T., Stelts, D., Pennline, K. J., Beavis, A. J.,

Smith, S. R., Egan, R. W., and Umland, S. P. (1995) T cells are necessary for Th2 cytokine production and eosinophil accumulation in airways of antigen-challenged allergic mice. *Clin. Immunol. Immunopathol.* **75**, 75–83.

270. Mozaffarian, D., and Rimm, E. B. (2006) Fish intake, contaminants, and human health: evaluating the risks and the benefits. *JAMA* **296**, 1885–1899.

APPENDIX A: ANIMAL USE PROTOCOL

Animal Care and Use Committee
East Carolina University
212 Ed Warren Life Sciences Building
Greenville, NC 27834
252-744-2436 office • 252-744-2355 fax

MEMORANDUM

TO: Benjamin Rockett
Department of Biochemistry

FROM: Dorcas O'Rourke, D.V.M.
University Veterinarian

SUBJECT: Certificate of Training
Training Date 8/19/08

DATE: September 12, 2008

This letter is provided to certify that you have completed training in humane methods of animal experimentation, proper handling of selected species of research animals, and methods for reporting deficiencies in animal care and treatment. The training was provided in accordance with U.S. Department of Agriculture (9 CFR 2.32) regulations and the Public Health Service Policy.

This training included information on ECU animal care organizational structure, regulatory requirements, IACUC procedures, program for veterinary and animal care, occupational health and safety program, and methods for reporting concerns. Information on biology and care, proper restraint and procedures, and allergies and zoonoses were also provided.

We suggest that you retain this letter in your training file for future reference.

East Carolina University
Animal Use Protocol (AUP) Form
Latest Revision, July, 2010

Project Title: High fat diets modulate adaptive immune responses

1. Personnel

1.1. Principal investigator and email: Saame Raza Shaikh ("Raz")
shaikhsa@ecu.edu

1.2. Department, office phone: Biochemistry & Molecular Biology
744-2585

1.3. Emergency numbers:

	Principal Investigator	Other (Co-I, technician, student)
Name:	Saame Raza Shaikh	Mitch Harris
Cell:	(317)409-9565	(919)943-9882
Pager:		
Home:		

FOR IACUC USE ONLY

AUP # C059a
New/renewal: Renewal
Date received: 5/23/11
Full Review and date: Designated Reviewer and date:
Approval date: 5/24/11
Study type: Obesity
Pain/Distress category: B
Surgery: Survival: Multiple:
Prolonged restraint:
Food/fluid restriction:
Hazard approval/dates: Rad: IBC: ✓ EH&S: LPS, transgenics
OHP enrollment/mandatory animal training completed:
Amendments approved:

1.4. Co-Investigators if any: None

1.5. List all personnel (PI, Co-I, technicians, students) that will be performing procedures on live animals and describe their qualifications and experience with these specific procedures. If people are to be trained, indicate by whom:

Name	Required ECU Training	Other Relevant Animal Experience/ Training
PI:Saame Raza Shaikh	Yes	Received formal training at Johns Hopkins as a postdoctoral fellow in animal care. Also received ECU's training
Others: Benjamin Drew Rockett	Yes	Received ECU's training
Mitch Harris	Yes	Received ECU's training
Heather Teague	Yes	Received ECU's training
Mark Melton	Yes	Received ECU's training

2. Regulatory Compliance

2.1 Non-Technical Summary

Using language a non-scientist would understand, please provide a 6 to 8 sentence summary explaining the overall study objectives and benefits of proposed research or teaching activity, and a brief overview of all procedures involving live animals (more detailed procedures are requested later in the AUP). Do **not** cut and paste the grant abstract.

Obesity is now regarded as an epidemic on a worldwide scale, a consequence of nutritional and genetic factors. High fat diets are major factors that promote the development of obesity, which results in disorders including diabetes mellitus, cardiovascular disease, hypertension, and immune dysfunction with increased susceptibility to infection. One major factor that predisposes obese individuals to infection is nutritional status. Our laboratory's focus is on identifying the targets and mechanisms by which dietary fatty acids modify the adaptive immune system. We are currently studying how differing fatty acids affect the adaptive immune system of mice. Using a combination of techniques, we are studying how different fatty acids affect the function of immune cells of the spleen, which play a vital role in combating infection and inflammation. Briefly, animals will be fed varying diets and sacrificed for specific tissues. In some studies, we will induce inflammation by injecting the animals with an inflammatory agent and then sacrifice

2.2. Duplication

Does this study duplicate existing research? Yes ☐ No X☐
If yes, why is it necessary? (note: teaching by definition is duplicative)

N/A

2.3 Alternatives to the Use of Live Animals

Are there less invasive procedures, other species, isolated organ preparation, cell or tissue culture, or computer simulation that can be used in place of the live vertebrate species proposed here? Yes X☐ No ☐
If yes, please explain why you cannot use these alternatives.

We can use cell culture studies and we do this routinely to avoid using animals. However, we cannot address whole body responses in a cell culture model. There are no other alternatives.

2.4 Literature Search to ensure that there are no alternatives to all potentially painful and/or distressful procedures

List the following information for each search (please do not submit search results but retain them for your records):

Date Search was performed: Initially performed Aug. 6, 2008 and performed again May 5, 2011 Database searched: Pubmed and Google Scholar Period of years covered in the search: All Keywords used and strategy: Obesity, infection, saturated fatty acids, monounsaturated fatty acids, n-3 and n-6 polyunsaturated fatty acids, antigen presentation, T cell proliferation, high fat diets, mechanisms, alternatives, immunological synapse, B-T cell synapse, lipid rafts, lipopolysaccharide (LPS), lymphocyte activation, membrane microviscosity Other sources consulted: Google Scholar
Narrative indicating the results of the search (2-3 sentences) and explaining why there are no alternatives to your proposed procedures that have the potential to cause pain and/or distress. If alternatives exist, describe why they are not adequate. Please use the concept of the 3 R's when considering alternatives (reducing the number of animals to what is necessary to obtain scientifically sound results; refining techniques to minimize pain and discomfort to animals; and replacing animal models with non-animal models whenever possible): When searching for the effects of high fat diets on the targets and mechanisms of adaptive immunity, the only alternative possibility is to use fatty acids in cell culture. However, this method does not depict the in vivo condition of consuming a high fat diet, and results from cell culture are often artifacts. In order to avoid these artifacts, feeding mice high fat diets and then isolating specific cell types for experiments is the closest to the in vivo condition. The basis of our animal studies will be based on findings from cell culture, in order to minimize the use of animals.

2.5 Hazardous agents

2.5a. Protocol related hazards

Please indicate if any of the following are used in animals and the status of review/approval by the referenced committees:

HAZARDS	Oversight committee	Status (Approved, Pending, Submitted)/Date	AUP Appendix 1 Completed?
Radioisotopes	Radiation	No	
Ionizing radiation	Radiation	No	

Infectious agents (bacteria, viruses, rickettsia, prions)	IBC	No	
Toxins of biological origins (venoms, plant toxins, etc.)	IBC	No	
Transgenic, Knock In, Knock Out Animals---breeding, cross breeding or any use of live animals or tissues	IBC	No	
Human tissues, cells, body fluids, cell lines	IBC	No	
Viral/ Plasmid Vectors/ Recombinant DNA or recombinant techniques	IBC	No	
Oncogenic/toxic/mutagenic chemical agents	EH&S	No	
Nanoparticles	EH&S	No	
Cell lines injected or implanted in animals (MAP test)	DCM	No	
Other agents		Yes, LPS	

2.5b. Incidental hazards

Will personnel be exposed to any incidental zoonotic diseases or hazards during the study (field studies, primate work, etc)? If so, please identify each and explain steps taken to mitigate risk:

No

3. Animals and Housing

3.1. Species and strains:	C57/BL6; BALB/c, TCR transgenics (OT-II and OT-I) which are on a C57/BL6 background. The OT-II are C57BL/6-Tg(TcraTcrb)425Cbn/J and OT-I are C57BL/6-Tg(TcraTcrb)1100Mjb/J. OT-II and OT-I are transgenic for the T cell receptor (TCR)
3.2. Weight, sex and/or age:	Males, 4-6 weeks of age, occasional females, also 4-6 weeks of age. Generally studies start off with a weight of 14-18g.

Total number of animals in treatment and control groups	Additional animals (Breeders, substitute animals)	Total number of animals used for this project
Total = 2250	See below	See below

3.3. Justify the species and number (use statistical justification when applicable) of animals requested:

There will be several different dietary conditions, which will require 12 animals per condition. The C57/BL6 species are ones that are routinely used in the field for high fat feeding studies. We have found based on previous studies (as a postdoctoral fellow) that 12 mice per condition are enough to warrant changes of 20% and greater to be statistically significant (based on one-way ANOVA and post hoc Dunnett's T test). We have recently verified this number with a statistician (Allied Health – Dr. Fang) who conducted a power analysis for our lab. We will use the C57/BL6 mice routinely. The TCR transgenics are needed for some other studies in which we will test the impact of the diet on T cells. The TCR transgenics (OT-II and OT-I) express T cell receptors that are specific for MHC molecules that we present to these cells ex vivo in the presence of varying peptide doses. This ensures that we are measuring an antigen-specific response in cell culture.

3.4. Justify the number and use of any additional animals needed for this study (i.e. breeder animals, inappropriate genotype/phenotype, extra animals due to problems that may arise, etc.):

Treatment groups	# of mice/study	# of studies over 3 years	# animals/group
C57BL/6 on 10 diets over time for 2 time points (3 and 14 weeks of feeding)	12 mice/time point x 2 time points for each study	a. B cell activation through TLR4 b. B cell activation through BCR c. MHC class I activation d. MHC class II activation e. In vivo LPS activation	12 mice per diet x 10 diets x 2 time points x 5 studies = 1200
OT-II (TCR transgenic)	12 mice/time point x 2 time points for each study	a. MHC class II activation b. Immune synapse	12 mice per diet x 10 diets x 2 time points x 2 studies = 480
OT-I (TCR transgenic)	12 mice/time point x 2 time points for each study	a. MHC class I activation b. Immune synapse	12 mice per diet x 10 diets x 2 time points x 2 studies = 480
OT-II for breeding	N/A	5 males and 5 females/year	10 x 3 years = 30
OT-I for breeding	N/A	5 males and 5 females/year	10 x 3 years = 30
C57BL/6 for breeding	N/A	5 males and 5 females/year	10 x 3 years = 30
Total = 2250 mice			

3.5. Will the phenotype of mutant, transgenic or knockout animals predispose them to any health behavioral, or physical abnormalities?
Yes X☐ No ☐ (if yes, describe)

The TCR transgenic are supposedly a bit more prone to infection. However, in the past few years, we have not experienced any problems. We handle the mice carefully and avoid handling excessively.

3.6. Are there any unusual husbandry and environmental conditions required? Yes x☐ No ☐ If yes, then describe conditions and justify the exceptions to standard housing (temperature, light cycles, sterile cages, special feed, feed on cage floor, prolonged weaning times, wire-bottom cages, no enrichment, social isolation, etc.):

Should we experience any problems with the TCR transgenic getting infected, we would administer antibiotics through the water. We will work with DCM should the need arise for antibiotics. Again, it is unlikely we will need this based on our experience in the past three years.

Another concern could be that will our diets render the animals to become insulin resistant. The answer is no. We are focusing mostly on n-3 polyunsaturated fatty acids and we would need very high doses (which we are not pursuing) to induce insulin resistance. Our saturated fat diets are relatively low in fat (~40% fat by weight); in comparison, one needs 60% fat by weight diets to induce insulin resistance and even then, long-term feeding beyond our time points.

3.7. If wild animals will be captured or used, provide permissions (collection permit # or other required information):

N/A

3.8. List all laboratories or locations outside the animal facility where animals will be used. Note that animals may not stay in areas outside the animal facilities for more than 12 hours without prior IACUC approval. For field studies, list location of work/study site.

N/A

4. Animal Procedures

4.1. Will procedures other than euthanasia and tissue collection be performed? Yes X☐ No ☐
If animals will be used exclusively for tissue collection following euthanasia (answer "no" above), then skip to Question 5 (Euthanasia).

4.2. Outline the Experimental Design including all treatment and control groups and the number of animals in each. If this is a breeding protocol, please describe the breeding strategy (pairs, trios, etc.) and method and age of genotyping (if applicable). Tables or flow charts are particularly useful to communicate your design.

Breeding
This will be done as we currently do, in pairs for several weeks for the C57BL/6 and OT transgenic mice.

Diets
Mice will be given one of ten experimental diets, which were developed with a nutritionist from Harlan-Teklad: (i) Normal diet (5% fat by weight) which is a standard purified diet. (ii) N-3 polyunsaturated fatty acid (PUFA) diet (5% fat by weight) made up of flaxseed and fish oil (1/1). (iii) Saturated fatty acid-rich (SFA) high fat diet (20% fat by weight) made up of coconut oil and milk fat (1/1). (iv) Monounsaturated fatty acid-rich (MUFA) high fat diet (20% fat by weight) made up of olive oil. (v) PUFA-rich high fat diet (20% fat by weight) made up of fish oil and flaxseed oil (1/1). (vi) Hydrogenated high fat diet (20% fat by weight) made up of hydrogenated vegetable oils. (vii) n-6 PUFA high fat diet (20% fat by weight) made up of soybean oil. (viii-x) will be either fish oil, flaxseed oil, or a specific ratio of fish to flaxseed (all at 5-10% fat by weight) depending on some data that we are currently analyzing. All of the high fat diets correspond to ~40% total kcal of energy from fat. The PUFA-rich diets are a mix of fish oil and flaxseed oil in order to minimize oxidation. Furthermore, diets are stored under nitrogen gas and changed every other day to further minimize oxidation. We will verify the lipid composition of the diets for the mice using gas chromatography.

Based on existing studies, we will conduct studies with different levels of fatty acids in the diet (~5-40% fat by weight) for different periods of feeding (time points fall within the 3-14 week range) to assess the effects of dose and time. Our diets have been tested with C57BL/6, OT-II and AND TCR transgenic mice. We have not observed any adverse effects. We will provide fresh food every other day and monitor food intake and body weights. Food intake is monitored every other day and body weights are taken at least once a week.

Cardiac puncture.
We will obtain blood via cardiac puncture on the day we are going to euthanize a set of mice fed different high fat diets. As we currently do, the mice will be placed in the CO_2 chamber and prior to death, we will insert a syringe with a ~22g needle to draw blood. The mouse will be immediately euthanized after taking the blood.

LPS Protocol

As described in extensive detail above, mice will be fed the differing diets. We will then inject i.p. the mice with ~0.5ml of sterile PBS containing E. Coli serotype 0111:B4 LPS (purchased from Sigma). The dose that we anticipate injecting will be 100μg LPS/20g body weight. Control mice will receive PBS alone. The mice will then be exposed to CO_2 inhalation and blood will be obtained via cardiac puncture. We will ensure the mice are dead using cervical dislocation. For these studies, we will first have to measure the kinetic response to the LPS. We anticipate euthanizing mice within 60 minutes after injection up to 3 days after injection. Once we establish the impact of the LPS on the cytokine profile from the isolated blood, then we will pursue experiments at select time points within 60 minutes up to 3 days.

Our protocol is based on a well-established method from the Philip Calder laboratory (UK Southampton), one of the leading experts in nutritional immunology. Their lab published their original protocol in Immunology 1999, vol 96, pgs. 404-410, entitled "Dietary lipids modify the cytokine response to bacterial lipopolysaccharide in mice". Should any of the mice fail to groom, become unresponsive, or display body loss greater than 20% of their body weight, the mice will be immediately terminated. Furthermore, we will initially ask Dr. Rosenbaum to assist us in the i.p. injections to ensure our methods are in agreement with standard practice for i.p. injections. Overall, the goal of these studies is to induce inflammation (i.e. inflammatory cytokine release from activated lymphocytes) and study the impact of diet on inflammation ex vivo; therefore, we are not modeling sepsis.

The majority of the mice will not be injected with LPS. It is difficult to predict how many mice will be injected; we will first start off with a pilot study of roughly 10 animals and test if fish oil enriched diets modify the ex vivo cytokine production in response to LPS. If we find an effect, we would anticipate another 120-240 animals that would be injected. Again, this is very difficult to predict until we get some data on this aspect of the project.

In sections 4.3-4.19 below, please respond to all items relating to your proposed animal procedures. If a section does not apply to your experimental plans, please leave it blank.

Note: Procedures covered by DCM and IACUC guidelines and policies are indicated by asterisk (*). Please refer to these and justify any departures.

4.3. Anesthesia/Analgesia/Tranquilization/Pain/Distress Management (for procedures other than surgery)

Adequate records describing anesthetic monitoring and recovery must be maintained for all species.

If anesthesia/analgesia must be withheld for scientific reasons, please provide compelling scientific justification as to why this is necessary.

Describe the pre-procedural preparation of the animals:

1a. Food restricted for _____ hours

1b. Food restriction is not recommended for rodents and rabbits and must be justified:

2a. Water restricted for _____ hours

2b. Water restriction is not recommended in any species for routine pre-op prep and must be justified:

	Agent	Concentration	Dose (mg/kg)	Volume	Route	Frequency	Duration
Pre-emptive analgesic							
Pre-anesthetic							
Anesthetic							
Analgesic Post procedure							
Other							

a. Reason for administering agent(s):

b. For which procedure(s):

c. Method of monitoring anesthetic depth:

d. Methods of physiologic support during anesthesia and recovery:

e. Duration of recovery:

f. Frequency of recovery monitoring:

g. Specifically what will be monitored?

h. When will animals be returned to their home environment?

i. Describe any behavioral or husbandry manipulations that will be used to alleviate pain, distress, and/or discomfort:

4.4 Use of Paralytics

Will paralyzing drugs be used?

For what purpose:

Please provide scientific justification for paralytic use:

Paralytic drug:

Dose:

Method of ensuring appropriate analgesia during paralysis:

4.5. Blood or Body Fluid Withdrawal/Tissue Collection/Injections/Tail Snip*/Gavage

Please fill out appropriate sections of the chart below:

	Location on animal	Needle/ catheter/ gavage tube size	Route of administration	Biopsy size	Volume collected	Compound and volume administered (include concentration and/or dose)	Frequency of procedure
Body Fluid Withdrawal							
Tissue Collection							
Injection/Infusion	I.P.	25g	I.P.	N/A	N/A	100μg LPS/20g body weight. The volume will be 0.5ml or less. PBS (control) will be added, also at 0.5ml	Depends on the results. We anticipate some kinetic measurements first with 10 animals followed by a study of 12mice/ diet x 10 diets x 2 time points
Tail snip*							
Gavage							
Other							

4.6. Prolonged restraint with mechanical devices

*Restraint in this context means **beyond routine care and use procedures** for rodent and rabbit restrainers, and large animal stocks. Prolonged restraint also includes **any** use of slings, tethers, metabolic crates, inhalation chambers, primate chairs and radiation exposure restraint devices.*

a. For what procedure(s):

b. Restraint device(s):

c. Duration of restraint:

d. Frequency of observations during restraint/person responsible

e. Frequency and total number of restraints:

f. Conditioning procedures:

g. Steps to assure comfort and well-being:

h. Describe potential adverse effects of procedures and provide humane endpoints (criteria for either humanely euthanizing or otherwise removing from study):

4.7 Tumor* and Disease Models/Toxicity Testing

a. Describe methodology:

b. Expected model and/or clinical/pathological manifestations:

c. Signs of pain/discomfort:

d. Frequency of observations:

e. Describe potential adverse effects of procedures and provide humane endpoints (criteria for either humanely euthanizing or otherwise removing from study):

4.8 Treadmills/Swimming/Forced Exercise

a. Describe aversive stimulus (if used):

b. Conditioning:

c. Safeguards to protect animal:

d. Duration:

e. Frequency:

f. Total number of sessions:

g. Describe potential adverse effects of procedures and provide humane endpoints (criteria for either humanely euthanizing or otherwise removing from study):

4.9 Projects Involving Food and Water Deprivation or Dietary Manipulation
(Routine pre-surgical fasting not relevant for this section)

a. Food Restriction
   i. Amount restricted and rationale:

   ii. Duration (hours for short term/weeks or months for long term):

   iii. Frequency of observation/parameters documented (weight, etc):

   iv. Describe potential adverse effects of procedures and provide humane endpoints (criteria for either humanely euthanizing or otherwise removing from study):

b. Fluid Restriction
   i. Amount restricted and rationale:

   ii. Duration (hours for short term/weeks or months for long term):

   iii. Frequency of observation/parameters documented:

iv. Describe potential adverse effects of procedures and provide humane endpoints (criteria for either humanely euthanizing or otherwise removing from study):

c. Dietary Manipulations

i. Compound supplemented/deleted and amount:

ii. Duration (hours for short term/weeks or months for long term):

As stated above, diets will be administered for 3 and 14 weeks.Mice will be given one of ten experimental diets, which were developed with a nutritionist from Harlan-Teklad: (i) Normal diet (5% fat by weight) which is a standard purified diet. (ii) N-3 polyunsaturated fatty acid (PUFA) diet (5% fat by weight) made up of flaxseed and fish oil (1/1). (iii) Saturated fatty acid-rich (SFA) high fat diet (20% fat by weight) made up of coconut oil and milk fat (1/1). (iv) Monounsaturated fatty acid-rich (MUFA) high fat diet (20% fat by weight) made up of olive oil. (v) PUFA-rich high fat diet (20% fat by weight) made up of fish oil and flaxseed oil (1/1). (vi) Hydrogenated high fat diet (20% fat by weight) made up of hydrogenated vegetable oils. (vii) n-6 PUFA high fat diet (20% fat by weight) made up of soybean oil. (viii-x) will be either fish oil or flaxseed oil alone, or a specific ratio of fish to flaxseed oil (at 5-10% fat by weight) depending on some data that we are currently analyzing. All of the high fat diets correspond to ~40% total kcal of energy from fat. The PUFA-rich diets are a mix of fish oil and flaxseed oil. We may have to adjust the fat levels based on data but anticipate they will remain in the range of 5-20% fat by weight.

iii. Frequency of observation/parameter documented:

The mice are fed on the range of 3-14 weeks depending on the study and the study results. Observations on body weight, especially of a new diet, are made on a weekly basis and food is administered every other day, which includes weighing the food and general health of the animal.

iv. Describe potential adverse effects of procedures and provide humane endpoints (criteria for either humanely euthanizing or otherwise removing from study):

We do not anticipate any adverse effects of the diets since our fat levels are below those that would induce insulin resistance. LPS injection will not lead so sepsis since the administered dose is very low. However, with any intervention, failure to groom and/or loss of >~20% body weight will result in euthanasia.

4.10
Endoscopy/Fluroscopy/X-Ray/Ultrasound/MRI/CT/PET/Other Imaging

a. Describe animal methodology:

b. Duration of procedure:

c. Frequency of observations during procedure:

d. Frequency/total number of procedures:

e. Method of transport to/from procedure area:

e. Please provide or attach appropriate permissions/procedures for animal use on human equipment:

4.11 Polyclonal Antibody Production*

a. Antigen/adjuvant used:

b. Needle size:

c. Route of injection:

d. Site of injection:

e. Volume of injection:

f. Total number of injection sites:

g. Frequency and total number of boosts:

h. What will be done to minimize pain/distress:

i. Describe potential adverse effects of procedures and provide humane endpoints (criteria for either humanely euthanizing or otherwise removing from study):

4.12 Monoclonal Antibody Production

a. Describe methodology:

b. Is pristane used: [ ] Yes [ ] No
- Volume of pristane:

c. Will ascites be generated: [ ] Yes [ ] No
d. Criteria/signs that will dictate ascites harvest:

e. Size of needle for taps:

f. Total number of taps:

g. How will animals be monitored/cared for following taps:

h. What will be done to minimize pain/distress:

j. Describe potential adverse effects of procedures and provide humane endpoints (criteria for either humanely euthanizing or otherwise removing from study):

4.13 Temperature/Light/Environmental Manipulations

a. Describe manipulation(s):

b. Duration:

c. Intensity:

d. Frequency:

e. Frequency of observations/parameters documented:

f. Describe potential adverse effects of procedures and provide humane endpoints (criteria for either humanely euthanizing or otherwise removing from study):

4.14 Behavioral Studies

a. Describe methodology/test(s) used:

N/A

b. If aversive stimulus used, frequency, intensity and duration:

N/A

c. Frequency of tests:

N/A

d. Length of time in test apparatus/test situation:

N/A

e. Frequency of observation/monitoring during test:

N/A

f. Describe potential adverse effects of procedures and provide humane endpoints (criteria for either humanely euthanizing or otherwise removing from study):

4.15 Capture with Mechanical Devices/Traps/Nets

a. Description of capture device/method:

b. Maximum time animal will be in capture device:

c. Frequency of checking capture device:

d. Methods to ensure well-being of animals in capture device:

e. Methods to avoid non-target species capture:

f. Method of transport to laboratory/field station/processing site and duration of transport:

g. Methods to ensure animal well-being during transport:

h. Expected mortality rates:

i. Describe potential adverse effects of procedures and provide humane endpoints (criteria for either humanely euthanizing or otherwise removing from study):

4.16 Manipulation of Wild-Caught Animals in the Field or Laboratory

a. Parameters to be measured/collected:

b. Approximate time required for data collection per animal:

c. Method of restraint for data collection:

d. Methods to ensure animal well-being during processing:

e. Disposition of animals post-processing:

f. Describe potential adverse effects of procedures and provide humane endpoints (criteria for either humanely euthanizing or otherwise removing from study):

4.17 Wildlife Telemetry/Other Marking Methods

a. Describe methodology (including description of device):

b. Will telemetry device /tags/etc be removed? If so, describe:

c. Describe potential adverse effects of procedures and provide humane endpoints (criteria for either humanely euthanizing or otherwise removing from study):

4.18 Other Animal Manipulations

a. Describe methodology:

b. Describe methods to ensure animal comfort and well-being:

c. Describe potential adverse effects of procedures and provide humane endpoints (criteria for either humanely euthanizing or otherwise removing from study):

4.19 Surgical Procedures

All survival surgical procedures must be done aseptically, regardless of species or location of surgery. Adequate records describing surgical procedures, anesthetic monitoring and postoperative care must be maintained for all species.

A. Location of Surgery (Room #):

B. Type of Surgery:

[ ] Nonsurvival surgery (animals euthanized without regaining consciousness)
[ ] Major survival surgery (major surgery penetrates and exposes a body cavity or produces substantial impairment of physical or physiologic function)
[ ] Minor survival surgery

[ ] Multiple survival surgery*
If yes, provide scientific justification for multiple survival surgical procedures:

C. Describe the pre-op preparation of the animals:

1a. Food restricted for [ ] hours

1b. Food restriction is not recommended for rodents and rabbits and must be justified:

2a. Water restricted for [ ] hours

2b. Water restriction is not recommended in any species for routine pre-op prep and must be justified:

D. Minimal sterile techniques will include (check all that apply):

Please refer to DCM Guidelines for Aseptic Surgery for specific information on what is required for each species and type of surgery (survival vs. non-survival).

[ ] Sterile instruments

- How will instruments be sterilized:

- If serial surgeries are done, how will instruments be sterilized between surgeries:

[ ] Sterile gloves
[ ] Cap and mask
[ ] Sterile gown
[ ] Sanitized operating area
[ ] Clipping or plucking of hair or feathers
[ ] Skin preparation with a sterilant such as betadine
[ ] Practices to maintain sterility of instruments during surgery
[ ] Non-survival (clean gloves, clean instruments, etc.)

E. Describe all surgical procedures:

1. Skin incision size and site on the animal:

2. Describe surgery in detail (include size of implant if applicable):

3. Method of wound closure:
   a. Number of layers

   b. Type of wound closure and suture pattern:

   c. Suture type/size / wound clips/tissue glue:

   d. Plan for removal of skin sutures/wound clips/etc:

F. Anesthetic Protocol:

If anesthesia/analgesia must be withheld for scientific reasons, please provide compelling scientific justification as to why this is necessary.

	Agent	Concentration	Dose (mg/kg)	Volume	Route	Frequency	Duration
Pre-emptive analgesic							
Pre-anesthetic							
Anesthetic							
Analgesic Post Op							
Other							

1. Criteria to monitor anesthetic depth, including paralyzing drugs:

2. Methods of physiologic support during anesthesia and immediate post-op period:

3. Duration of recovery from anesthesia (immediate post-op period):

4. Frequency/parameters monitored during immediate post-op period:

5. Describe any behavioral or husbandry manipulations that will be used to alleviate pain, distress, and/or discomfort during the immediate post-op period:

6. List criteria used to determine when animals are adequately recovered and when the animals can be returned to their home environment:

G. Recovery from Surgical Manipulations (after animal regains consciousness and is returned to its home environment)

1. What parameters will be monitored:

2. How frequently will animals be monitored:

3. How long post-operatively will animals be monitored:

H. Surgical Manipulations affecting animals

1. Describe any signs of pain/ discomfort/ functional deficits resulting from the surgical procedure:

2. What will be done to manage any signs of pain or discomfort/ (include pharmacologic and non-pharmacologic interventions):

3. Describe potential adverse effects of procedures and provide humane endpoints (criteria for either humanely euthanizing or otherwise removing from study):

5. Euthanasia

**Please refer to the 2007 AVMA Guidelines on Euthanasia and DCM Guidelines to determine appropriate euthanasia methods.*

5.1 Euthanasia Procedure. If a physical method is used, the animal should be first sedated/anesthetized with CO_2 or other anesthetic agent. If prior sedation is not possible, a **scientific justification** must be provided. All investigators, even those doing survival or field studies, must complete this section in case euthanasia is required for humane reasons.

Overdose with CO_2, followed by cervical dislocation.

5.2. Method of ensuring death (can be a physical method, such as pneumothorax or decapitation for small species and assessment method such as auscultation for large animals):

Absence of heartbeat

5.3. For field studies, describe disposition of carcass following euthanasia (If carcass will be kept for genetic/morphological/phylogenetic analysis, please include preservation, transportation, and storage technique):

I acknowledge that humane care and use of animals in research, teaching and testing is of paramount importance, and agree to conduct animal studies with professionalism, using ethical principles of sound animal stewardship. I further acknowledge that I will perform only those procedures that are described in this AUP and that my use of animals must conform to the standards described in the Animal Welfare Act, the Public Health Service Policy, The Guide For the Care and Use of Laboratory Animals, the Association for the Assessment and Accreditation of Laboratory Animal Care, and East Carolina University.

Please submit the completed animal use protocol form via e-mail attachment to iacuc@ecu.edu. You must also carbon copy your Department Chair.

APPENDIX 1 - HAZARDOUS AGENTS			
Principal Investigator: S.R. Shaikh	Campus Phone:744-2484		Home Phone:317-409-9565
IACUC Protocol Number:C059	Department:Biochemistry		E-Mail:shaikhsa@ecu.edu
Secondary Contact:Mitch Harris Department:Biochemistry	Campus Phone:744-2119	Home Phone:919-943-9882	E-Mail:harrismit@ecu.edu
Chemical Agents Used:LPS		Radioisotopes Used:none	
Biohazardous Agents Used:none		Animal Biosafety Level:2	Infectious to humans?no
PERSONAL PROTECTIVE EQUIPMENT REQUIRED:			
Route of Excretion:			
Precautions for Handling Live or Dead Animals:			
Animal Disposal:			
Bedding / Waste Disposal:			
Cage Decontamination:			
Additional Precautions to Protect Personnel, Adjacent Research Projects including Animals and the Environment:			
Initial Approval Safety/Subject Matter Expert Signature & Date _____			

PI Signature: e-mail Date: 5/23/11

Veterinarian: Karen A. Oppelt Date: 5/24/11

IACUC Chair: [signature] Date: 5/24/11

APPENDIX 1 - HAZARDOUS AGENTS			
Principal Investigator: S.R. Shaikh	Campus Phone:744-2484		Home Phone:317-409-9565
IACUC Protocol Number:C059	Department:Biochemistry		E-Mail:shaikhsa@ecu.edu
Secondary Contact:Mitch Harris Department:Biochemistry	Campus Phone:744-2119	Home Phone:919-943-9882	E-Mail:harrismit@ecu.edu
Chemical Agents Used:LPS		Radioisotopes Used:none	
Biohazardous Agents Used:none		Animal Biosafety Level:2	Infectious to humans?no
PERSONAL PROTECTIVE EQUIPMENT REQUIRED:			
Route of Excretion:Not applicable			
Precautions for Handling Live or Dead Animals:Gloves			
Animal Disposal: Standard methods of disposal			
Bedding / Waste Disposal: Standard			
Cage Decontamination: Standard			
Additional Precautions to Protect Personnel, Adjacent Research Projects including Animals and the Environment:None required (spoke to Eddie Johnson for this form)			
Initial Approval Safety/Subject Matter Expert Signature & Date Edward A. Johnson, Jr. 5/23/2011 prospective health / biological safety			

East Carolina University

1907-2007 CENTENNIAL

Animal Care and Use Committee
212 Ed Warren Life Sciences Building
East Carolina University
Greenville, NC 27834

252-744-2436 office
252-744-2355 fax

November 19, 2009

Raza Shaikh, Ph.D.
Department of Biochemistry
Brody 5E-124
ECU Brody School of Medicine

Dear Dr. Shaikh:

The Amendment to your Animal Use Protocol entitled, "High Fat Diets Modulate Adaptive Immune Responses", (AUP #C059) was reviewed by this institution's Animal Care and Use Committee on 11/19/09. The following action was taken by the Committee:

"Approved as amended"

A copy of the Amendment is enclosed for your laboratory files. Please be reminded that all animal procedures must be conducted as described in the approved Animal Use Protocol. Modifications of these procedures cannot be performed without prior approval of the ACUC. The Animal Welfare Act and Public Health Service Guidelines require the ACUC to suspend activities not in accordance with approved procedures and report such activities to the responsible University Official (Vice Chancellor for Health Sciences or Vice Chancellor for Academic Affairs) and appropriate federal Agencies.

Sincerely yours,

Robert G. Carroll, Ph.D.
Chairman, Animal Care and Use Committee

RGC/jd

enclosure

The Brody School of Medicine
Office of Prospective Health
East Carolina University
188 Warren Life Sciences Building • Greenville, NC 27834
252-744-2070 office • 252-744-2417 fax

Occupational Medicine
Employee Health
Radiation Safety
Infection Control
Biological Safety

TO: Dr. Saame Raza Shaikh
Department of Biochemistry and Molecular Biology

FROM: Eddie Johnson/Nick Chaplinski
Biological Safety Officers

RE: Registration Final Approval

Date: May 23, 2011

Your Biological Safety Protocol, Shaikh S, 08-01, *"High Fat Diets Modulate Adaptive Immune Responses"* (Amendment) has received **final approval** to be conducted at Biosafety Level 2 based on your registration/revisions submitted,

using: A. Biohazards

- ☐ Infectious Agent(s)
- ☒ Biotoxin(s)
- ☐ Allergen(s)
- ☐ Prion(s)
- ☒ Human blood, fluid, cells, tissue or cell cultures
- ☐ Transformed cells
- ☐ Other

and/or B. ☒ NIH Use of Recombinant DNA (or RNA) molecules, microorganisms use or breeding transgenic or techniques (plasmids, viral vectors, transfection); of transgenic animals or plants at NIH Category III-F Exempt.

This approval is effective for a period of 3 years and may be renewed with an updated registration if needed at that time. Your laboratory will be inspected periodically (every 1-3 years) depending upon the materials/techniques used.

Please notify the Animal Care staff before beginning work with Biohazard agents in animals. Also please keep in mind all individuals who will be exposed to or handle human-derived biohazardous agents will be due for Blood Borne Pathogens refresher training annually.

Please do not hesitate to contact Biological Safety at 744-2070 if you have any questions, concerns, or need any additional information. Best wishes on your research.

cc: Dr. Jeff Smith, Chair, Biosafety Committee
Dr. Phillip Pekala, Chair
Janine Davenport, IACUC
Dr. Scott Gordon, IACUC
Dale Aycock, IACUC

The Brody School of Medicine
Office of Prospective Health
East Carolina University
188 Warren Life Science Building • Greenville, NC 27834
252-744-2070 office • 252-744-2417 fax

Occupational Medicine
Employee Health
Radiation Safety
Infection Control
Biological Safety

TO: Dr. Saame Raza Shaikh ("Raz")
Department of Biochemistry and Molecular Biology

FROM: Eddie Johnson/John Williams
Biological Safety Officers

RE: Registration Final Approval

Date: December 5, 2008

Your Biological Safety Protocol Shaikh S ("Raz"), 08-01 *"High Fat Diets Modulate Adaptive Immune Responses"* has received **final** approval. This approval is effective for a period of 3 years and may be renewed with an updated registration if needed.

Please do not hesitate to contact Biological Safety at 744-2070 if you have any questions or concerns.

cc: Dr. Jeff Smith, Chair, Biosafety Committee
Dr. Phillip Pekala, Interim Chair
Janine Davenport, IACUC

11/4/09

Amendment to C059

Davenport, Janine

From: Shaikh, Saame Raza
Sent: Tuesday, November 03, 2009 4:28 PM
To: Davenport, Janine
Subject: amendment to animal protocol for Shaikh

Hi Janine,

Rob Carroll asked me to send you the changes to the animal protocol that I had submitted to him earlier this week:

Use of metabolic cages. Throughout the period in which we will feed mice special diets (for which the time can range from 24 hours to several months as indicated in our protocol), we will place the mice into the metabolic cages. We will follow the standard protocol for metabolic cage studies, which includes checking the animals twice a day in addition to husbandary needs. The mice will be housed one per cage at room temperature on a 12 hour light/12 hour dark cycle in order to measure oxygen consumption, food intake, locomotor activity, etc. The mice will placed into the cages at the time point at which lights come on in the morning (7am). The mice will be placed in the cages for 2 days for adaptation and then up to an additional 2 days for data collection. The food will continue to be changed on a regular basis to prevent oxidation, as we currently do.

Number of mice to be utilized for the metabolic cages. The number of animals proposed for metabolic cage housing is: six mice at a given time on the diet x 3 (triplicates) x 4 times on the diet = 72 mice per study x 10 studies over the next two years = 720 mice

Thank you,

Raz.

Saame Raza Shaikh, Ph.D.
Assistant Professor
Dept. of Biochemistry & Molecular Biology
Brody School of Medicine - East Carolina University
Office: 252-744-2585 Lab: 252-744-2119

Karen A. Oppelt
11/19/09

11/4/2009

APPENDIX B: SUPPLEMENTAL TABLES AND FIGURES

Supplemental Table 2.1: Fatty acid analysis of experimental diets

Fatty Acid	CD	LF (n-3) PUFA	HF (n-3) PUFA	HF (n-6) PUFA
14:0	0.5	3.1	3.7	4.6
16:0	12.2	14.6	13.6	10.0
16:1	0.1	4.3	4.9	0.1
18:0	6.9	8.7	7.2	7.5
18:1 *trans*	0.5	1.5	0.9	0.5
18:1 *cis*	20.5	16.0	15.7	15.5
18:2 (n-6)	48.0	13.6	12.1	58.3
18:3 (n-3)	6.5	24.1	26.9	1.4
20:5 (n-3)	0.0	4.4	5.0	0.1
22:2 (n-6)	0.2	0.7	0.6	0.0
22:5 (n-3)	0.1	0.8	0.8	0.0
22:6 (n-3)	0.0	3.3	3.5	0.1
∑SFA	20.4	27.0	25.0	22.6
∑MUFA	23.0	24.3	24.0	17.1
∑PUFA (n-3)	6.6	32.6	36.2	1.5
∑PUFA (n-6)	50.0	16.1	14.8	58.7

Fatty acids were extracted from the diets and analyzed with gas chromatography. Values are the percentage of total fatty acids. Values less than 0.5 are omitted for clarity.

Supplemental Figure 2.1

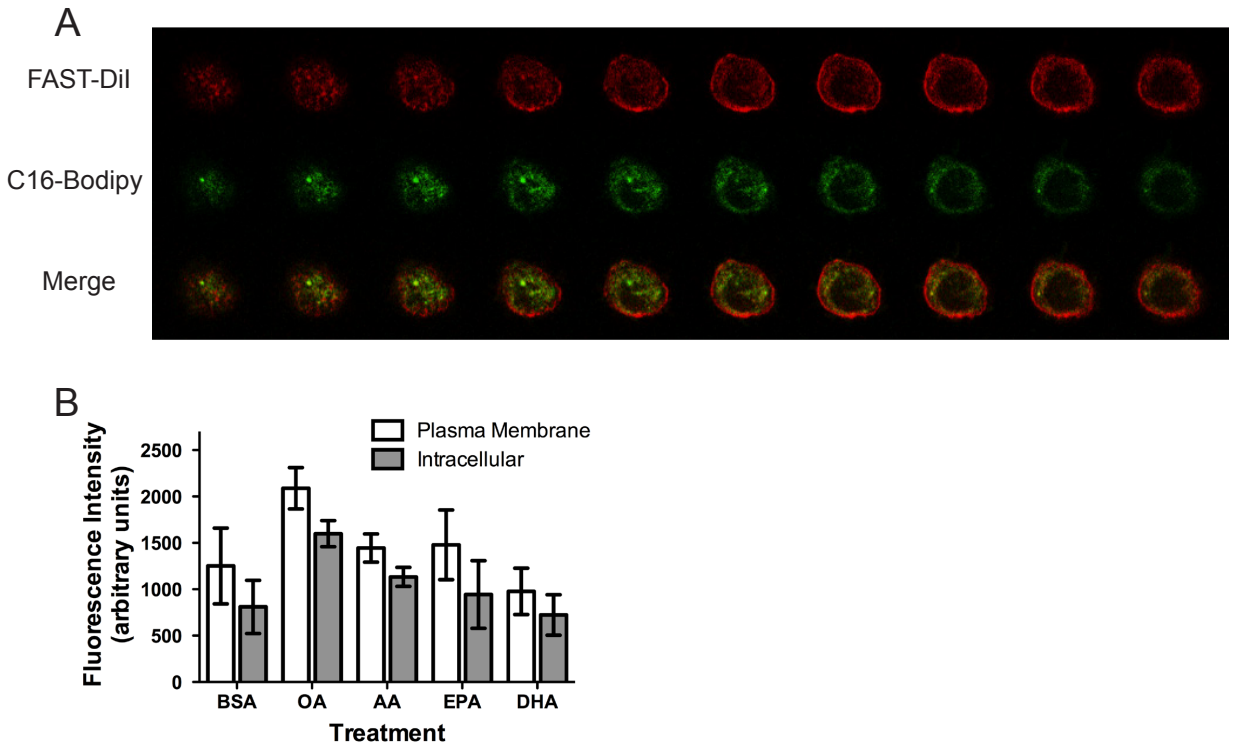

Supplemental Figure 2.1: C16-Bodipy imaging studies. (A) EL4 cells were co-stained with FAST-DiI and C16-Bodipy. The images are from a single z-stack used to calculate percent co- localization. The data are representative of 2 separate experiments. Co-localization is indicated by orange in the merge. (B) Average C16-Bodipy intracellular and plasma membrane image intensity for EL4 cells treated overnight with BSA, OA, AA, EPA, and DHA. Data are means ± SEM, n= 4.

Supplemental Figure 2.2

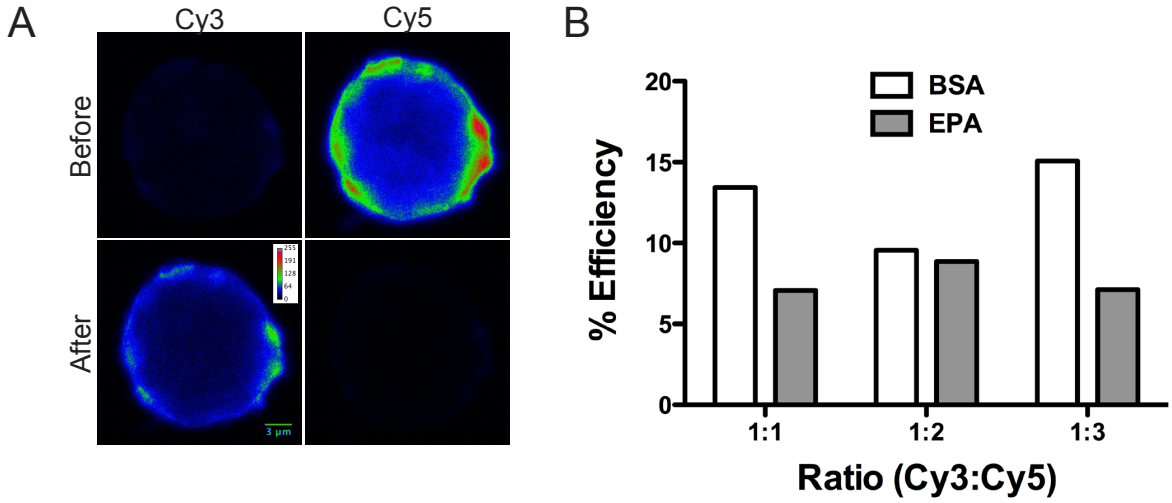

Supplemental Figure 2.2: MHC class I molecules were randomly distributed on EL4 cells. (A) Positive control before and after photobleaching images of EL4 cells stained with Cy3 (donor) and Cy5 (acceptor) labeled antibodies against MHC I. FRET efficiency increased by ~80%. (B) Sample data from a single experiment to show BSA or EPA treatment did not modifiy MHC I clustering since efficiency values did not increase with increasing donor:acceptor ratio. However, note EPA treatment lowered FRET values relative to BSA.

Supplemental Figure 2.3

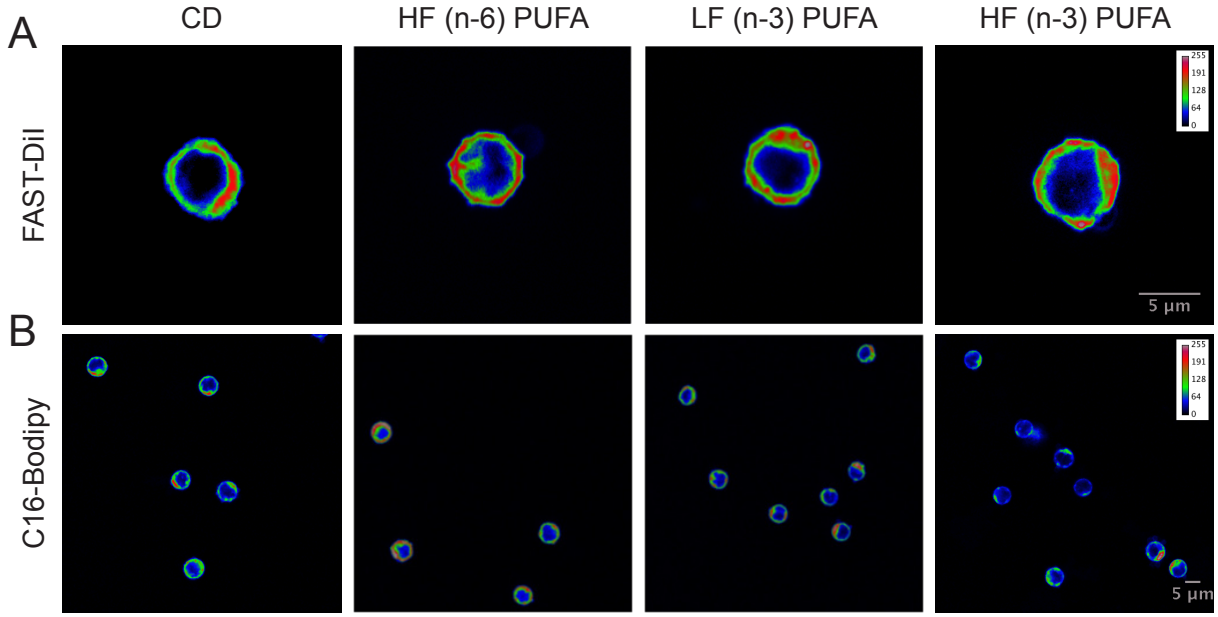

Supplemental Figure 2.3: (n-3) PUFA diets did not increase FAST-DiI accumulation but HF (n-3) PUFA diet lowered C16-Bodipy uptake. (A) Fluorescent images of B cells isolated from C57BL/6 mice fed CD, HF (n-6), LF or HF (n-3) PUFA diets and stained with FAST-DiI. (B) Fluorescent C16-Bodipy images of B cells isolated from mice fed differing diets. Images are on a rainbow palette to discriminate differences in relative fluorescence intensity. Red and blue values, respectively, indicate high and low fluorescence intensity.

Supplemental Figure 2.4

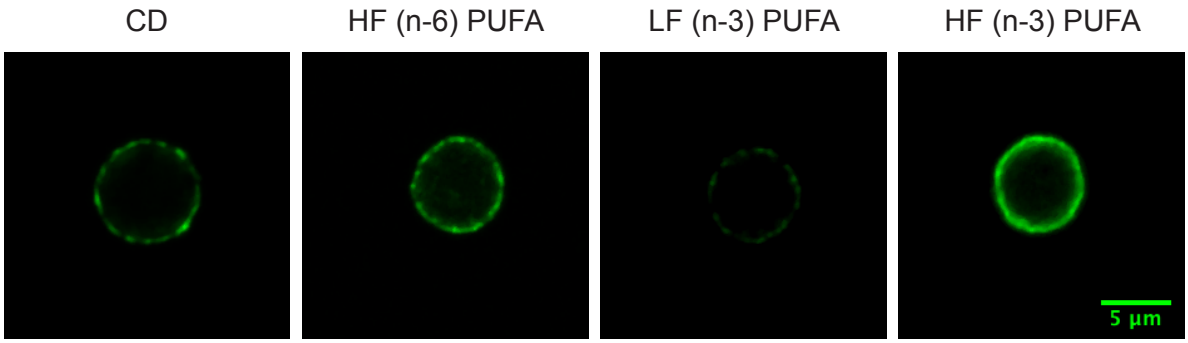

Supplemental Figure 2.4: HF (n-3) PUFA diet disrupted lipid raft clustering.

Fluorescent images of B cells isolated from C57BL/6 mice fed CD, HF (n-6), LF or HF (n-3) PUFA diets and stained for lipid rafts.

Supplemental Table 4.1: Analysis of major fatty acids in mouse diets.

Fatty Acid	Control	Fish oil
14:0	0.2	6.7
16:0	11.7	24.6
16:1	0.1	13.1
18:0	5.2	6.3
18:1 *trans*	0.1	0.1
18:1 *cis*	21.6	12.6
18:2 (n-6)	53.7	3.1
18:3 (n-6)	0.3	0.6
18:3 (n-3)	6.9	1.7
20:4 (n-6)	0.0	1.3
20:5 (n-3)	0.0	15.7
22:5 (n-3)	0.0	0.3
22:6 (n-3)	0.0	11.2
∑SFA	17.2	37.6
∑MUFA	21.9	25.8
∑(n-6) PUFA	54.0	5.5
∑(n-3) PUFA	6.9	28.8

Supplemental Figure 4.1

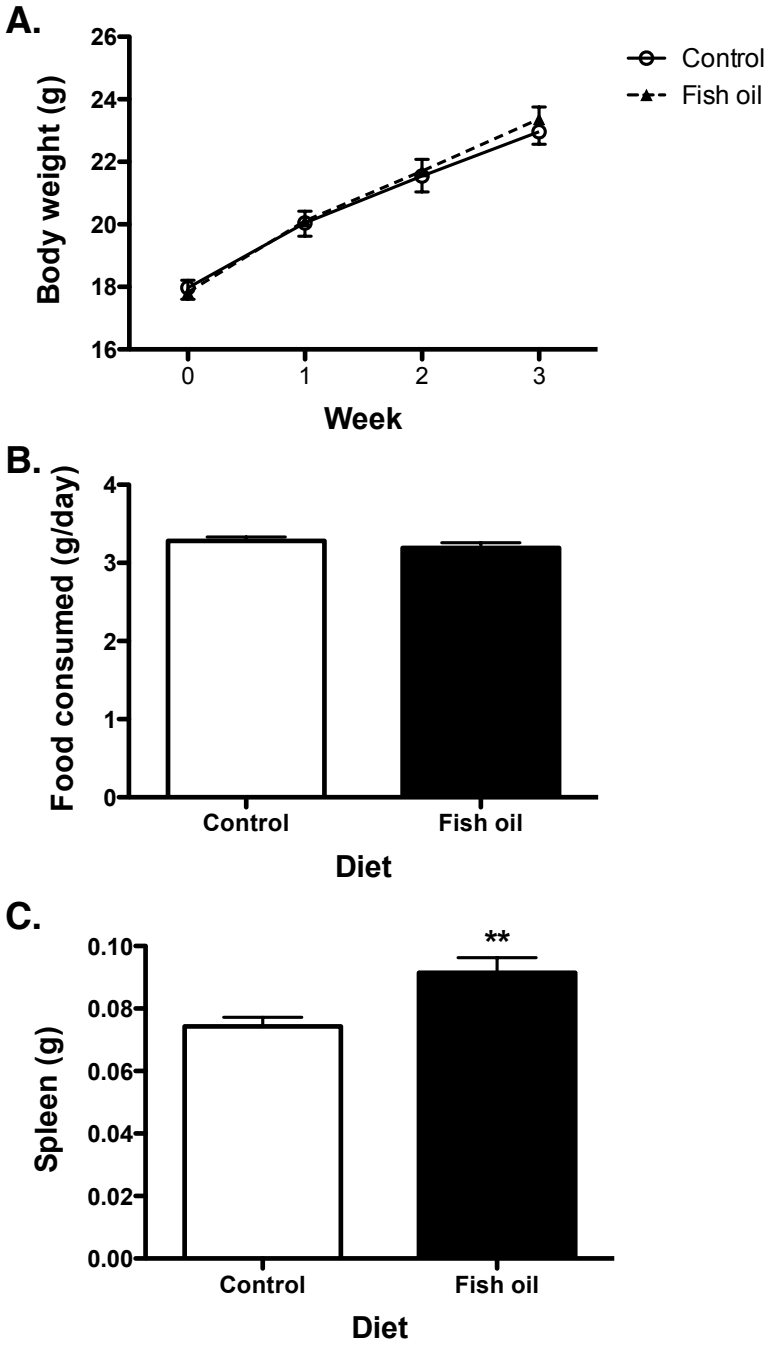

Supplemental Figure 4.1: FO increased spleen size. (A) Body weights as a function of time for mice fed a control or FO diet. (B) Average daily food consumption. (C) Spleen weight after 3 weeks. Values are means ± SEM, n = 20-30 mice. Asterisks indicate different from control: **P< 0.01.

Supplemental Figure 4.2

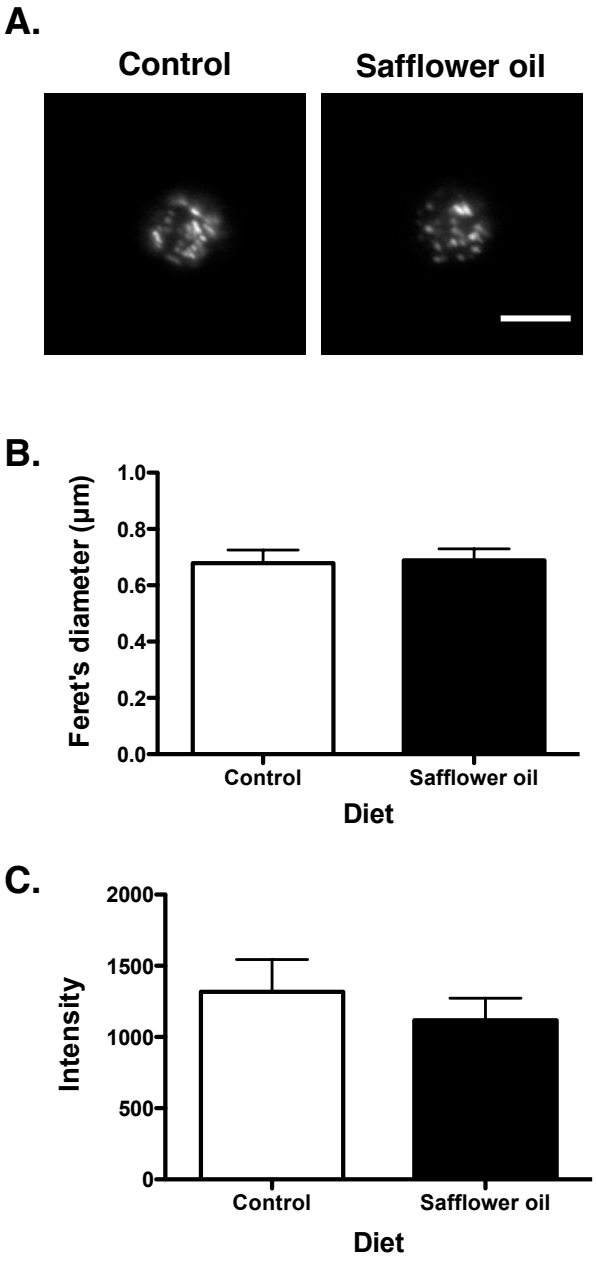

Supplemental Figure 4.2: Safflower oil-enriched diet did not increase lipid raft size. (A) TIRF microscopy images of B cell lipid rafts, induced upon cross-linking, from mice fed a control or safflower-enriched diet for 3 weeks. (B) Quantification of lipid raft size. (C) CTxB fluorescence intensity after cross-linking. Values are means ± SEM, n = 4.

Supplemental Table 4.2: Cholesterol levels in DRM and DSM fractions from ex vivo and in vitro studies. Mice were fed for 3 weeks a control or FO diet; EL4 cells were treated overnight with BSA, EPA, and DHA, as described in the Methods. Cholesterol values are fluorescence per μg of protein. Values are mean ± SEM from 4-5 independent experiments. P values are for the DRM/DSM ratio.

	DRM	DSM	DRM/DSM	p value
Control	419.8 ± 285.5	66.9 ± 6.1	7.1 ± 5.3	
Fish Oil	305.6 ± 91.6	68.1 ± 3.5	4.6 ± 1.5	0.66
BSA	4962.6 ± 988.0	190.2 ± 31.0	27.2 ± 4.9	
EPA	2390.2 ± 395.4	207.1 ± 25.9	12.7 ± 2.9	0.08
DHA	3425.4 ± 1490.9	204.5 ± 21.5	15.5 ± 5.7	0.08

Supplemental Figure 4.3

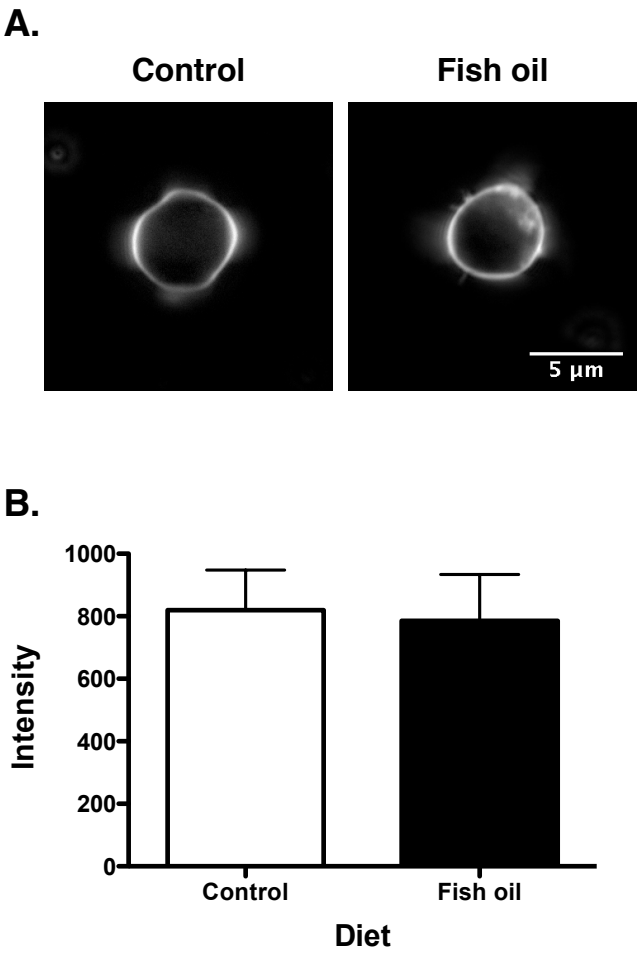

Supplemental Figure 4.3: FO had no impact on non-raft organization as measured by uptake of DiIC$_{18}$. (A) Sample images of B cells from control and FO fed mice stained with DiIC$_{18}$. (B) Quantification of DiIC$_{18}$ intensity. Values are means ± SEM, n = 3-4.

Supplemental Figure 4.4

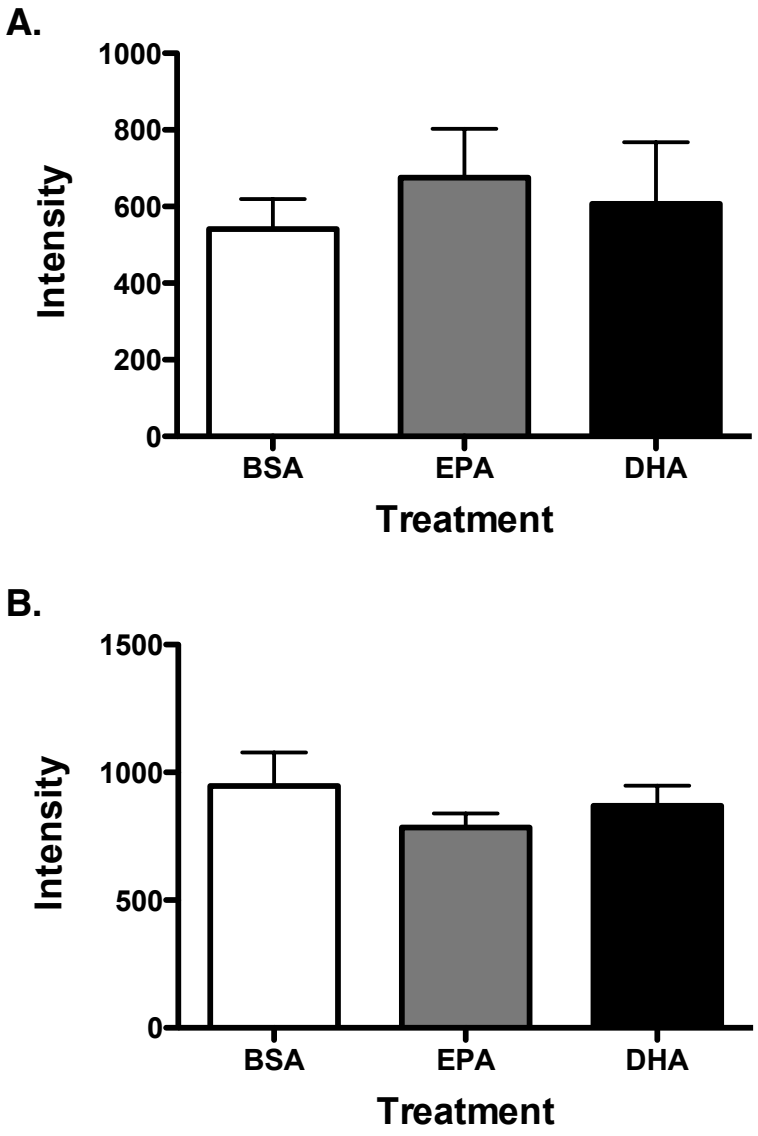

Supplemental Figure 4.4: EPA and DHA treatment had no effect on GM1 surface levels. GM1 surface levels (A) before and (B) after cross-linking rafts with CTxB upon treatment of EL4 cells with EPA or DHA relative to BSA. Values are means ± SEM, n = 4.

Supplemental Figure 5.1

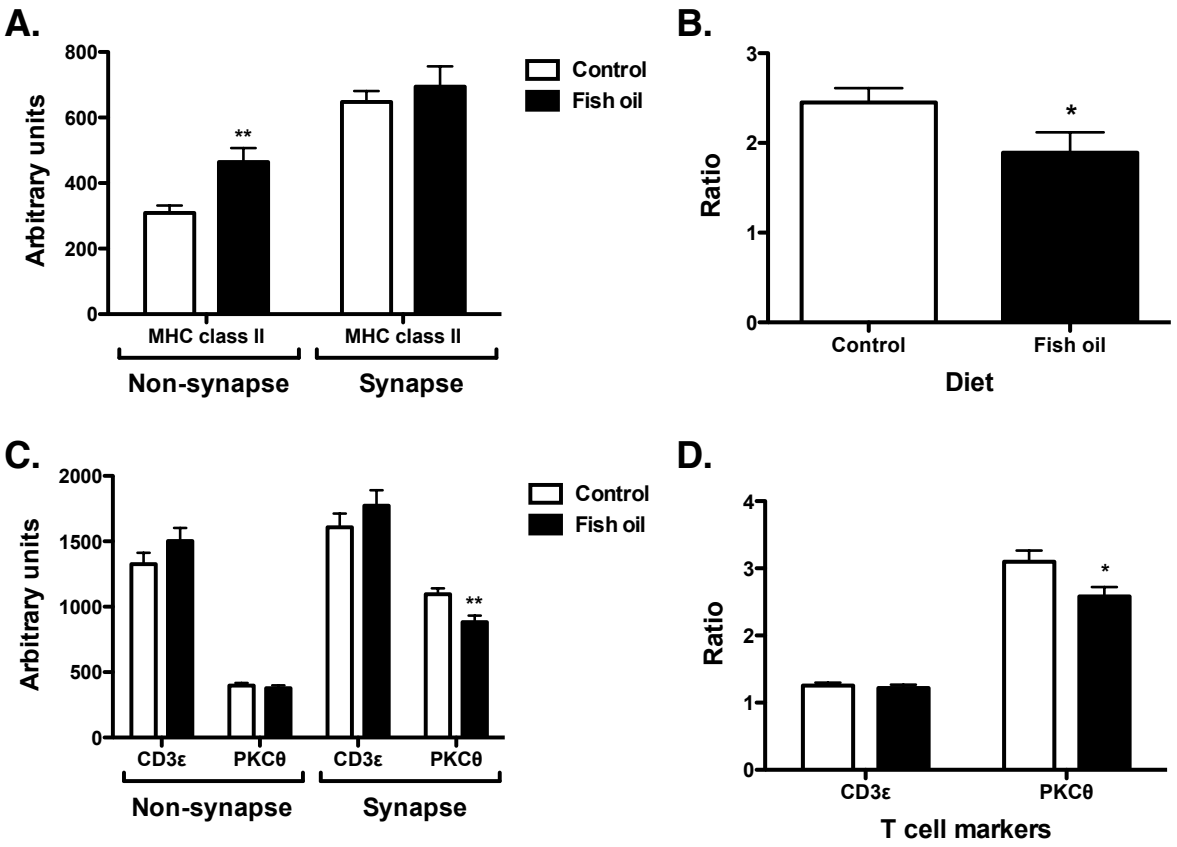

Supplemental Figure 5.1: Fish oil disrupts the B-T cell immunological synapse. A) Fluorescent intensity of MHC class II staining outside (Cell) and inside (Synapse) the immunological synapse for B cells from control (white) or fish oil (black) fed mice. B) Ratio of fluorescent intensity Synapse/Cell values for MHC class II staining. C) Fluorescent intensity of CD3ε and PKCθ staining outside (Cell) and inside (Synapse) the immunological synapse for B cells from control or fish oil fed mice. D) Ratio of fluorescent intensity Synapse/Cell values for CD3ε and PKCθ staining. Values are means ± SEM (n = 4 with 66 - 69 cells analyzed per diet). Asterisks indicate different from control: *$P < 0.05$; **$P < 0.01$.

Supplemental Figure 5.1

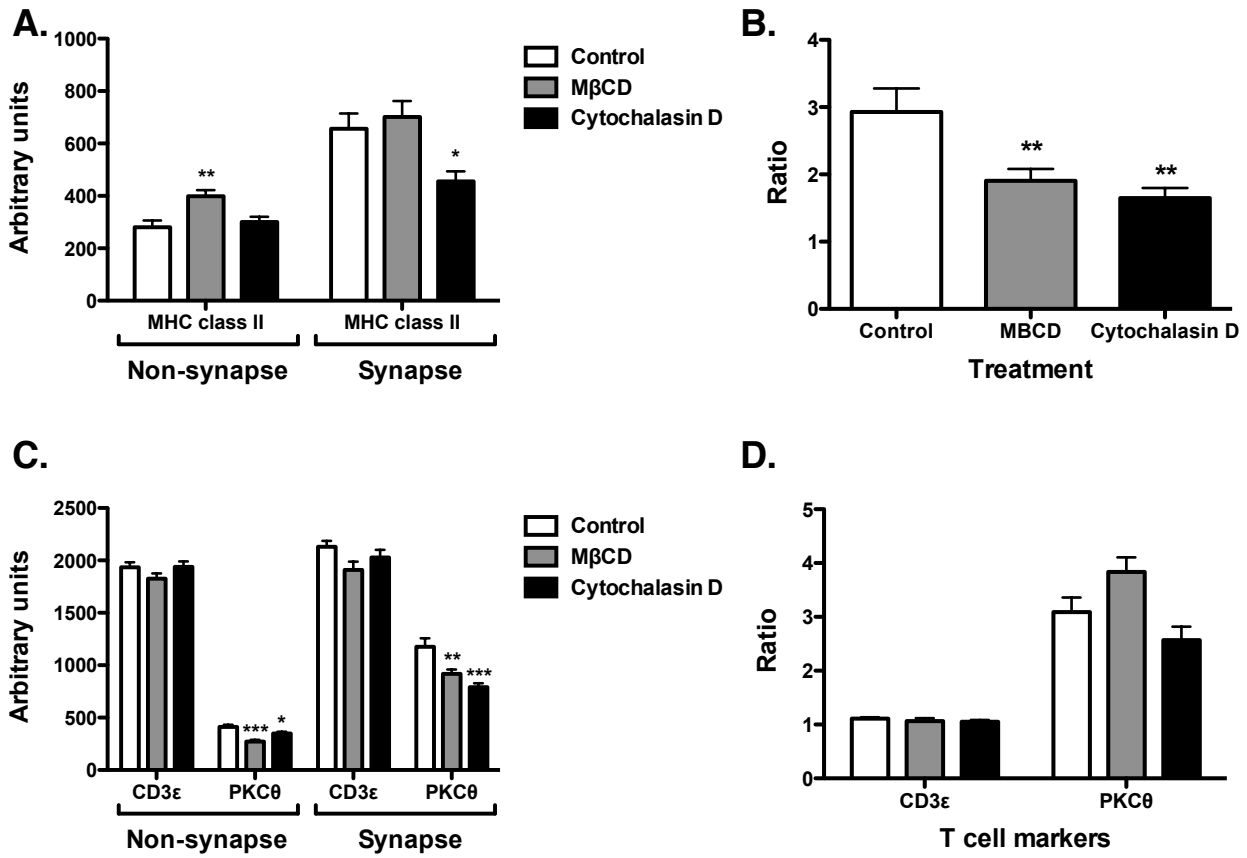

Supplemental Figure 5.2: Pharmacological agents disrupt the B-T cell immunological synapse. A) Fluorescent intensity of MHC class II staining outside (Cell) and inside (Synapse) the immunological synapse for B cells from control (white) or MβCD (grey) and cytochalasin D (black) treatment. B) Ratio of fluorescent intensity Synapse/Cell values for MHC class II staining. C) Fluorescent intensity of CD3ε and PKCθ staining outside (Cell) and inside (Synapse) the immunological synapse. D) Ratio of fluorescent intensity Synapse/Cell values for CD3ε and PKCθ staining. Values are means ± SEM (n = 4 with 66 - 69 cells analyzed per diet). Asterisks indicate different from control: *$P < 0.05$; **$P < 0.01$.